WIDE AREA CONTROL THROUGH AGGREGATION OF POWER SYSTEMS

Arash Vahidnia

B.Sc, M.Sc in Electrical Engineering

A Thesis submitted in partial fulfilment of the requirements for the degree of

Doctor of Philosophy

School of Electrical Engineering and Computer Science

Faculty of Science and Engineering

Queensland University of Technology

Queensland, Australia

February 2013

Keywords

Aggregation of Power Systems, Dynamic Reduction, FACTS Devices, Generator Coherency, Inter-area Oscillations, Kalman Filter, Phasor Measurement Units, Power System Stability, State Estimation, System Identification, Transient Stability, Wide-area Control, Wide-area Measurement

Abstract

The power systems are operating closer to their capacity limits to improve the efficiency of the system operation. This has increased the risk of system failures in the event of possible contingencies. The electricity supply industries need tools for dealing with system-wide disturbances that can cause widespread blackouts in power networks. When a major disturbance occurs in the system, the protection and controlling systems play the greatest role to prevent further degradation of the system, restore the system to a normal state, and minimize the impact of the disturbance. Synchronized phasor measurement units (PMU) can be installed in the network to improve the performance of the power systems in the event of faults by wide-area monitoring and control systems.

Due to the complexity of power systems and large number of dynamic states, the conventional control designs based on wide-area measurements require extensive computational effort which is not practical for dealing with large disturbances in the network. In order to reduce the complexity of the power system, unimportant dynamics and states can be excluded for the control design by obtaining a reduced dynamic model containing major system states that have higher effect on the system stability.

In this research, a feasible wide-area control approach based on dynamic reduction and aggregation of power systems is presented to improve the performance of the system in the event of severe faults. The model reduction is an important part of this research which is performed on the entire network to obtain a reduced model with measurements. The nonlinear reduced model is first obtained based on the available model of the power system and a Kalman filter is applied to estimate the

reduced system states using measurements. The reduction process relies on identification of the coherent generators in the network. This is addressed in this research by developing a method to find the coherent generators and areas which stay coherent for a wide range of operating conditions.

A more general dynamic reduction approach is achieved by identifying the parameters of the nonlinear reduced model by online processing of the data obtained from phasor measurement units. The reduced model is integrated with a nonlinear Kalman filter to estimate the angles and frequencies of the equivalent areas which represent the inter-area oscillations of the power system. The main goal of this research is achieved by integrating the developed reduction and estimation methods to obtain a feasible wide-area control system. The control approach addresses both first swing and damping stability of power systems by applying switching laws based on Kinetic energy of the system. It is shown that the proposed wide-area control approach can improve the dynamic performance of the power system following severe disturbances.

Table of Contents

List of Figures

List of Tables

List of Abbreviations

CCT	Critical Clearing Time
COA	Centre of Angle
CSC	Controllable Series Capacitor
DAE	Differential and Algebraic Equations
DFT	Discrete Fourier Transform
FACTS	Flexible AC Transmission System
KE	Kinetic Energy
MPC	Model Predictive Control
PMU	Phasor Measurement Unit
PSD	Power Spectral Density
SVC	Static VAR Compensator
UEP	Unstable Equilibrium Point

Statement of Original Authorship

The work contained in this thesis has not been previously submitted to meet requirements for an award at this or any other higher education institution. To the best of my knowledge and belief, the thesis contains no material previously published or written by another person except where due reference is made.

Signature: 

Date: 27 Feb 2013

Acknowledgements

First of all, I would like to convoy my sincerest and deepest thanks to my principal supervisor, Professor Gerard Ledwich for his patience, support and guidance throughout my doctoral research. It has been a privilege for me to work under his supervision and be a part of his research team.

I also wish to extend my sincere appreciation to my associate supervisors, Professor Arindam Ghosh and Dr. Ed Palmer for their invaluable support and advice during my PhD.

Last but not least, I would like to express my heartiest appreciation to my beloved wife, Sadaf for her endless encouragement and support during this period.

Chapter 1: Introduction

1.1 Background and motivation

The energy demand is rapidly growing and the network expansion is not following the pace of load growth in many power systems across the world. This has led the inter-connected systems to operate very close to their capacity limits, which makes them more vulnerable to any possible disturbance. One of the important issues in planning and operation of power systems is transient stability analysis which is performed by utilities to guarantee stable and reliable operation of power systems under contingencies. In addition, the expansion and rapid increase in penetration of renewable energy sources increase the complexity of power systems and highlight the need for advanced operation and control methods. Therefore, there is an increasing value for enhancement methods to maintain the stability of power systems.

After a severe disturbance, the kinetic energy of the system can cause instability of some generators and the whole system consequently. There are some preventive and protective schemes in power system stability which protect the system from cascading events resulting in system blackout. Most of the current controllers in the network are linear controllers which use local measurements of the system states. These controllers are designed and tested for a range of operating conditions based on the best available models of the system. The uncertainty in modelling of the system and effect of large disturbances which result in nonlinear system behaviour affect the performance of these controllers.

To achieve a better performance for dealing with the complexity and nonlinearity of power systems, improved control schemes based on nonlinear control design and remote measurements seem necessary. These controllers rely on wide-area measurements which means the control system will be based on the behaviour of the power system in all regions, not only on the measurements at the local power stations. The synchronized phasor measurement units (PMUs) which are installed throughout the network are used to implement the wide-area measurement and control systems and provide online controlling actions in the event of disturbance.

The wide-area control system should be able to make correct and in time decisions after a severe disturbance in the network. Due to the large number of dynamic states and measurement devices in wide-area measurement, extensive computational effort is required to implement the online control and this is not practical in dealing with the system disturbances. One way to provide a feasible online control approach is to reduce the complexity of the control system by excluding the unimportant states and dynamics in the control design. This can be achieved by obtaining a reduced model which contains major system states that highly affect the system stability. Therefore, dynamic aggregation of power systems is an important part of the online control approach which is presented in this research. The proposed aggregation methods reduce the entire network based on coherent areas and the PMUs are used for online identification of the reduced system parameters and estimation of dynamic states. It will be shown that the online control design based on aggregated regional model is capable of providing good performance for both first swing and damping stability of power systems.

1.2 Aims and objectives of the thesis

The main objective of the research is to provide a feasible wide-area control approach for improving the stability of power systems. The controllable devices throughout the network are employed to increase the robustness of the system against contingencies. The control approach relies on the reduced model of the system which contains important system states to reduce the computation and decision time. This highlights the importance of the system dynamic reduction in the process of online control. The following research aims are integrated to deliver the main goal of this research:

- Development of a methodology for power system model reduction to create a simplified area based model for entire system
- Development of a method for generator coherency detection and area identification for multiple operating conditions
- Development of tools for online identification of nonlinear dynamic parameters of the aggregated area based models
- Development of a system dynamic state estimation approach using phasor measurement units
- Designing the nonlinear control tools to address both first swing and damping stability of power systems for nonlinear large disturbances
- Integration of the developed tools and methods for implementing the wide-area control system

1.3 Significance of this research

The increasing demand for energy along with the environmental issues regarding global warming highlights the need for renewable energies. Transferring the power generated from large renewable energy sources to loads needs significant improvement in power transmission systems. Due to the huge cost of investment in new transmission lines, making greatest use of the current transmission capacity is very important. The increased stress on the transmission network makes the system more vulnerable to contingencies. Therefore, advanced control approaches are required to keep the system stable during severe disturbances. This research provides a feasible wide-area control approach to improve the robustness of the power transmission systems.

1.4 Key innovations of the research

The main contribution of this research is developing a wide-area control algorithm which can be implemented online to improve the inter-area performance of power systems following severe disturbances. In order to achieve the main goal of this work, the control approach is designed based on the reduced models of the systems. Therefore, accurate reduction of the system into an aggregated model is a main part of this research. In order to achieve the main objectives of this research, the following are accomplished:

1. A new system reduction approach is developed for forming a simplified area based model of the system. In most of the available reduction approaches the reduction is applied to the portion of the system outside the study area to

simplify power system studies. The advance in the proposed approach is to develop a process for reduction of entire system.

2. A new approach is introduced for defining the coherent generators and areas in large power systems. The entire project relies on generator coherency for system reduction and wide-area control. The developed method finds the coherent generators and non-generator buses which stay coherent in a wide range of operating conditions.

3. The method for obtaining the aggregated dynamic model is enhanced to be entirely based on the measurements. The system dynamic reduction in (1) relies on the available model of the entire system while the proposed method identifies the nonlinear dynamic parameters of the aggregated area based model using the measurements in the system.

4. A nonlinear state estimation approach is presented to estimate the angles and velocities of the aggregated system using phasor measurement units. The estimator is used to enhance the nonlinear parameter identification in (3) to provide a dynamic live aggregated model of the system.

5. A nonlinear control approach is presented to address both first swing and damping stability of power systems for nonlinear large disturbances.

6. All of the developed tools and methods are integrated to achieve the main goal of the research. The control approach is designed based on the aggregated regional model obtained from measurements and is then applied to the system to improve the system stability following severe disturbances.

1.5 Structure of the thesis

This thesis is organized in seven chapters. An overview of the research along with aims and contributions are outlined in **Chapter 1**. A literature review is presented in **Chapter 2** to outline the justification for doing this research. The approach for obtaining the aggregated model of power systems is described in **Chapter 3**. The entire power system is reduced based on the available model of system and the aggregated model represents the inter-area interactions of the system. A state estimation method is also presented to integrate the measurements with the aggregated model and implement the reduced dynamic model with synchronized phasor measurement. The generator grouping and area based model reduction are performed for the nominal operating conditions. To provide a more general approach, the coherent generators and areas should be identified for a wide range of operating conditions which is addressed in **Chapter 4**. The coherent generators and their correspondent non-generator buses are identified by applying spectrum analysis on the angle and velocity signals resulting from a distributed disturbance on the system. By combing the ideas of the Chapter 3 and 4, a new approach is presented in **Chapter 5** for obtaining the aggregated regional model of the power system based on measurements. Unlike the method described in Chapter 3, the parameters of the dynamic reduced model are identified online through wide-area measurement. An improved nonlinear state estimator is then designed to provide a more accurate estimation of area angles and frequencies which represent the dynamic states of the aggregated system. All of the developed tools and methods in previous chapters are integrated to achieve the main goal of the research which is presented in **Chapter 6.** The developed control approach targets both first swing and damping stability of power systems. The online nonlinear control design is based on the aggregated model

obtained from wide-area measurement which is then applied to improve the system stability.

Conclusions drawn from this research and recommendations for future works are given in **Chapter 7**. The list of references and a list of publications arising from this research are provided after the last chapter. The parameters of the dynamic systems used in the simulations are presented in Appendix.

Chapter 2: Literature Review

2.1 Introduction

Power system stability is one of the most important issues in power systems which deals with the response of the system to the disturbances occurred in the network. Rotor angle stability is one of the classified categories of the power system stability which refers to the ability of the synchronous machines to maintain synchronism after a disturbance. Considering the characteristics of the disturbances, rotor angle stability analysis can be classified as below [1]:

Dynamic Stability: Deals with small signal disturbances in the network. In this case the system is modelled as a linear system and the response of the system to the disturbances can be directly analysed using linear tools.

Transient Stability: In this case, the response of the system to large disturbances is investigated and because of the nonlinear behaviour of the system against these kinds of disturbances, the system cannot be modelled in linear form and other tools are required for transient stability analysis.

Large-disturbance rotor angle stability or transient stability is the ability of the power system to maintain synchronism when subjected to a severe disturbance, such as a short circuit on a transmission line or bus. In large power systems, instability does not only occur in first swing because of the effects of other modes resulting instability beyond the first swing [2]. The conventional method for determination of transient stability in power systems is solving the equations of the system to obtain a

time solution of variables and parameters for a certain scenario [3]. The other way for transient stability analysis is to determine the stability directly. Transient energy function method is the mostly preferred way for direct transient stability analysis of power systems [4, 5]. Several methods such as *Approximate Unstable Equilibrium Point (UEP)* and *Potential Energy Boundary Surface (PEBS)* methods have been proposed for direct transient stability analysis and prediction [4, 6-9]. These methods have advantages and disadvantages where each method can be used according to the application.

2.2 Wide-area measurement and control

In modern power systems, wide area measurement systems have been applied for various issues such as stability and security assessment and enhancement [10]. The availability of simultaneous data from Synchronised phasor measurement units provides the opportunity to monitor the nature of power system oscillations before and after possible system disturbances. One of the major problems in application of PMU data is the difficulty of characterizing the large amount of data captured by wide-area measurements over widely separated locations in the power system [11].

Synchronised phasor measurement units have a vast range of application in power system stability, including improving the dynamic stability in power systems [12]. One of the major problems in implementation of wide-area measurement as a tool for stability enhancement is the delay in signal transmission. The reliability of the communication network is another major concern with wide-area measurement based control [13-15].

Wide-area measurement system also provides the opportunity to analyse and characterize some dynamic characteristics of interconnected power systems such as

inter-area and local oscillations. It may be also required to reject these dynamic effects from measurement for specific studies so the measurement data will not include any inter-area or local modes [16]. Fast stability assessment is necessary after a disturbance in the system and the wide-area measurement system can provide additional data for the controlling system to monitor the characteristics of the system so that better decisions can be made after fault clearance [17].

Phasor measurement units as a wide-area measurement system can also act as a wide-area protection system on large power systems which is presented in [18]. When a fault happens in the system, the wide-area protection system uses the online measurement data to detect the nearest buses to the fault and consequently the faulted line is detected. Synchronised PMUs are playing a great role in recent studies related to power system transient stability. The data extracted from PMUs have been used for inter-area damping calculations as well as estimation of power systems properties such as inter-area dynamics [19-21]. It is clear that, phasor measurement units can provide tools for facilitating various applications such as improved control approaches in power system stability.

2.3 Power system oscillations and coherency

Interconnected power systems show various kinds of oscillations when subjected to a perturbation. Some of the oscillations are related to a single unit, some others are related to a closely connected power generation units and some other oscillations are related to a group of generators that are connected through weak connections such as tie-lines. The oscillations of a group of generators against other group or groups of generators in a power system are known as inter-area or inter-region oscillations while the oscillations associated with the closely connected

machines are called local modes [22, 23]. One of the common methods for studying power system oscillations is small signal analysis using modal techniques, where the eigenvalues represent the modes and eigenvectors define the relationship between each mode and participating generators in that mode [24]. Monitoring and control of inter-area modes is very important due to the effect of these modes on the stability of entire power system.

In the case of a disturbance in multi-machine power systems, some of the machines exhibit similar responses to the disturbance which means the difference between their swing curves is so small that they can be considered to be oscillating together and coherent. In power system dynamic performance, coherency is an important characteristic of the generators which has been used in several applications including dynamic reduction of power systems and emergency protection and control schemes.

Due to the importance of coherency detection in transient stability and control studies, several methods have been introduced to define the coherent groups of generators and areas in inter-connected power systems. Some of these methods use time-domain analysis on the linear dynamic model of power systems [25] while frequency response analysis have been implemented in [26]. Direct stability analysis methods such as Unstable Equilibrium Point (UEP) have been also applied for solving the generator coherency detection problem [27]. In the methods using the linearized dynamic model such as slow coherency method, the coherency between generators is obtained for the specific operating point and the change in the operating conditions may change the coherency indices between the generators which should be investigated. Therefore, methods such as continuation method [28] have been applied to trace the coherency characteristics in the network. In [29] a method is

proposed to use the phase of the oscillations to determine coherency using Hilbert–Huang transform. Application of wide area angle and generator speed measurement is another helpful tool in tracking the generator coherency in inter-connected power systems [30]. There have been also approaches which have used spectrum analysis in detecting coherent generators [31, 32].

In many applications such as system dynamic reduction and islanding, defining the non generator buses which belong to each area is important; this task is addressed in few research works [33]. Therefore, in order to provide a general area detection scheme, generators and load buses related to each area should be defined. This leads into detection of boundary buses and lines to divide the entire network to coherent areas. Most of the mentioned methods, define the coherent generators and areas for a single operating condition; however, a multiple operating point approach can provide a more accurate scheme to be applied in applications such as dynamic reduction and control.

2.4 Generator aggregation and dynamic reduction

A multi machine system when subjected to a disturbance can be represented as a multi area system based on generator coherency. The first step in the dynamic reduction process is the identification of coherent generators, a process which is well addressed in literature [26, 29, 34]. As a simple method, the network reduction can be performed to preserve the balanced steady state power flow conditions of the system while replacing the groups of generators by aggregated machines in the network [35]. When the system is subjected to a perturbation, the generators which are coherent in slow modes (low frequency modes) are called slow coherent generators and they usually define an area of the system. These generators can be

aggregated so a reduced dimension power system dynamic model is produced. Slow coherency based aggregation is a common method for aggregating coherent generators [36, 37] while other approaches have also been implemented for recognition and aggregation of the machines in the coherent areas [38, 39]. Based on the control theory, synchrony which is a generalization of the concept of slow coherency can be used for creating dynamic equivalent of the power systems by aggregation [38]. In this case, the area refers to synchronic group of generators instead of coherent groups and these generators can be aggregated to form an equivalent machine representing the machines in the area.

In order to simplify the dynamic model of large power systems in stability studies, several methods have been introduced to provide dynamic equivalents with high accuracy. In [40] a dynamic equivalent is obtained by aggregating generators based on their relative participation in the group while a non-iterative method is introduced in [41] to form aggregated dynamic equivalents based on preservation of coefficient matrices in time domain. In most of the proposed dynamic reduction techniques, the system is divided into study area and external area and the reduction is performed on the external area [42-44]. Aggregation is the main tool for forming dynamic equivalents in the methods discussed so far, but dynamic equivalents can be also obtained using online identification techniques using measurements [45, 46].

It can be observed that majority of the works on dynamic reduction and aggregation use the linear methods to obtain the reduced model of the system and the main focus is to reduce the external part (zone) of the system which is not studied. This highlights the need for new approaches to obtain the reduced nonlinear model of entire power systems.

2.5 Power system identification and state estimation

The parameters of system models are identified using measurements and identification techniques [47]. Due to the importance of dynamic models in power systems stability, various methods have been proposed for identification of power system dynamic models and parameters such as loads [48-51]. The identification algorithm presented in [52] is applied to obtain a linear low order model from a detailed system model where the transfer function of the linear model is identified from input and output samples. It is shown in [53] that phasor measurement units can be applied for identification of power system dynamic characteristics.

In order to accurately monitor the power systems, many electrical quantities of the network should be measured. This requires a huge amount of investment which is not economically efficient and control systems will be very vulnerable to measurement errors or failures. Therefore, state estimation methods have been proposed to determine the optimal estimation of the system states, including unmeasured parameters based on the system models and other measurements in the network [54]. There are various well known methods for estimation of power system state where *Least Square* based methods are very common. In the least square method by considering an error for each of the measurement, the best estimation of remaining parameters of the system is calculated.

Beside Least Square based methods, *Kalman filtering* is an optimal state estimation method applicable to dynamic systems containing random perturbations [55, 56]. The approach based on Kalman filtering is presented in [57] for optimal estimation of dynamic phasors and other dynamic parameters in energy processing systems. In [58] a Kalamn filtering based method shows a good estimation

performance on modal damping changes in power systems based on measurement data.

It is discussed that, wide area measurement systems can be applied for various stability assessment and enhancement issues by utilizing phasor measurement units. In [20, 21] it is shown that synchronized phasor measurements can be used for estimation of power systems properties such as inter-area dynamics. The Kalman filtering based methods in [59-61] have demonstrated good performances in various aspects of power systems using the phasor measurement units where in [60], a Kalman estimator is applied for designing an adaptive controller for damping of power system oscillations.

In summary, it is seen the approaches based on Kalman filtering have a huge range of application in various fields of power systems. The identification and estimation approaches can use Kalman filter to estimate the unknown system states and parameters using a limited number of measurement devices in the network.

2.6 Control approaches for improving power system stability

The conventional control systems try to keep the power systems stable for all operation conditions. However, large disturbances may lead into the failure of these controllers in stabilizing the system. If the disturbance is large enough to make a severe risk for the network, some emergency strategies must be planned and implemented on the system to prevent possible cascading which can lead to system-wide blackouts.

Most of the current control approaches in power systems are based on linear control design, which have been tested over a range of system operating conditions.

Due to the nonlinear characteristics of power system dynamics, these controllers are more suitable for the cases when disturbances and state changes are small [62]. This underlines the need for advanced nonlinear control approaches for stabilizing the system in the case of large disturbances which may involve flexible AC transmission system (FACTS) devices [63, 64].

Several control approaches have been proposed for stability enhancement of power systems using FACTS devices. Owing to the increasing power demand, improving the first swing stability is a key tool to increase the utilization of existing transmission networks. It is shown in [65] that various FACTS devices can improve the first swing stability performance of large power system while the control strategy presented in [66] demonstrated good first swing stability performance using shunt FACTS devices.

One of the concerns in power systems stability is the damping of oscillations, particularly inter-area modes, in the network [67]. Controllable series capacitors have shown to provide good damping for inter-area modes of inter-connected power systems in [68] and application of local and wide-area measurement in damping stability is demonstrated in [69]. Despite the nonlinear characteristics of power systems, linear control algorithms have also been implemented to damp the oscillations [70].

Several methods have been proposed for designing the first swing and damping stability controllers in power systems while the controllers based on Lyapunov energy function are among the widely applied control approaches [71]. The approach presented in [72] uses controllable series FACTS devices for damping the oscillations based on Lyapunov theory and shows good performance can be achieved by only using local measurements. Due to the complexity of the energy function

based controllers, the kinetic energy part of the Lyapunov energy function is used in [73] for control design which could successfully address both first swing and damping stability of power systems.

Beside energy based control approaches, the short horizon model predictive control (MPC) presented in [74] demonstrated near optimal first swing stability performance for large disturbances. The approach in [75] showed that a wide-area control system using synchronized phasor measurement can be facilitated by obtaining the aggregate model of the power system. The proposed method uses FACTS devices such as Thyristor Controlled Series Compensators (TCSC) for damping the electromechanical oscillations in power systems. This approach shows the feasibility of the wide-area control through aggregation of the systems which is the main aim of this research.

If all the control actions fail to keep the system stable, the emergency actions such as load shedding [76-78] and controlled islanding [79-82] should be applied to restrict the extent of system instability. These emergency approaches are considered as the last defense line for protecting the system from a system-wide blackout. However, the outcome of these actions is not completely desirable as some part of the network may face blackout. Therefore, more effort should be devoted for design and implementation of wide-area control systems to improve the stability performance of power systems following severe disturbance and reduce the possibility of blackouts.

2.7 Summary

In this chapter, a brief review is presented based on the previous research works on power system stability. Transient stability deals with the ability of power

systems to withstand the large disturbances and several methods have been proposed for direct and indirect transient stability analysis. Due to complexity of the power systems, advanced methods for monitoring and control of power systems seem necessary. Therefore, synchronized phasor measurement units are used for implementing the wide-area measurement and control systems to improve the stability of power systems. In order to provide a feasible wide-area control approach the processing and control decision time should be reduced which can be achieved by reducing the system model for control design. Most of the proposed dynamic reduction and aggregation methods deal with linear models and reduce a part of the system known as external zone which highlights the need for nonlinear approaches to reduce the entire network.

Identifying coherent generators and areas is the first step in dynamic reduction which is addressed by few approaches which mostly define the coherent generators for a single operating condition and do not consider non-generator buses. Therefore, the coherent generators and load buses should be defined for multiple operating points to provide a general approach. It is shown that Kalman filtering based approaches can be used for identification and estimation of unknown parameters and states of the power systems which implies the applicability of Kalman estimator in the wide-area control based on PMU measurements.

In order to avoid blackouts and load shedding in the event of severe disturbances, advanced control systems are necessary. It is seen that, controllable FACTS devices can be applied for dealing with first swing and damping stability of power systems. The Lyapunov energy function based control algorithms are among the widely applied methods and demonstrated good performance in transient stability enhancement of power systems. Therefore, the wide area control system can

integrate the energy based control algorithm with the dynamic reduction and estimation approaches to improve the first swing and damping stability of the inter-connected power systems.

Chapter 3: Dynamic Model Reduction with Phasor Measurement Units

3.1 Introduction

In this chapter a new approach is presented for state estimation of angles and frequencies of equivalent areas in large power systems with synchronized phasor measurement units. A multi machine system can be represented as a multi area system based on generator coherency when it is subjected to a disturbance. The first step in dynamic reduction process is identification of coherent generators which is well addressed in literature [26, 29, 34]. When the system is subjected to a perturbation, the generators which are coherent in slow modes (low frequency modes) are called slow coherent generators and they are usually considered to be in the same area. These generators can be aggregated so the reduced power system dynamic model is produced.

In order to simplify the dynamic model of large power systems in stability studies, several methods have been introduced to provide dynamic equivalents with high accuracy [40, 41]. In most of the proposed dynamic reduction techniques, the system is divided into study area and external area and the reduction is performed on the external area [42-44]. Unlike these efforts on dynamic reduction, the aim of proposed method is not to reduce the external area of the system; instead dynamic equivalents are obtained for each coherent area of the system. The approach consists of two major steps. By defining the generators in each area based on coherency, the system is reduced such that each area is represented by a generator then the reduced system parameters are obtained. At the next step a Kalman estimator is designed for

the linear system and modified to be implemented on the nonlinear reduced system to finalize the reduced dynamic model with synchronized phasor measurement. The method is simulated on two test systems to evaluate the feasibility of the proposed method.

3.2 Dynamic system model and reduction

In this section the mathematical approach of the proposed reduction method is presented for a general multi machine power system, and the proposed system simplification into reduced power system model is discussed. Like other dynamic systems, in a multi machine system, dynamic state model is represented by:

$$\dot{\boldsymbol{x}} = f(\boldsymbol{x}, u)\,, \quad \boldsymbol{y} = g(\boldsymbol{x}, u) \tag{3.1}$$

This is a general dynamic model of the power systems where $f(\boldsymbol{x}, u)$ is a nonlinear function of state variables in the state vector $\mathbf{x}$ and input vector u. Variables of the state vector are dependent to the order and shape of the state differential and algebraic equations (DAE). Differential equations are based on dynamic modeling of different parts of the power system including generators (machines) and their related devices in power plants such as excitation systems, loads, transmission lines and all the network components. The algebraic equations are related to the steady state equations for lines in power systems. For power system stability studies, state vector may consist of machine angles, velocities, and other machine related variables such as fluxes. Various parts of the system can be dynamically modeled by different order of differential equations such that there are several model orders of synchronous machines. Depending on the purpose of studies, a suitable order of equations is chosen to be applied in the simulations. For transient

stability studies a classical machine model of machines is usually sufficient. The dynamic model of a m machine system is given by:

$$J_i\ddot{\delta}_i + D_i\omega_i = P_{mi} - P_{ei}$$

$$\omega_i = \dot{\delta}_i = \omega_i^a - \omega_s \quad , \quad i = 1, ..., m \tag{3.2}$$

Where J_i is the inertia ratio, δ_i is the angular position, D_i is damping ratio, ω_i is the angular speed deviation, ω_i^a is the angular speed, m is the number of machines, P_{mi} and P_{ei} are the mechanical power input and electrical power output of the i^{th} machine, and ω_s is the nominal synchronous speed. Electrical power P_{ei} depends on the load modeling in the system and by modeling them as constant impedances the differential algebraic equations will be simplified. Using the classical machine model (3.1), the state variables of the system state model are $\boldsymbol{x} = [\boldsymbol{\delta} \quad \boldsymbol{\omega}]^{\boldsymbol{T}}$, where $\boldsymbol{\delta}$ and $\boldsymbol{\omega}$ are the angle and velocity vectors of generators. In order to simplify the state model it can be linearized at an operating point and the linearized state model is then obtained:

$$\dot{x} = Ax + Bu \quad , \quad y = Cx + Du \tag{3.3}$$

In this model, matrix A is the state matrix and the eigenvalues of this matrix represent system modes while the eigenvectors represent the relationship between system states for specific modes. The matrix C represents the relationship between output variables or measurements perturbation y and state variable perturbation x, while B and D provide the relationship between control vector u and system states and outputs. The A matrix has m eigenvalues called modes as below:

$$\lambda_i = \sigma_i \pm j2\pi f_i \tag{3.4}$$

For each of the eigenvalues, f_i is the frequency of mode i and σ_i is the damping factor of this mode. The type of each mode can be defined by considering the frequency and damping ratio of the correspondent eigenvalue and also the structure of normalized eigenvector. The linear model is needed to perform the dynamic reduction process and the first step state estimation using a Kalman filter. The linear state model (3.3) can be transferred into a modal representation using the eigenvector matrix *V*, and to create a modal position and velocity form of equations with low frequency modes first, the *P* matrix transformation as in [83] is applied .

$$P = \begin{bmatrix} 1 & 1 & 0 & 0 & \cdots & \cdots & 0 & 0 \\ \lambda_1 & \lambda_1^* & 0 & 0 & \cdots & \cdots & 0 & 0 \\ 0 & 0 & \vdots & \vdots & \vdots & \vdots & \vdots & \vdots \\ \vdots & \vdots & \vdots & \vdots & \vdots & \vdots & \vdots & \vdots \\ \vdots & \vdots & \vdots & \vdots & 1 & 1 & 0 & 0 \\ \vdots & \vdots & \vdots & \vdots & \lambda_{m-1} & \lambda_{m-1}^* & 0 & 0 \\ 0 & 0 & \cdots & \cdots & 0 & 0 & 1 & 0 \\ 0 & 0 & \cdots & \cdots & 0 & 0 & 0 & 1 \end{bmatrix} \tag{3.5}$$

$$T = PV^{-1} \tag{3.6}$$

$$\dot{z} = TAT^{-1}z + TBu \tag{3.7}$$

$$A_m = TAT^{-1} \tag{3.8}$$

$$\dot{z} = A_m z + TBu \tag{3.9}$$

Equation (3.9) is the modal representation of the system where *z* is the system state expression in terms of position and velocity perturbation of the system modes. The dynamics of the modal form are summarized in A_m matrix. The modal representation is the basis for the proposed system reduction approach which is applied such that coherent generators in each area form an equivalent machine representing all the machines in the area.

Using the classical machine model (3.2), three types of modes are observed in the system behavior, the common, local, and inter-area modes. Local modes have the higher frequency comparing to the inter-area modes and are described as the oscillation of each machine against other machines inside an area. The inter-area modes are related to low frequency oscillations related to the oscillation of a group of generators inside an area against other generator groups in the other areas. The oscillation frequency in these modes is usually below 1 Hz and inter-area modes have smaller damping ratios comparing to the local modes [23]. Therefore, different modes can be observed and defined by having the eigenvalues of A matrix. The eigenvalues matrix $[\lambda]$ is a diagonal matrix of eigenvalues of the system and for the classical model of machines it will be as below showing different modes.

$$[\lambda] = \begin{bmatrix} \lambda_{loc_1} & 0 & \cdots & \cdots & \cdots & \cdots & \cdots & \cdots & \cdots & \cdots & \cdots & 0 \\ 0 & \lambda^*_{loc_1} & 0 & \ddots & \ddots & \ddots & \ddots & \ddots & \ddots & \ddots & \ddots & \vdots \\ \vdots & 0 & \ddots & \ddots & \ddots & \ddots & \ddots & \ddots & \ddots & \ddots & \ddots & \vdots \\ \vdots & \ddots & \ddots & \lambda_{loc_a} & 0 & \ddots & \ddots & \ddots & \ddots & \ddots & \ddots & \vdots \\ \vdots & \ddots & \ddots & 0 & \lambda^*_{loc_a} & 0 & \ddots & \ddots & \ddots & \ddots & \ddots & \vdots \\ \vdots & \ddots & \ddots & \ddots & 0 & \lambda_{int_1} & 0 & \ddots & \ddots & \ddots & \ddots & \vdots \\ \vdots & \ddots & \ddots & \ddots & \ddots & 0 & \lambda^*_{int_1} & 0 & \ddots & \ddots & \ddots & \vdots \\ \vdots & \ddots & \ddots & \ddots & \ddots & \ddots & 0 & \ddots & \ddots & \ddots & \ddots & \vdots \\ \vdots & \ddots & \ddots & \ddots & \ddots & \ddots & \ddots & \ddots & \lambda_{int_b} & 0 & \ddots & \vdots \\ \vdots & \ddots & \ddots & \ddots & \ddots & \ddots & \ddots & \ddots & 0 & \lambda^*_{int_b} & 0 & \vdots \\ \vdots & \ddots & \ddots & \ddots & \ddots & \ddots & \ddots & \ddots & \ddots & 0 & \lambda_{com1} & 0 \\ 0 & \cdots & \cdots & \cdots & \cdots & \cdots & \cdots & \cdots & \cdots & \cdots & 0 & \lambda_{com2} \end{bmatrix} \quad (3.10)$$

Equation (3.10) contains all the eigenvalues of the system such that the number of local modes λ_{loc} is defined by a and there are b number of inter-area modes λ_{int} in the system. For the system reduction approach, high frequency local modes are ignored in the modal equation (3.9) such that A_m matrix is segmented in respect to different modes types and the segments associated with local modes are omitted in the matrix structure. In this case the reduced eigenvalues matrix $[\lambda_r]$ and modal equation will be defined as below:

$$[\lambda_r] = \begin{bmatrix} \lambda_{int_1} & 0 & \cdots & \cdots & \cdots & \cdots & 0 \\ 0 & \lambda^*_{int_1} & 0 & \ddots & \ddots & \ddots & \vdots \\ \vdots & 0 & \ddots & \ddots & \ddots & \ddots & \vdots \\ \vdots & \ddots & \ddots & \lambda_{int_b} & 0 & \ddots & \vdots \\ \vdots & \ddots & \ddots & 0 & \lambda^*_{int_b} & 0 & \vdots \\ \vdots & \ddots & \ddots & \ddots & 0 & \lambda_{com1} & 0 \\ 0 & \cdots & \cdots & \cdots & \cdots & 0 & \lambda_{com2} \end{bmatrix} \tag{3.11}$$

$$\dot{z}_r = A_{mr} z_r + (TB)_r u \tag{3.12}$$

Where A_{mr} is the lower right segment of the A_m matrix and z_r is the reduced modal perturbation vector representing inter-area modes of the systems. In order to have the state representation of the reduced *m* machine system to an *n* area system, the state vector *x* is replaced by the reduced state vector $\mathbf{x_r} = [\boldsymbol{\delta_r}\ \boldsymbol{\omega_r}]^T$ where $\boldsymbol{\delta_r}$ and $\boldsymbol{\omega_r}$ are the vectors of equivalent angles and velocities of coherent areas. To obtain the reduced system state model, the relationship between full state vector **x** and the reduced state vector $\mathbf{x_r}$ must be found. Considering the coherency of machines inside an area, the coherent machines are aggregated using a slow coherency based aggregation. In this method, slow aggregate variables are considered to represent the area angle and velocity and δ_r and ω_r of each area *k* are calculated:

$$\delta_{rk} = \sum_{i \in k} J_i \delta_i \Big/ \sum_{i \in k} J_i \tag{3.13}$$

$$\omega_{rk} = \dot{\delta}_{rk} = \sum_{i \in k} J_i \omega_i \Big/ \sum_{i \in k} J_i \tag{3.14}$$

The equations above are defined such that the aggregated δ and ω of each area can be represented by inertia *J* weighted sum of velocity and angle of the machines in each area. Applying (3.13)-(3.14) on the machines of each area, the aggregated angle and velocity of the area is calculated. Therefore, a relation between full system state vector and reduced system state vector is then obtained:

$$\mathbf{x_r} = \mathrm{H}\mathbf{x} \quad \Rightarrow \quad x_r = Hx \tag{3.15}$$

The relationship between reduced system state vector x_r and the original system state vector x is defined by H which is a $2n \times 2m$ matrix. The procedure is continued by calculating the relationship between the reduced state vector and the modal vector of the full system as below:

$$x_r = HT^{-1}z \tag{3.16}$$

$$S = HT^{-1} \tag{3.17}$$

$$x_r = Sz \tag{3.18}$$

The reduced state perturbation vector x_r and full system modes *z* are related by matrix *S* which has the same dimension of *H* matrix. To obtain the relation between x_r and reduced modal perturbation vector z_r, the same reduction method that has been applied on A_m matrix will be applied on *S* matrix by ignoring the local modes in the matrix structure and producing the S_r matrix. Then the state equation can be written for the reduced system model:

$$x_r = S_r z_r \tag{3.19}$$

$$\dot{x}_r = S_r A_{mr} S_r^{-1} x_r + S_r (TB)_r u \tag{3.20}$$

$$A_r = S_r A_{mr} S_r^{-1} \tag{3.21}$$

$$B_r = S_r (TB)_r \tag{3.22}$$

$$\dot{x}_r = A_r x_r + B_r u \tag{3.23}$$

Equation (3.23) represents the linearized state equation of the reduced system where A_r matrix is the state matrix of the reduced system and the eigenvalues of this matrix are just representing inter-area and common modes.

3.3 Nonlinear reduced system model with measurement

In this section the procedure for building a nonlinear reduced model and state estimator of equivalent area angles and frequencies is presented. In Section 2 the linear state model is obtained as a result of system dynamic reduction based on coherency for one particular operating point. The linear model is usually applied in small signal dynamic studies while for transient stability analysis a nonlinear model gives more confidence of stability at wide range of operating points. To represent the dynamic reduced system by a nonlinear model, the parameters of the reduced system model including the aggregated machines and reduced system characteristics should be calculated.

The reduced system state matrix A_r should represent a linear multi-machine model similar to the system *A* matrix. Using the classical machine models, the linear state matrix of the original system *A* as in (3.3), consists of four $m \times m$ sub-matrices:

$$A = \begin{bmatrix} A_{11} & A_{12} \\ A_{21} & A_{22} \end{bmatrix} \tag{3.24}$$

Each of the sub-matrices of *A* matrix has specific characteristics. A_{11} is a zero matrix, A_{12} is an identity matrix, A_{22} is a diagonal matrix where its diagonal elements represent the damping over the inertia of machines (D_i / J_i). Submatrix A_{21} has two important characteristic relations between each of its elements a_{ij} as below:

$$\sum_{j=1}^{m} a_{ij} = 0 \tag{3.25}$$

$$a_{ii} = -\sum_{\substack{j=1 \\ j \neq i}}^{m} a_{ij} \tag{3.26}$$

The reduced state matrix A_r must have similar properties to the A matrix as described above, such that it can be represented as four $n \times n$ sub-matrices as $A_r = \begin{bmatrix} Ar_{11} & Ar_{12} \\ Ar_{21} & Ar_{22} \end{bmatrix}$. The sub-matrices should also have similar properties to the sub-matrices of the A matrix. The reduction method in Section 3.2 may results in small errors in the produced A_r matrix but to increase the accuracy of the linear and nonlinear reduced model, a modification is applied on the A_r matrix. We find the smallest variation of the elements of Ar_{21} and Ar_{22} using a least square based method such that these sub-matrices have the similar properties to the ones of the original system. Therefore, the modified Ar_{22} will become a diagonal matrix with the diagonal elements representing the damping over inertia of equivalent generators representing each area $\left(Dr_i / Jr_i\right)$ and the elements ar_{ij} of modified Ar_{21} will have the characteristics as below which are all satisfied with the lowest variation using the least square method:

$$\sum_{j=1}^{n} ar_{ij} = 0 \quad \& \quad ar_{ii} = -\sum_{\substack{j=1 \\ j \neq i}}^{n} ar_{ij} \tag{3.27}$$

This modification may change the eigenvalues and eigenvectors of the A_r matrix. To reduce the possible error, a weighted least square method could be applied based on the sensitivity index of A_r elements to the eigenvalues. According to the

results on test systems, the change in eigenvalues is very small so this sensitivity weighted version of the least square method may not be necessary.

To obtain the parameters required for the nonlinear representation of the reduced system, the linearized classical machine model is expressed as below while the damping ratio is neglected and bus voltages are considered to be very close to each other and around *1 pu*.

$$J_i \Delta\ddot{\delta}_i = -\left(\sum_{\substack{j=1 \\ j\neq i}}^{n} \cos\delta_{ij0} \left(\frac{1}{X_{ij}} \right) \right) \Delta\delta_i + \sum_{\substack{j=1 \\ j\neq i}}^{n} \cos\delta_{ji0} \left(\frac{1}{X_{ij}} \right) \Delta\delta_j \tag{3.28}$$

***While**:* $\cos\delta_{ij0} = \cos\delta_{ji0} \qquad \forall i, j \quad i \neq j$

In (3.28) X_{ij} is the reactance between bus *i* and *j*, and considering this equation for the reduced system, the unknown parameters will be the inter-area admittances and aggregated inertia ratios. The parameter $\cos\delta_{ij0} = \cos\delta_{ji0} = const.$ is defined by linearizing over a known δ_{ij0}. The original *A* matrix is produced by a linearization around the steady state operating point of the system. Therefore, the best assumption for the δ_{i0} of area *i* is the inertia based aggregation as for the stable operating points [37]. In this case δ_{i0} is the steady state operating point of the reduced system as $\delta_{i0} = \sum_{k\in i} J_k \delta_{k0} \Big/ \sum_{k\in i} J_k$ where the steady state angle δ_{k0} for every machine *k* inside area *i* is known.

The inter-area power transfer equation is required along with (3.28) to obtain the unknown parameters of the reduced system. Knowing the steady state power transfer between areas and the aggregated steady state δ_{i0}, the inter-area admittances can be obtained. To define the inter-area power transfer, the border buses and tie-line

should be defined and inter-area power transfer is then calculated based on the prior full system steady state power flow equations. For more accurate calculation of the inter-area power transfer, the power transfer measurement data can be used. The single phase circuit equivalent power flow equation for the inter-area power transfer between area *i* and area *j* is as below:

$$P_{ij} = E_i E_j \sin(\delta_i - \delta_j) / X_{ij} \tag{3.29}$$

In the equation above the equivalent reduced areas are assumed to be connected via lossless lines which are represented by the line reactance X_{ij}. Equation (3.28) is the key part of the sub-matrix A_{21} of the original system and Ar_{21} of the reduced system respectively. Therefore, knowing the variables of this equation as described above and calculating the Ar_{21} matrix, inter-area admittances and aggregated machine inertia ratios can be calculated for the reduced system using the least square method and also considering the power transfer between areas as described by equation (3.29). Having the equal inertia ratio J_i for each area *i*, the damping ratio of the area D_i can be calculated based on the Ar_{22} sub-matrix using a similar least square method. Identifying all the parameters, the nonlinear reduced system model is obtained. The equal load and generation are also considered as the sum load and generation at each area shown in (3.30)-(3.31) for the area i.

$$Pm_i = \sum_{k \in i} Pm_k \tag{3.30}$$

$$Load_i = \sum_{k \in i} Load_k \tag{3.31}$$

The method can combine many different PMU measurements, and provided observability conditions are met, the state estimator can be obtained. Potentially

improved estimation can be found through optimal placement to ensure the best places for PMUs to reflect inter-area modes [84], however local modes may still be visible in the data obtained from the phasor measurement units in large power systems. To overcome this problem, state estimation of the inter-area modes is added to the model described before, based on wide-area measurement in the system such that local modes are suppressed by the estimator. Kalman filtering is one of the best and most accurate state estimation methods which has been widely applied in various aspects of power systems [58, 61]. The Kalman filter needs an explicit representation of noise; therefore, the linearized state equation is extended to form the equations to be applied to the estimator and obtain the Kalman gain:

$$\dot{x} = Ax + Bu + Gw \tag{3.32}$$

$$y = Cx + Du + v \tag{3.33}$$

Equation (3.32) is the extended form of linearized state equation with unbiased process noise w which is related to system state by gain matrix G and equation (3.33) is the output equation which links the measurements in the system with the measurement noise v. These noise parameters are considered as uncorrelated zero mean Gaussian white noises which are defined by their covariances as below:

$$E\{ww^T\} = Q \tag{3.34}$$

$$E\{vv^T\} = R \tag{3.35}$$

The Kalman estimator in stationary operation is designed based on the system state and measurement equations considering the process and measurement noises. For this approach, the process covariance Q is a segmented diagonal matrix where the segment related to velocity states is set to unity to excite these states while other

segments are zero. Equal disturbance is chosen since there is no prior information of whether the disturbance will perturb any particular machine. The measurement noises from PMUs are independent from each other and have similar characteristics; therefore, the measurement noise covariance R is set to be a diagonal matrix. The local mode noise from a system disturbance may be known to have a higher probability at certain measurements and in that case the R matrix element is modified. For this work we take $R = \sigma \times I$ with a comparatively low value for σ to represent an equal effect of local modes.

$$\hat{\dot{x}} = (A\hat{x} + Bu) + L(y - \hat{y}) \quad , \quad \hat{y} = C\hat{x} \tag{3.36}$$

The Kalman estimator in (3.36) represents the system dynamic model considering the measurement data where $\hat{x}$ is the estimation of state vector perturbation, and $\hat{y}$ is the estimation of measurement perturbation. The first part of equation as $(A\hat{x} + Bu)$ predicts the evolution of system state and is updated with the correction term $(y - \hat{y})$ through the filter gain L. The Kalman gain L is calculated for the system based on the system and measurement equations and the correspondent noises.

$$L = MC^T R^{-1} \tag{3.37}$$

$$\dot{M} = AM + MA^T - MC^T R^{-1} CM + GQG^T \tag{3.38}$$

Where M is the covariance of the state estimation error in steady state and is the only positive solution of the algebraic Riccati equation (3.38) when $\dot{M} = 0$. Based on the system reduction procedure described in Section 3.2, Kalman estimator is obtained for the reduced system by neglecting the effect of local modes.

$$\hat{\dot{x}}_r = A_r \hat{x}_r + B_r u + L_r (y - \hat{y}) \quad , \quad \hat{y} = C_r \hat{x}_r \tag{3.39}$$

Equation (3.39) represents the reduced linear dynamic system model with PMU measurement where $\hat{x}_r$ denotes the estimation of reduced state perturbation. As an approach we consider the linear Kalman gain for one operating point can be applied for the nonlinear system which will result in nonlinear system state estimation for the reduced system:

$$\hat{\dot{\mathbf{x}}}_\mathbf{r} = f(\hat{\mathbf{x}}_\mathbf{r}, u) + L_r (\mathbf{y} - \hat{\mathbf{y}}) \quad , \quad \hat{\mathbf{y}} = C_r \hat{\mathbf{x}}_\mathbf{r} \tag{3.40}$$

Based on the equation above, a dynamic nonlinear state estimation for reduced power system based on phasor measurement units is obtained; where $\hat{\mathbf{x}}_\mathbf{r}$ is the estimation of the equivalent area angles and velocities, $\mathbf{y}$ is the measurement from PMUs, and $\hat{\mathbf{y}}$ is the estimation of measurements. This filter describes how to combine PMU measurements in the evaluation of estimation of inter-area modes. Therefore, the inter-area oscillations in a multi area multi machine system with wide area measurement are estimated with substantial reduction of interference by local modes. In the proposed Kalman filter, local modes are considered as noise to be filtered; therefore if the estimator is well designed, the output of estimator ignores local modes and represents only the inter-area modes. This is the basis of the measurement based model of the reduced system.

3.4 Simulation case A - four machine test system

In the first case, the test system is a simple four machine system where the generators are represented by a classical machine model and the transmission lines are represented as constant impedances with zero resistance. For this case, all the

transmission lines are assumed to have a reactance of *0.1 pu* except for line connecting buses 6 and 7 which has the reactance of *0.5 pu* as illustrated in Fig. 3.1.

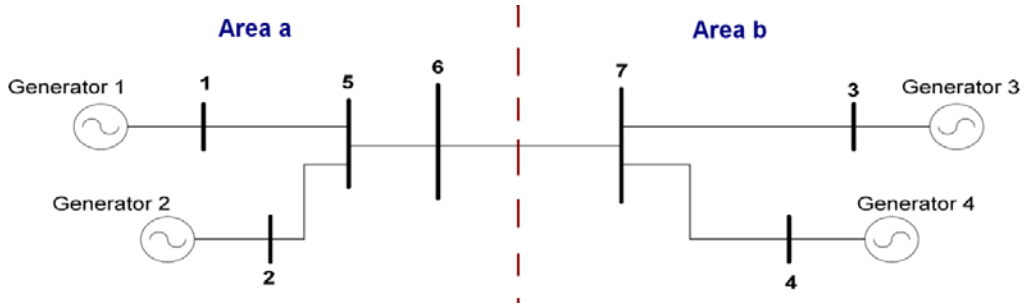

Fig. 3.1 Test case A - four machine two area test system

The value of the *A* matrix can be found from the nonlinear equations by a state perturbation method. The eigen properties of the *A* matrix describe the system behavior and the oscillations of different machines in the case of contingencies. For this study the eigenvalues and eigenvectors of the *A* matrix are calculated and the system is transformed into modal form. From the frequencies and modes shapes this system is found to have two local modes, one for each area, and one inter-area mode as shown in Table 3.1.

Table 3.1 The eigenvalues of test system A

Mode Type	**Eigenvalue**
Local Modes	-0.5401 ± j5.5244
	-0.1783 ± j3.6077
Inter-area Mode	-0.1999 ± j1.2018

This system can be considered as a two area system based on the slow coherency approach. The eigenvector correspondent to the inter-area mode defines the coherency of the generators in the low frequency modes which defines the areas in the system. The normalized inter-area eigenvectors in the system are illustrated in Fig. 3.2 showing the generators in two areas of the test system.

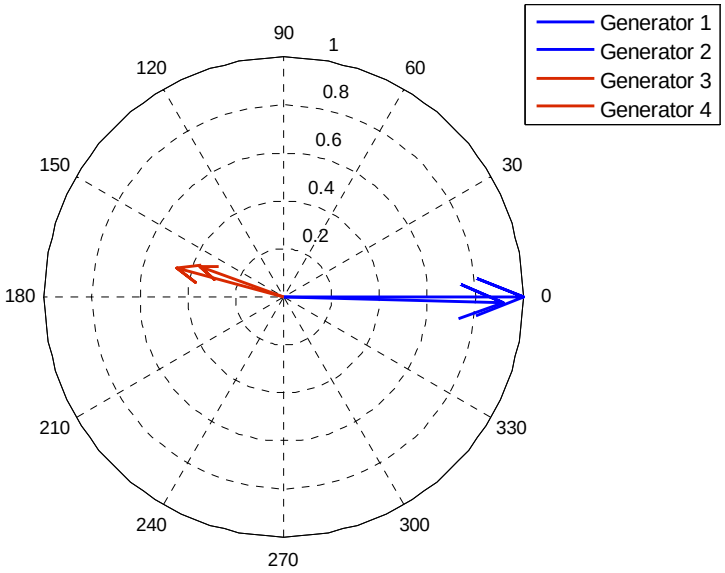

Fig. 3.2 Eigenvectors of inter-area mode of the test system

The reduction method described in Section 3.2 is applied to the system of test case A to obtain the reduced linear model of this system. To obtain the parameters of nonlinear reduced system, the procedure in Section 3.3 is applied such that the system can be represented by two generators each representing a coherent area with a transmission line between them as shown in Fig.3.3. In order to obtain the reduced system parameters the modification described in Section 3.3 is applied to the process. The eigenvalue of the modified reduced system is "-2.0024 ± j1.2018" which implies the change in the inter-area eigenvalue of Table 3.1 is negligible.

Fig. 3.3 Reduced equivalent system

In the next step, the nonlinear Kalman estimator is designed for the reduced system to complete the measurement based reduced model of the system. In this system, the PMUs are considered to be installed on bus 6 and 7 (one measurement at non-generator buses of each area) so the Kalman gain of the reduced system L_r is obtained as described in previous sections. To demonstrate the results of the reduced system, the original system is simulated considering a self clearing fault at bus 5 and the angle oscillations of the generators are illustrated in Fig. 3.4.

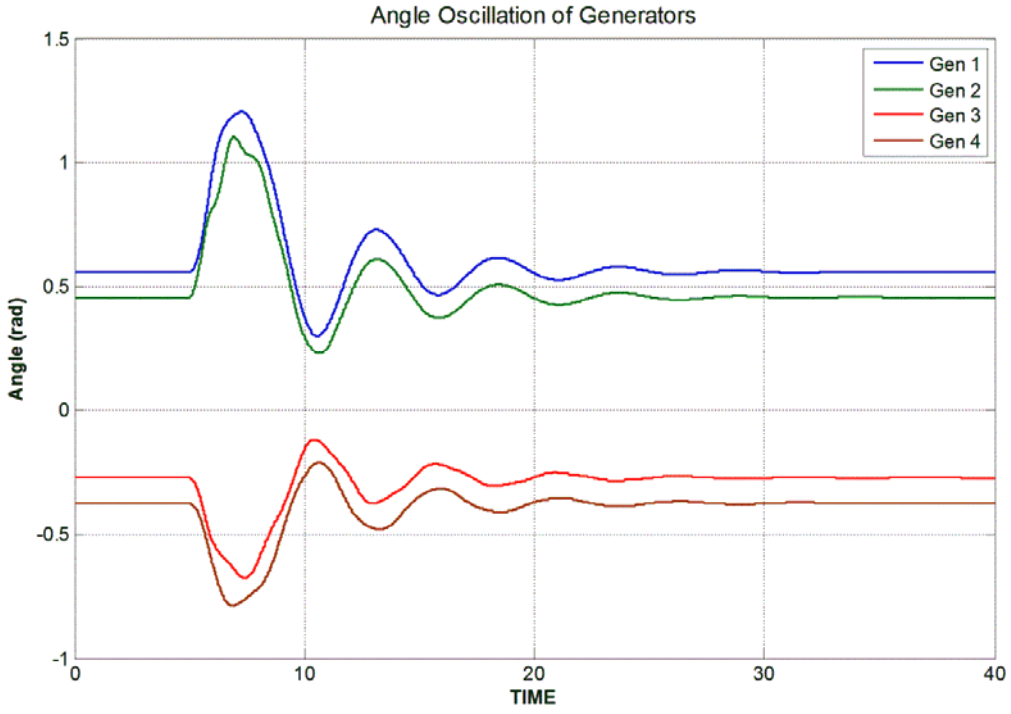

Fig. 3.4 Generator angle oscillations of the original system

The nonlinear Kalman estimator is designed for the reduced system which represents the inter-area oscillations of the system. To show the performance of the estimator, measurement data from installed PMUs is required which is obtained by simulation of the full faulted system. The simulation output of the nonlinear Kalman estimator is illustrated in Fig. 3.5 showing the angle oscillations of the reduced system for the original system fault.

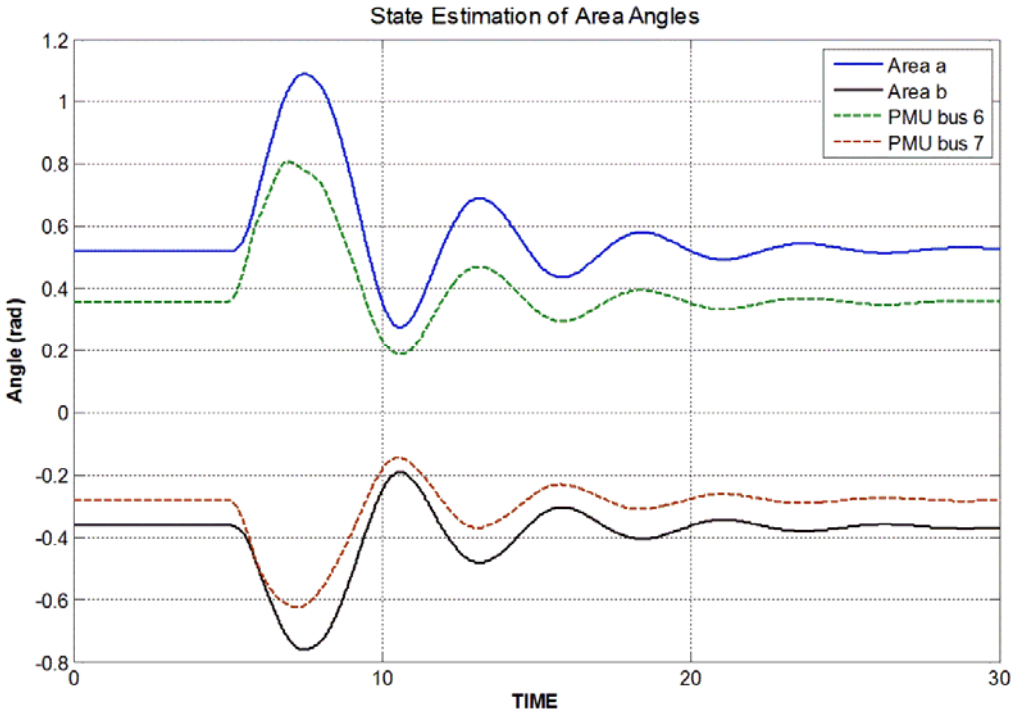

Fig. 3.5 State estimation of area angle oscillations

For comparison, the angle oscillations of the buses with PMU measurement are also illustrated in Fig. 3.5. The results show that, the approach is very effective in estimation of inter-area modes in a multi area system. Despite the presence of local modes in measurement data (particularly from the PMU at bus 6), local modes are not visible in the reduced system estimator output and the results only express the inter-area modes of the system. For another simulation, the system is excited with

another fault at bus 7 and the Kalman filter estimated the angle oscillations of the equivalent reduced system which is illustrated in Fig. 3.6.

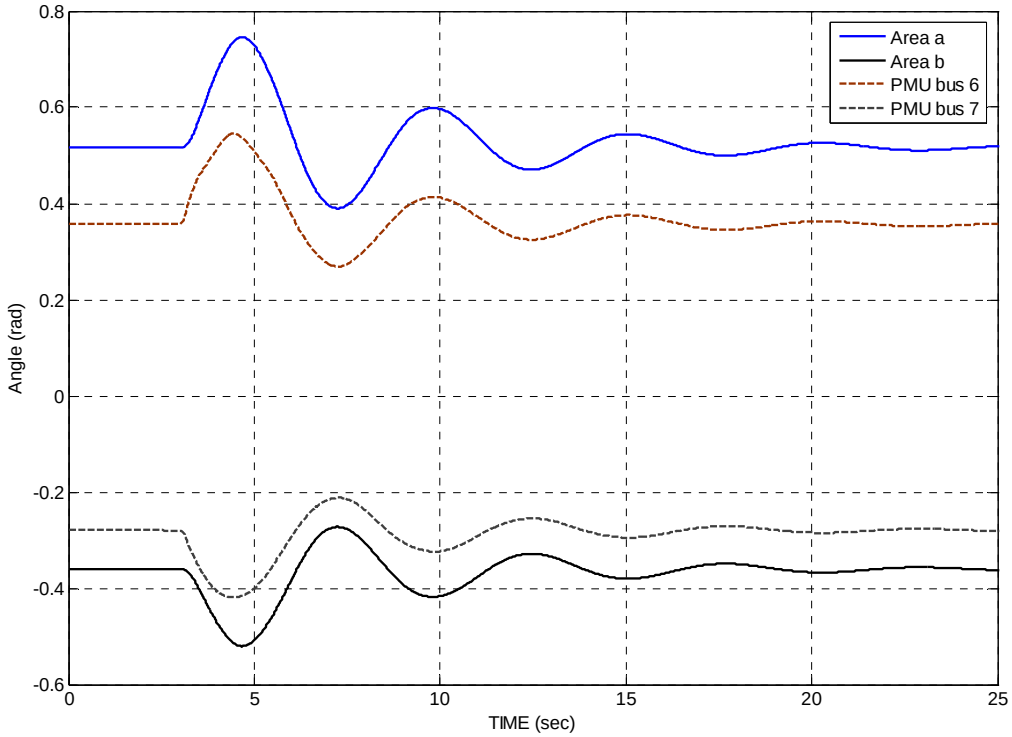

Fig. 3.6 . State estimation of area angle oscillations with the fault on bus 7

Similar to the previous fault case, the PMU measurements which contain local modes are also shown in the figure. It can be seen that the Kalman estimator is very effective by representing only the inter-area oscillations and ignoring the local modes in the estimated area angles.

3.5 Simulation case B - 16 machine test system

To demonstrate the feasibility of the proposed method in large power systems, it is simulated on a more complex test system namely the modified 68 bus, 16 machine system [23]. In order to apply this method, the lines are considered to be lossless and the system loads are modified but general system properties remained

unchanged. Under these operating conditions, this system can be divided into five coherent areas based on the slow coherency approach similar to the test case A as illustrated in Fig.3.7.

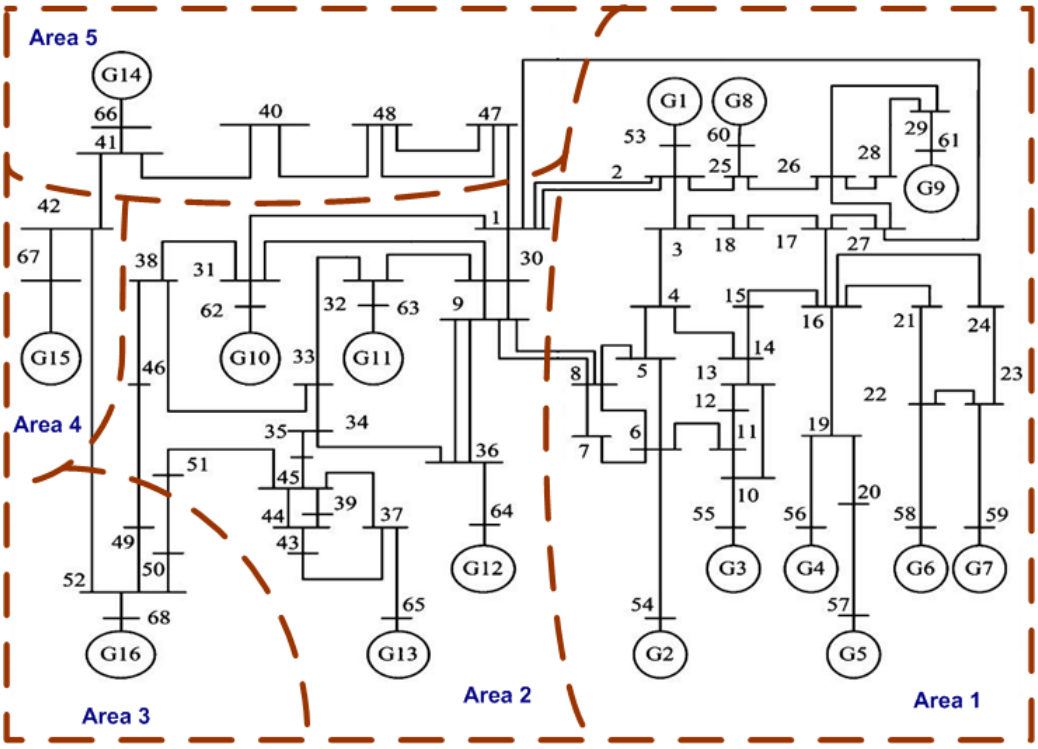

Fig. 3.7 Test system B and coherent areas

The reduction procedure similar to the test case A is performed on this test system and the linear reduced model is obtained. The parameters of the nonlinear reduced system are obtained as described in Section 3.2 and 3.3 such that the system is represented by 5 generators and the connecting link between them based on the area borders shown in Fig. 3.7. The inter-area modes of the original system and eigenvalues of the reduced system are presented in Table 3.2 to show the accuracy of reduction and modification process. To facilitate the reduced nonlinear model for this system, the Kalman estimator is designed considering PMU in each area on buses 11,

15, 24, 32, 36, 41, 42, and 52. . This case specifically considers the effect of multiple PMUs in each area, and the procedure shows how to combine multiple measurements to obtain a single area angle for the reduced system modeling the inter-area modes.

Table 3.2 Comparison between inter-area modes of the original system and the eigenvalues of the reduced system

Original system inter-area eigenvalues	**Eigenvalues of modified A_r matrix**
-0.4380 ± j5.1730	-0.4379 ± j5.1728
-0.3347 ± j4.0153	-0.3339 ± j4.0166
-0.3793 ± j2.9897	-0.3794 ± j2.9895
-0.3743 ± j2.0233	-0.3772 ± j2.0254

The measurement data is obtained by simulating the original system for the designated disturbance. Therefore, the system is simulated for a self clearing fault at bus 21 and angle oscillation of the buses, where PMUs are installed, is illustrated in Fig. 3.8. The nonlinear Kalman estimator is then simulated for the reduced system considering the same fault and using the obtained measurement data to compute the estimation of area angle oscillations as illustrated in Fig. 3.9.

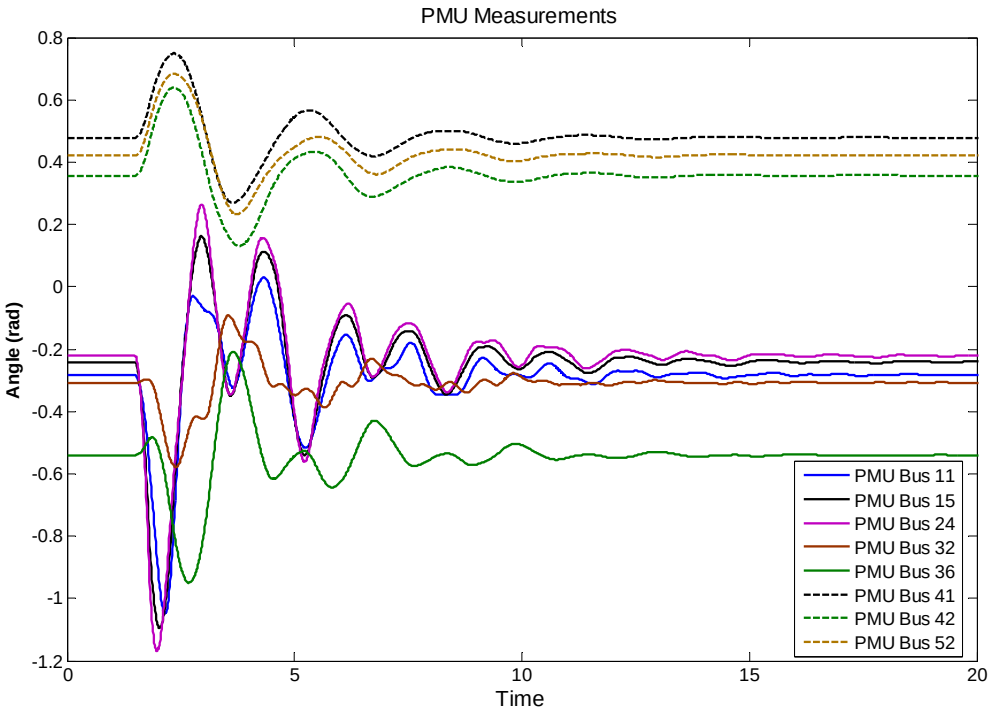

Fig. 3.8 Angle oscillation of the buses with PMU in the original system

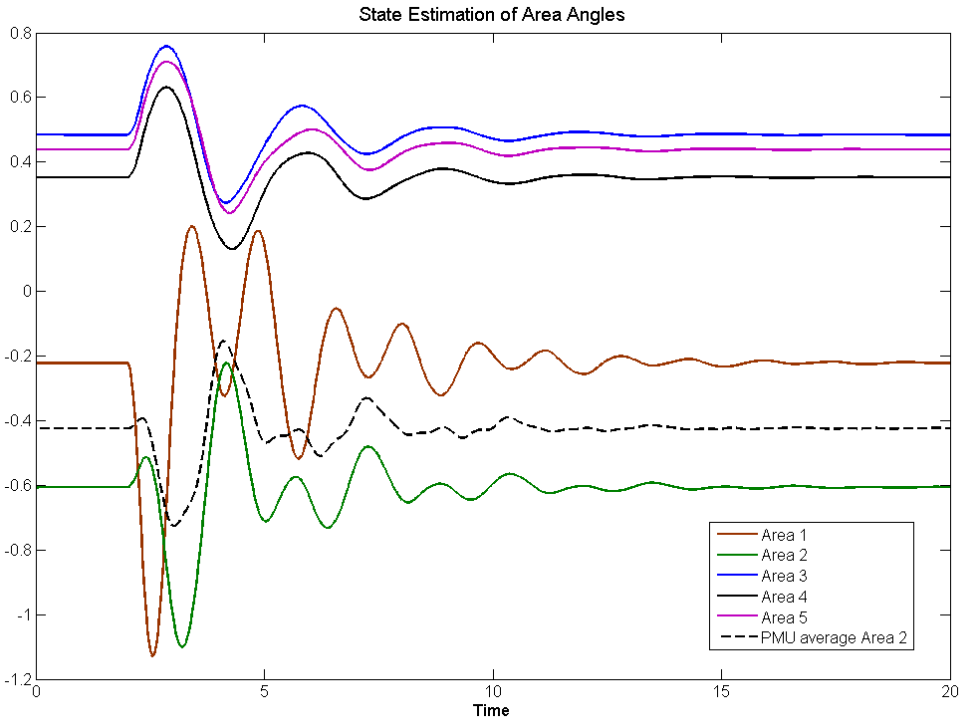

Fig. 3.9 State estimation of area angle oscillations

The results of the nonlinear Kalman estimator show the effectiveness of the proposed method in large power systems as the results express the inter-area oscillations of the test system and all the local modes have been suppressed in the state estimation. In order to decrease the effect of local modes in measurement, PMUs placement design can be performed to find the best buses to install the measurement devices. Although this reduces the effect of local modes in the measurement, presence of these modes in the measurements obtained from PMUs is inevitable. To examine the robustness of the approach, consider a change in the locations and number of PMUs. In each of these cases the Kalman gain for the reduced system will be different, but will yield a correct estimator for the reduced system. One naive approach to estimate area angles is to average the PMU measurements at each area. This however results in visibility of local modes as can be seen for area 2 in Fig. 3.9 while the proposed method shows good performance by ignoring the local modes in the estimated angles. Any frequency estimate obtained from the averaging method would also show an error due to the presence of local oscillation modes.

3.6 Summary

A new approach for estimation of angle and frequencies of coherent areas in large power systems by dynamic equivalents using synchronized phasor measurement units is presented in this chapter. By defining the coherent generators and their related buses based on slow coherency approach, coherent areas within the power systems are identified. The reduction is applied on the system such that each area is replaced by an equivalent generator representing the area and transmission lines by equivalent connections between areas. The aim of this approach is to

develop an estimator based on a reduced model which reflects only the inter-area oscillations of the original system. The parameters of the reduced nonlinear model are obtained using the linear reduced model and the system operating conditions. The nonlinear Kalman estimator is then designed for the reduced system to provide the reduced system state estimator based on phasor measurements. The approach is simulated on two test systems to show the feasibility of this method on both simple and complex networks. The results of the simulation in both cases demonstrate successful reduction of dynamic systems as the results of the nonlinear Kalman estimator only reflect the inter-area oscillations of the systems.

Chapter 4: Identification of Coherent Generators and Areas

4.1 Introduction

In this chapter a new general approach is presented for defining coherent generators in power systems which stay coherent in a wide range of operating conditions. In power system dynamic performance, coherency between generators is an important factor which has several applications including dynamic reduction of power systems and emergency protection and control schemes.

Due to the importance of coherency detection in transient stability and control studies, several methods have been introduced to define the coherent groups of generators and areas in inter- connected power systems [27, 29]. In this chapter, a new method is proposed to find a general grouping of generators based on coherency by providing a distributed disturbance on the network which is applied by low level randomly changing of the load in all of the load buses. In the frequency range of electromechanical oscillations the load changes can be considered as white noise. This process is called as random walk process and has been applied for estimation of modal parameters [85]. The spectrum analysis is then applied on the generator velocity swings to obtain the significant inter-area modes and generator coherency to form the areas in the network. In order to provide a general area detection scheme, load buses related to each area are defined, which leads to detection of boundary buses, lines and the whole system is thus divided into areas. Defining areas for multiple operating points also provides more accurate schemes to facilitate online control of inter-area dynamics.

4.2 Generator coherency and area detection

Defining the areas in large inter-connected power systems consists of two steps, including finding coherent generators which form a group and assigning the non-generation buses to these groups. The generators which have similar behaviour after the disturbances in the systems are called coherent generators and usually the term “coherency” refers to the coherency of generators in the slow inter-area modes. To study the generator coherency a classical machine model is usually considered to be sufficient [26, 40] which is presented in Chapter 3:

In most of the power system transient stability simulations, a disturbance is considered as a fault on a line or bus and the analysis is performed based on the single perturbation of the power system. In this approach instead of single disturbance in the system, the disturbance is distributed within the system to guarantee the excitation of all modes. This has been implemented by low level randomly changing of the load at all load buses which resembles the real load changes in power systems. This load change has the effect of a distributed disturbance in the power system, and will cause the generators to swing in a range of different frequencies related to different oscillation modes.

By applying the mentioned load disturbance, the velocity changes of all the machines in the system can be studied and spectrum analysis is applied to the output velocity of the generators. The Discrete Fourier Transform (DFT) is a common method for spectrum analysis of discrete time signals as shown below:

$$X_f = \sum_{n=0}^{N-1} x_n H e^{-\frac{i2\pi}{N} fn} \quad , \quad f = 0, \ldots, N-1 \tag{4.1}$$

Where X_f is DFT, x_n is the sampled velocity of each generator, N is the number of samples, and H is the window function. The inter-area modes are usually between 0.1 and 1 Hz and depending on the sampling frequency the number of samples should be chosen big enough to ensure all low frequency modes are extracted.

The kinetic energy of machines plays a significant role in the importance of each mode in power systems. By having the kinetic energy of each machine and also the total kinetic energy of the system over the spectrum, the important modes with the higher kinetic energy and low frequency can be considered as the possible inter-area modes. The kinetic energy of machines and total kinetic energy of the system over the spectrum is calculated as (4.2)-(4.3), where $E_i(f)$ is the kinetic energy of each machine and $E_T(f)$ is the total kinetic energy of the system across the spectrum.

$$E_i(f) = 1/2\, J_i \omega_i(f)^2 \tag{4.2}$$

$$E_T(f) = \sum_{i=0}^{n} E_i(f) \tag{4.3}$$

To obtain the kinetic energy of each machine and total kinetic energy of system respectively over the spectrum, the DFT of generator velocities ω_i is calculated by (4.1) and obtained $\omega_i(f)$ s are squared and multiplied by inertia ratio J_i according to (4.2) to define the spectral distribution of kinetic energy of each machine. Then referring to (4.3) the total kinetic energy across the spectrum can be easily calculated by adding the obtained kinetic energy of each generator. Then the obtained total kinetic energy is checked for low frequency to find the important inter-area modes.

As it is seen in the test results, the inter-area modes usually have the low oscillation frequency of 0.1 – 1 Hz while the kinetic energy analysis will also assist in defining inter-area oscillation frequencies. By studying the coherency of generators in the range of inter-area modes, the coherent generators are found and generator grouping is achieved. For the chosen disturbance, the velocity of generators can be considered as the random process and these signals are analysed in the inter-area frequency band. Therefore, the generators velocity signals are low pass filtered using a low pass digital signal filter such as Chebyshev filter to exclude the higher frequency oscillations. In this case for the filtered velocities, signal correlation coefficient is calculated as below:

$$r_{ij} = \frac{\sum_{k=1}^{N} (f\omega_{ik} - \overline{f\omega_i})(f\omega_{jk} - \overline{f\omega_j})}{\sqrt{\sum_{k=1}^{N} (f\omega_{ik} - \overline{f\omega_i})^2 \sum_{k=1}^{N} (f\omega_{jk} - \overline{f\omega_j})^2}} \tag{4.4}$$

Where $f\omega_{ik}$ and $f\omega_{jk}$ are the k th element of filtered velocity signal of machine i and j, $\overline{f\omega_i}$ and $\overline{f\omega_j}$ are the sample means of these signals, and r_{ij} is the correlation coefficient between mentioned velocity signals. The resulting r_{ij} is a real number such that $-1 < r_{ij} < 1$ and its sign shows if the pairs are positively or negatively correlated.

Coherent groups of generators are identified by calculating the correlation coefficients for the low pass filtered velocities of generators as described above. Based on the results for each pair of generators, highly positive correlated generators will define the coherent groups of generators. This method is very efficient in large power systems as highly correlated generators in the inter-area frequencies are considered to form groups. In some cases, some generators may not only correlate

with one group but also have higher correlations with other groups. In such cases and also for more accurate grouping and characterizing inter-area oscillations between areas, further analysis is performed on velocity of generators. To achieve this, the coherence and cross spectral density functions will be applied on the velocity changes of machines [86]. The coherence (magnitude-squared coherence) [87] between two velocity signals related to machine i and j is calculated as:

$$C_{ij}(f) = \frac{\left|P_{ij}(f)\right|^2}{\left|P_{ii}(f)P_{jj}(f)\right|} \tag{4.5}$$

Where $P_{ij}(f)$ is the cross spectral density of velocity of generators i and j, $P_{ii}(f)$ and $P_{jj}(f)$ are the power spectral density (PSD) of ω_i and ω_j calculated as (4.6)-(4.7). It can be inferred that cross spectral density and PSD functions are Discrete Fourier Transforms of cross-correlation $R_{ij}(n)$ and auto-correlation $R_{ii}(n)$ functions which can be obtained by (4.8)-(4.9) where $E\{\}$ is the expected value operator.

$$P_{ij}(f) = \sum_{n=0}^{N-1} R_{ij}(n) e^{-\frac{i2\pi}{N} fn} \quad , \quad f = 0,...,N-1 \tag{4.6}$$

$$P_{ii}(f) = \sum_{n=0}^{N-1} R_{ii}(n) e^{-\frac{i2\pi}{N} fn} \quad , \quad f = 0,...,N-1 \tag{4.7}$$

$$R_{ij}(n) = E\left\{\omega_i(m+n)\omega_j(m+n)^*\right\} \tag{4.8}$$

$$R_{ii}(n) = E\left\{\omega_i(m+n)\omega_i(m+n)^*\right\} \tag{4.9}$$

The coherence function (4.5) defines the coherency of the velocity output of machines across the frequency range and defines how the machines are correlated. This coherence function is not sufficient to define the coherent group of generators as it does not indicate if the generators are positively or negatively coherent in each frequency. To overcome this issue, the angle of cross spectral density function $P_{ij}(f)$ can show the angle that generators are correlated in each frequency at the range of inter-area modes. So if the angle is close to zero the machines are positively coherent and belong to a group and if it is close to 180 degrees, means the machines are negatively coherent for that frequency so they cannot be grouped and belong to different machine groups.

Comparing the coherence functions and cross spectral density angle between pairs of generators, the inter-area oscillation frequency band of every group of generators can be defined. In this approach, the generators in one group are highly and positively coherent with each other in that frequency band, while they are highly but negatively coherent to generators belonging to the other group. Therefore, generators in each area along with the inter-area oscillation frequency between different areas will be defined. This method is also applicable for the generators located in the area boundaries which can have high correlations with both of the neighbouring areas. These generators are checked for the specific inter-area frequency band of two areas to see their relation to each of the generator groups. In this case if the disputed generators are positively coherent at the inter-area oscillation frequency band with all of the generators in a group, these generators can be considered as a part of that group.

To define the concept of general coherency, the load and generation have to be randomly changed for several cases to check the coherency of generators over

different loading scenarios. The purpose is to check if the grouping of generators is robust against the load changes in the system or grouping will change by changing the load in network. It is proven that load changes can affect the coherency characteristics of the power systems. In this case, some generators specially the generators in the boundaries may be swapped between the neighbouring areas.

Defining the coherent generator groups is the essential part of area detection in power systems. The second part will be to identify the non-generator buses located in each area. To determine which load and switching bus should be considered in an area, the angle swing of all load buses are obtained. For this reason, the loads can be considered as constant impedances and by having the generators angle swings the angle swings in load buses are obtained.

$$I = YV \tag{4.10}$$

$$\begin{bmatrix} I_G \\ I_L \end{bmatrix} = \begin{bmatrix} Y_{11} & Y_{12} \\ Y_{21} & Y_{22} \end{bmatrix} \begin{bmatrix} V_G \\ V_L \end{bmatrix} \tag{4.11}$$

$$V_L = Y_{22}^{-1} Y_{21} V_G \tag{4.12}$$

$$\delta_L = angle\,(V_L) \tag{4.13}$$

In the equations above V_G and I_G refer to the voltage and current injection at generators while V_L and I_L are the voltage and current at non-generation buses and Y is admittance matrix of the system.

As the inter-area oscillation frequency bands of neighbouring areas are known, the load buses located in each of the areas can be defined. Similar to the generators, the angle swing in non-generation buses are low pass filtered using a low pass digital

signal filter to include only the low frequency inter-area modes and, signal correlation coefficient is calculated for the filtered angle swings.

$$rl_{ij} = \frac{\sum_{k=1}^{N_l} (f\delta_{ik} - \overline{f\delta_i})(f\delta_{jk} - \overline{f\delta_j})}{\sqrt{\sum_{k=1}^{N_l} (f\delta_{ik} - \overline{f\delta_i})^2 \sum_{k=1}^{N_l} (f\delta_{jk} - \overline{f\delta_j})^2}} \tag{4.14}$$

Similar to (4.4) $f\delta_{ik}$ and $f\delta_{jk}$ are the k th element of filtered angle swing signal of non-generation buses i and j, $\overline{f\delta_i}$ and $\overline{f\delta_j}$ are the sample means of these signals, N_l is the number of non-generation buses, and rl_{ij} is the correlation coefficient between these signals. Calculating the correlation coefficient for the filtered angle swing of non-generation buses, highly positive correlated buses are considered to be in the same area. This method is applicable to large systems to assign highly correlated buses to each area. To exactly define the border lines (lines connecting the areas) and border buses (buses at each end of border lines) coherence function is calculated for each pair of the non-generation buses using (4.6)-(4.9) and replacing the generator velocity ω by angle swing δ_L in the mentioned equations. Each of the neighbour border buses connected through a border line belong to different areas. Therefore, the target is to find the neighbour non-generator buses which are negatively coherent in the inter-area oscillation frequencies and the border lines are obtained consequently.

In some cases same as the generators, it might be difficult to assign some of the non-generation buses to any area. These buses will usually swap between the areas depending on the load and generation changes in the system. Therefore, the border lines and buses may change due to the changes of the load and generation in the system.

4.3 Simulation on test systems 1

The first case is a simple 4 machine test system in Chapter 3 as illustrated in Fig. 3.1 with different generator parameters. The system is considered to be operating in its nominal operating point and the disturbance is applied on the system by randomly changing the loads in load buses. In this case the load change is considered to be a random change with 1% variance at each bus and applied at each time step which is 0.01 sec. As mentioned in previous section, the load change has the effect of continuous distributed disturbance on the system and causes the generators to swing as illustrated in Fig. 4.1 by velocity swings of the generators over a 10 sec period.

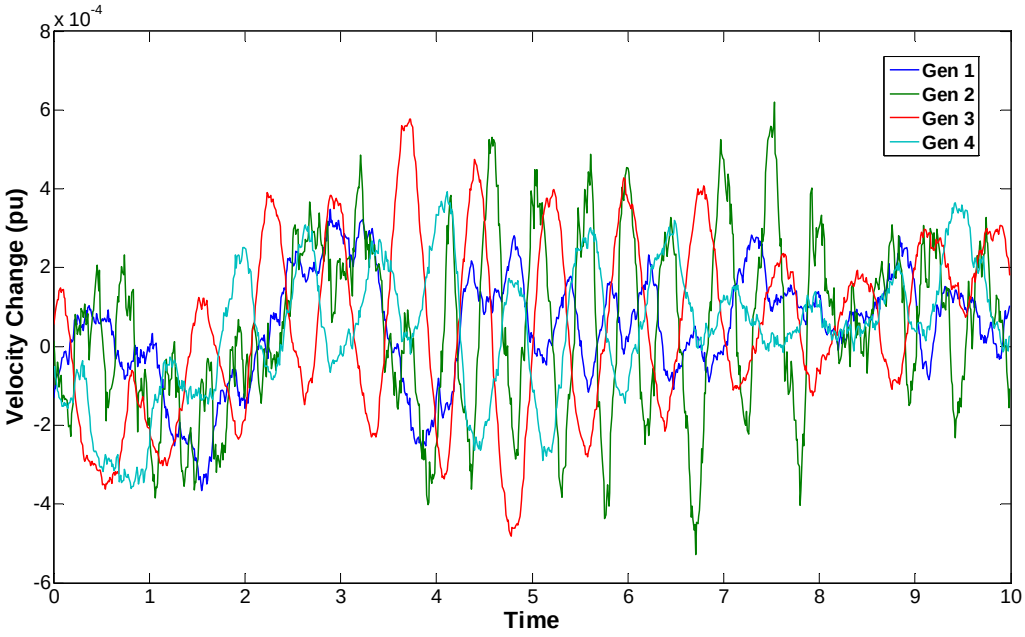

Fig. 4.1 Velocity changes in generators due to the disturbance

To obtain the oscillation frequencies of the generators, spectrum analysis is applied on the velocity output of the generators. The simulation is performed on the

system with a long simulation time and repeated to increase the accuracy of the obtained spectrum. For a more accurate result, DFT is calculated in several time frames and the average results are obtained as the spectrum output of the velocity swings shown in Fig. 4.2 along with the spectrum distribution of kinetic energy of whole system.

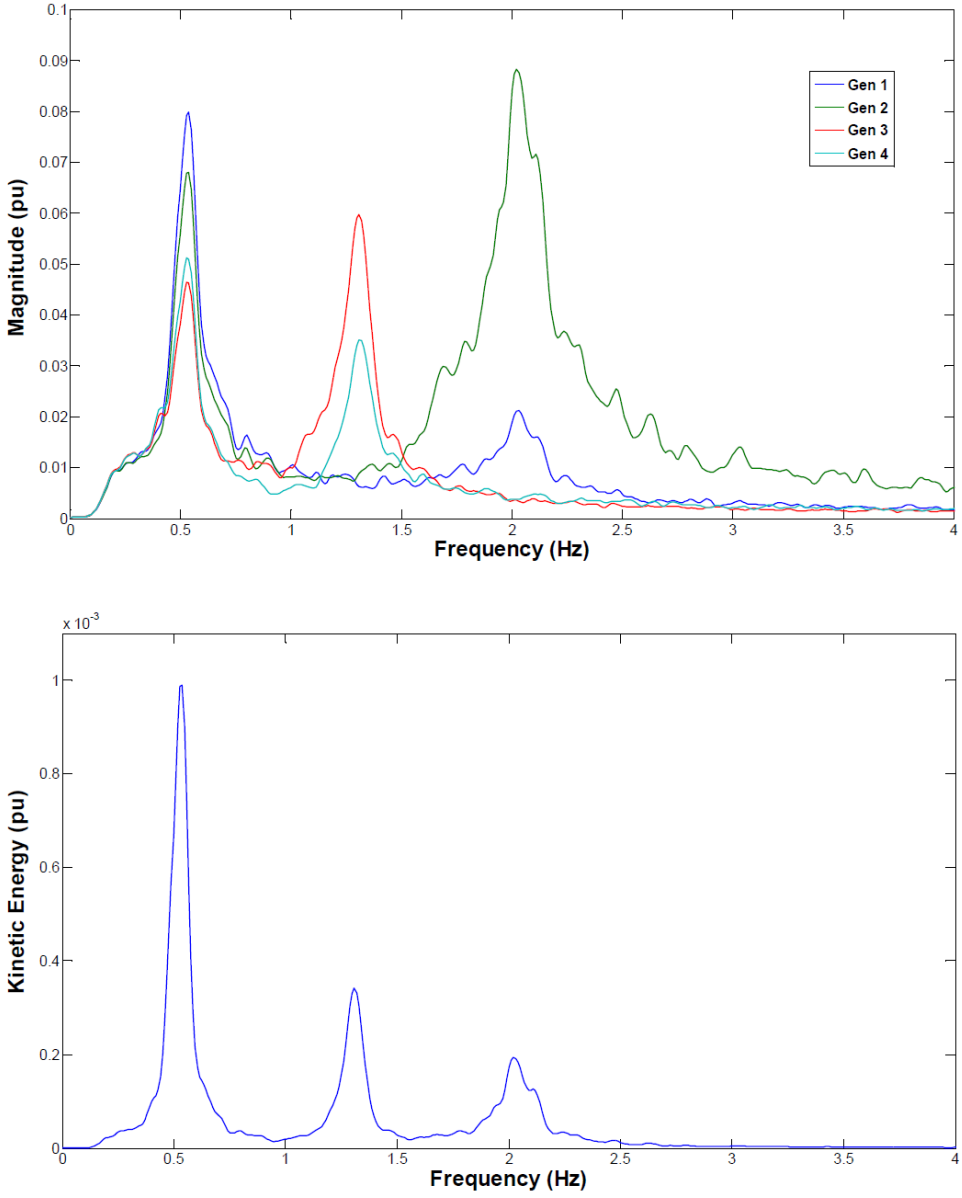

Fig. 4.2 Spectrum analysis of the generator velocity changes; and distribution of kinetic energy of whole system across the spectrum

The kinetic energy spectrum can define the important system oscillation frequencies and for this system three major oscillations can be observed. Inter-area modes usually have the frequency below 1 Hz and this example system has only 1 inter-area mode with the frequency of around 0.53 Hz. By checking the spectrum results of the generators velocity it can be observed that only in the inter-area oscillation frequency all the machines are oscillating while in all other major oscillation frequencies not all of the machines are participating in the oscillations which shows that the mentioned inter-area oscillation frequency is the sole inter-area mode of the system.

The system has only one inter-area mode which means it can be considered as two areas so the next step is to find the generators in each of the areas. Referring to the spectrum analysis, higher frequencies can be filtered from the velocity signals to preserve only the inter-area mode and correlation coefficient r_{ij} for the low pass filtered signals will define the generator grouping in the system which is shown in Table 4.1.

Table 4.1 Correlation coefficient of low-pass filtered generator velocity signals

i , j	r_{ij}	i , j	r_{ij}
1 , 2	0.987	2 , 3	-0.769
1 , 3	-0.788	2 , 4	-0.705
1 , 4	-0.725	3 , 4	0.959

It can be inferred from Table 4.1 that generators 1 and 2 are highly and positively correlated while being negatively correlated to generators 3 and 4 which

means they belong to a same group. Similar result is observable for generators 3 and 4 which means these two generators are also forming a group. To clarify the grouping as mentioned in section 2, the coherence function and the angle of cross spectral density between pairs of generators are calculated as the generator in same groups are highly and positively coherent in the inter-area frequency band. The results are illustrated in Fig. 4.3.

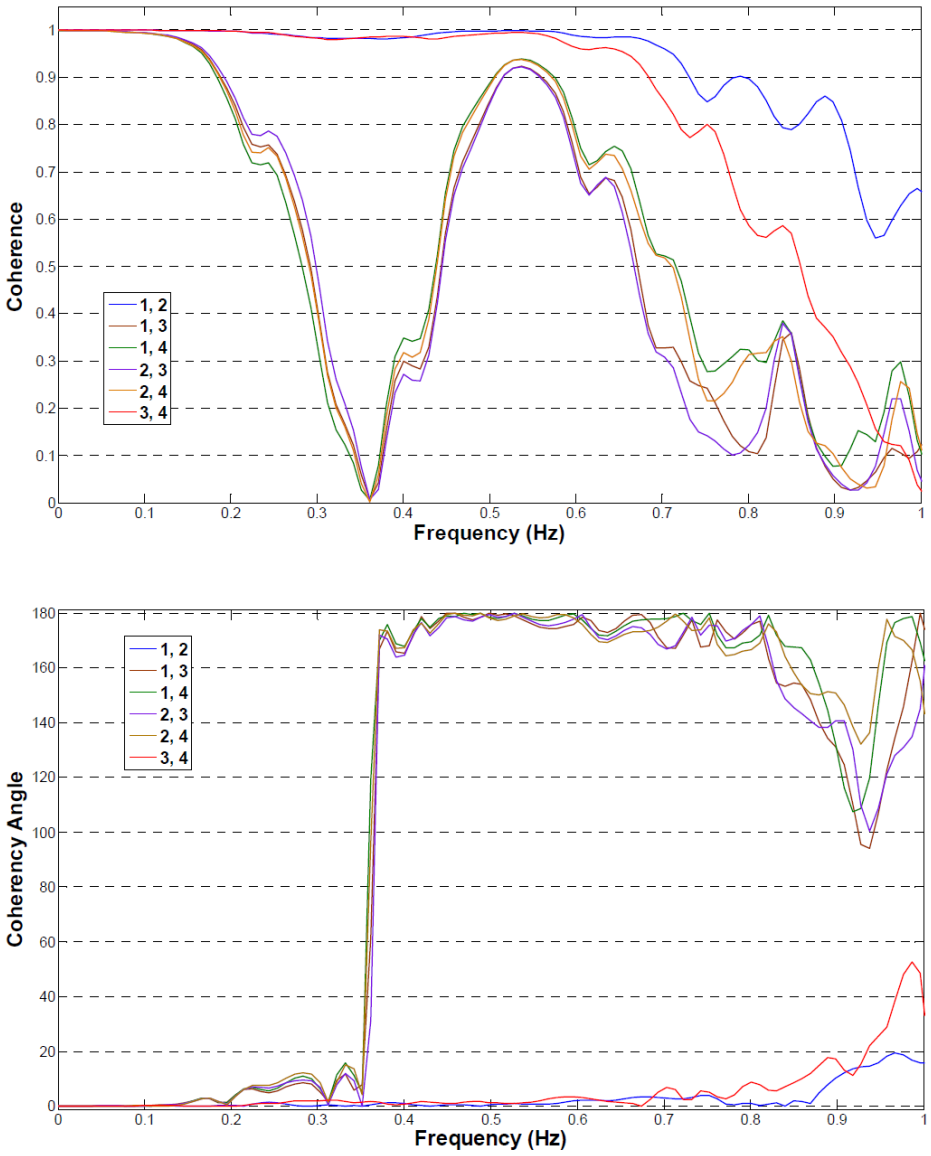

Fig. 4.3 Magnitude-squared coherence and angle of coherency between pairs of generators in test system 1

The coherency results also validate the grouping obtained previously as it can be observed from Fig. 4.3 only the generator groups 1, 2 and 3, 4 are highly and positively coherent in the inter-area frequency band which is around 0.53 Hz. These results also show that at the inter-area frequency, machines belong to other groups are highly but negatively coherent which validated the defined inter-area frequency to be the inter-area mode of system. Both of the proposed methods resulted in the same solution and defined the coherent group of generators. The next step is to define the load buses in each area and boundary buses between areas which will lead into finding the boundary lines connecting the areas.

This system consists of two neighbouring areas with one inter-area mode with the frequency of approximately 0.53 Hz. The angle swings in all of the non-generation buses are calculated using (4.10)-(4.13) and filtered to preserve only the inter-area frequency band. The correlation coefficient (4.14) is then calculated for these filtered signals and highly correlated non-generation buses are defined to be included in each area as shown in Table 4.2.

Table 4.2 Correlation coefficient of low-pass filtered angle swings of load buses

i , j	rl_{ij}
5 , 6	0.999
5 , 7	-0.969
6 , 7	-0.960

It can be inferred from the results in Table 4.2 that load buses no. 5 and 6 are highly and positively correlated in the inter-area frequency band which means they

belong to the same group while they are highly and negatively correlated with bus no. 7. The buses 6 and 7 are neighbour buses and as they are negatively correlated they can be called border buses and the line connecting these two buses as border line. In this case calculating the coherency function for the angle swings might not be necessary as the correlation results defined the load bus grouping with a high accuracy.

4.4 Simulation on test systems 2

In the second case, the proposed method is simulated and tested on a more complex system containing 68 bus and 16 machines In order to apply this method and run the simulations, the system loads and line impedances are modified to accelerate the simulation process but general system properties remained unchanged.

The system is operating at a stable operating point and in this case the simulation is performed using random load deviation of 2% of the load amount at load buses at each time step which is considered to be the same as previous case. This random load change disturbs the system as the distributed disturbance and the generators will swing similar to the case 1. The velocity swing of the generators over a 20 sec period is illustrated in Fig. 4.4.

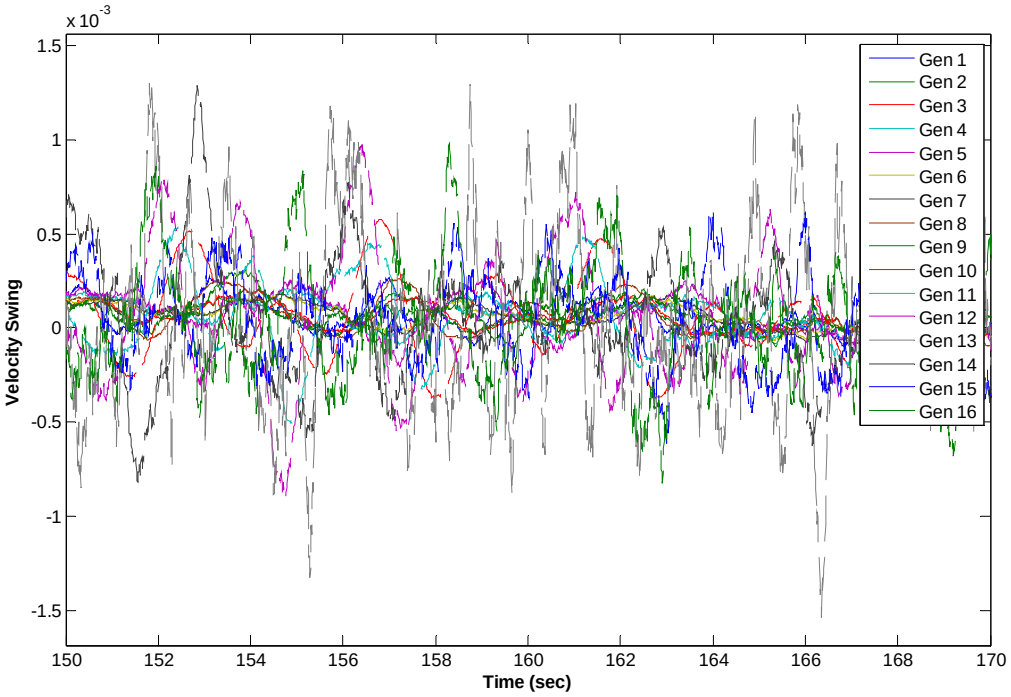

Fig. 4.4 Velocity swing in generators due to the disturbance

Running the simulation for a long simulation time, the oscillation frequencies of the generators can be obtained by applying the spectrum analysis on the obtained generator velocity changes. The average DFT is calculated for several simulation time frames similar to the previous case to obtain the spectrum analysis of the generator velocities which is illustrated in Fig. 4.5 along with the distribution of total kinetic energy of system across the spectrum.

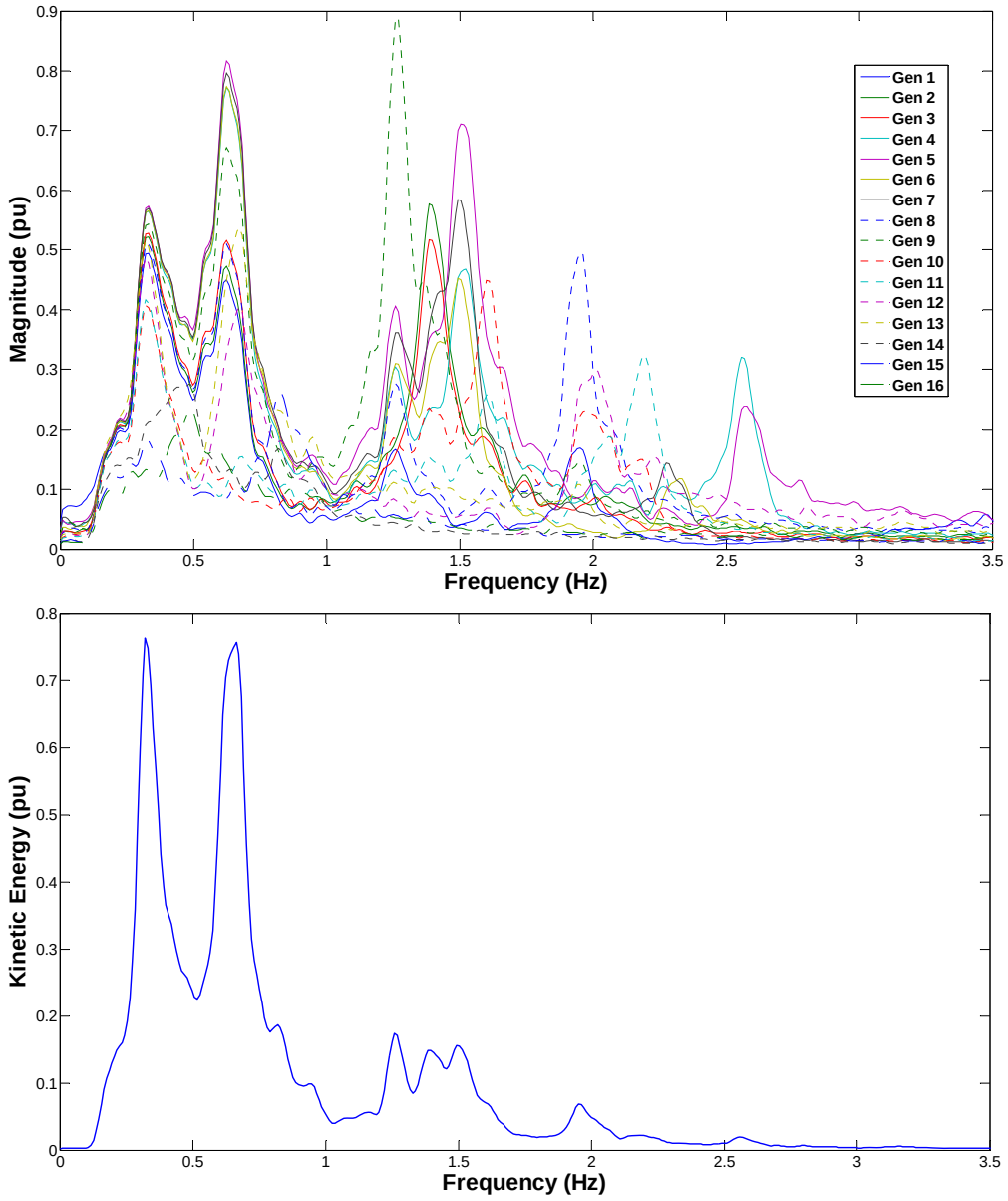

Fig. 4.5 Spectrum analysis of the generator velocity changes; and distribution of kinetic energy of whole system across the spectrum in 16 machine system

The kinetic Energy spectrum shows the important and high energy low frequency inter-area oscillations which are mostly below 1 Hz. Unlike the previous case, it is not easy to find the inter-area frequencies based on the kinetic energy spectrum. The velocity spectrums of most generators show higher frequency

oscillations in the range of 1- 1.5 Hz and regardless of frequency and lower energy, these oscillations might be considered as inter-area modes. Therefore for more accurate assumption about the range of inter-area frequencies more analysis is required on the velocity signals.

Considering the inter-area modes to be in the range of below 1 Hz, the velocity signals are low pass filtered to exclude all the higher frequencies. The correlation coefficient is then calculated for every pair of these filtered signals to find the highly correlated signal which is given in Table 4.3.

Table 4.3 Correlation coefficient of low-pass filtered generator velocity signals for 16 machine test system

i / *j*	**1**	**2**	**3**	**4**	**5**	**6**	**7**	**8**
1	**X**	1.00	1.00	0.96	0.95	0.97	0.96	1.00
2	1.00	**X**	1.00	0.96	0.95	0.96	0.96	0.99
3	1.00	1.00	**X**	0.97	0.96	0.98	0.97	1.00
4	0.96	0.96	0.97	**X**	1.00	1.00	1.00	0.97
5	0.95	0.95	0.96	1.00	**X**	0.99	0.99	0.96
6	0.97	0.96	0.98	1.00	0.99	**X**	1.00	0.98
7	0.96	0.96	0.97	1.00	0.99	1.00	**X**	0.98
8	1.00	0.99	1.00	0.97	0.96	0.98	0.98	**X**
9	0.98	0.97	0.98	0.98	0.97	0.98	0.98	0.99
10	0.83	0.84	0.81	0.67	0.65	0.67	0.67	0.80
11	0.67	0.68	0.64	0.47	0.45	0.48	0.46	0.63
12	0.33	0.34	0.30	0.10	0.07	0.10	0.09	0.28
13	0.21	0.22	0.17	-0.03	-0.05	-0.03	-0.04	0.16
14	0.13	0.11	0.11	0.08	0.08	0.08	0.08	0.12
15	0.00	-0.01	-0.01	-0.02	-0.02	-0.02	-0.02	-0.01
16	-0.06	-0.07	-0.07	-0.08	-0.08	-0.08	-0.08	-0.06

i / *j*	**9**	**10**	**11**	**12**	**13**	**14**	**15**	**16**
1	0.98	0.83	0.67	0.33	0.21	0.13	0.00	-0.06
2	0.97	0.84	0.68	0.34	0.22	0.11	-0.01	-0.07
3	0.98	0.81	0.64	0.30	0.17	0.11	-0.01	-0.07
4	0.98	0.67	0.47	0.10	-0.03	0.08	-0.02	-0.08
5	0.97	0.65	0.45	0.07	-0.05	0.08	-0.02	-0.08
6	0.98	0.67	0.48	0.10	-0.03	0.08	-0.02	-0.08
7	0.98	0.67	0.46	0.09	-0.04	0.08	-0.02	-0.08
8	0.99	0.80	0.63	0.28	0.16	0.12	-0.01	-0.06
9	**X**	0.71	0.53	0.16	0.03	0.09	-0.02	-0.07
10	0.71	**X**	0.97	0.79	0.70	0.19	0.04	0.04
11	0.53	0.97	**X**	0.91	0.86	0.16	0.04	0.05
12	0.16	0.79	0.91	**X**	0.99	0.09	0.03	0.00
13	0.03	0.70	0.86	0.99	**X**	0.07	0.02	-0.02
14	0.09	0.19	0.16	0.09	0.07	**X**	0.34	0.03
15	-0.02	0.04	0.04	0.03	0.02	0.34	**X**	0.22
16	-0.07	0.04	0.05	0.00	-0.02	0.03	0.22	**X**

Based on the calculated value of r_{ij} in the table above, it can be inferred that generators 1 to 9 are highly and positively correlated in the mentioned frequency range which means they can be considered as a group. Generators 11 to 13 also have a high correlation and can be considered as another group of generators. The correlation coefficients related to machines 14 to 16 are not significantly high and these generators can not be grouped with any of other machines. The only remaining machine is generator 10 which has a high correlation with both of the defined

generator groups but as it has a higher correlation with its neighbouring machine 11 we can consider it as a part of second group. This classification is based on the low pass filtered signals for the frequencies below 1 Hz while by changing the frequency cut off band for several cases from 1 to 1.5 Hz the general grouping did not change.

For a more accurate grouping especially for the generators that have high correlation with generators in two groups, the coherence function and the angle of cross spectral density between pairs of generators are calculated. The generators belong to the same area are highly and positively coherent in the range of inter-area frequency band. Therefore, the disputed generators can be checked for the inter-area oscillation frequency of the two groups so these generators will be assigned to the group of generators which are highly and positively coherent with them for that frequency. The results of coherence function and the angle of cross spectral density between selected pairs of generators are illustrated in Fig. 4.6.

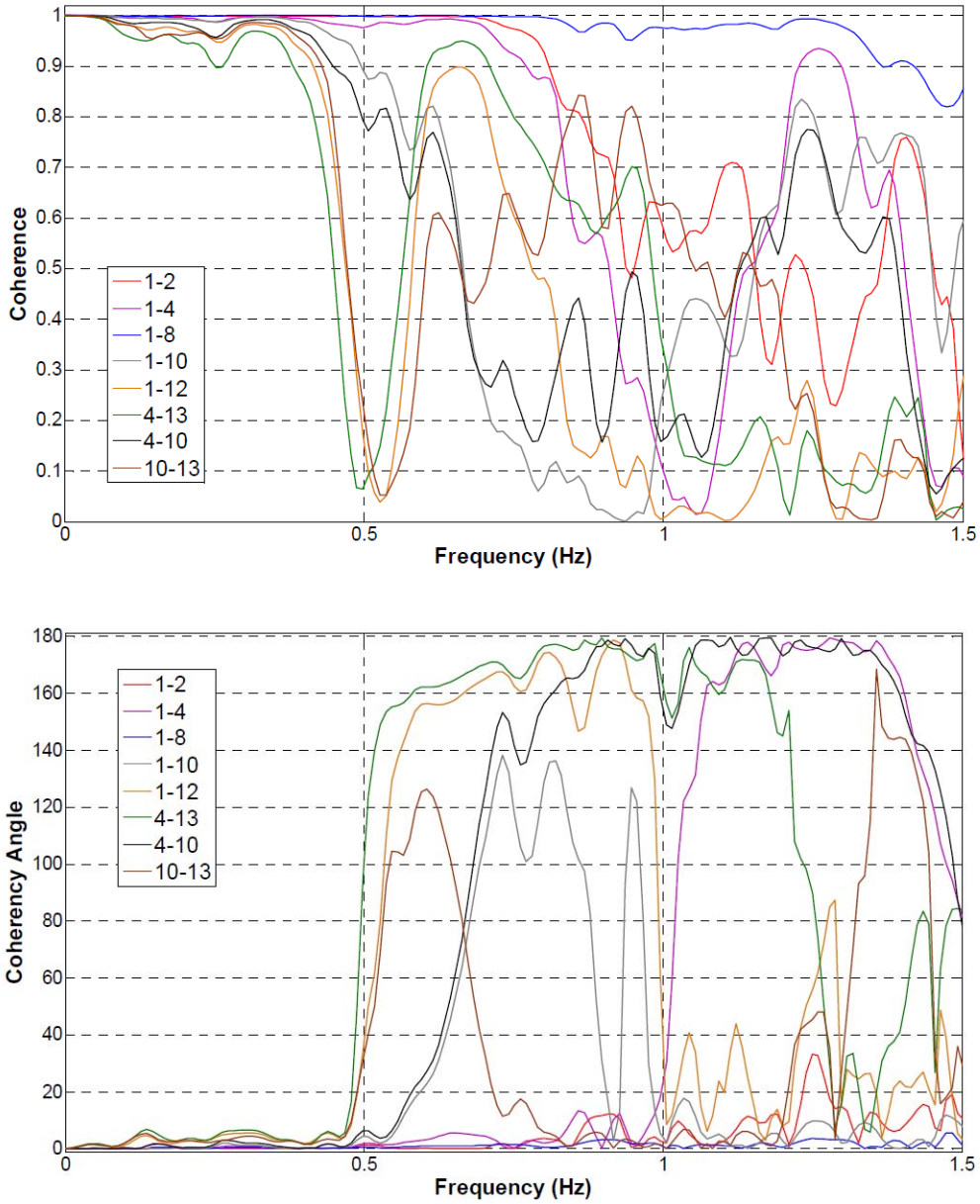

Fig. 4.6 Coherence and angle of coherency between selected pairs of generators in test system 2

The result of the coherency analysis provides useful information about the system grouping and inter-area oscillation frequency range. It can be inferred that generators which are assumed to be in the same group based on the previous results, are not highly and positively coherent for the frequencies more than 1 Hz. Therefore, no big group of generators can be found to be coherent in the frequencies over 1 Hz

which means those frequencies are not in the range of inter-area modes. Furthermore, the results provide more accurate results for the boundary generators which were difficult to be assigned to a group such as generator number 10 in this case. Based on the results shown in Fig. 4.6, machines 1 to 9 and 11 to 13 are oscillating against each other with the frequency around 0.62 Hz and in that frequency generator 10 has higher coherency with the first group while having higher coherency in other frequencies in the range of inter-area modes with the second group. Therefore, machine 10 is highly coherent with both of the groups and depending on the oscillation mode it can be assigned to one of the two groups.

By defining the coherent groups of generators the next step is to find the load buses in each area and boundary buses and lines between the areas by analysis the angle swing of non-generator buses as described in previous section and case 1. The angle oscillation of selected non-generator buses is illustrated in Fig. 4.7 where the mean of the signal is subtracted from recorded data for to focus on the oscillations.

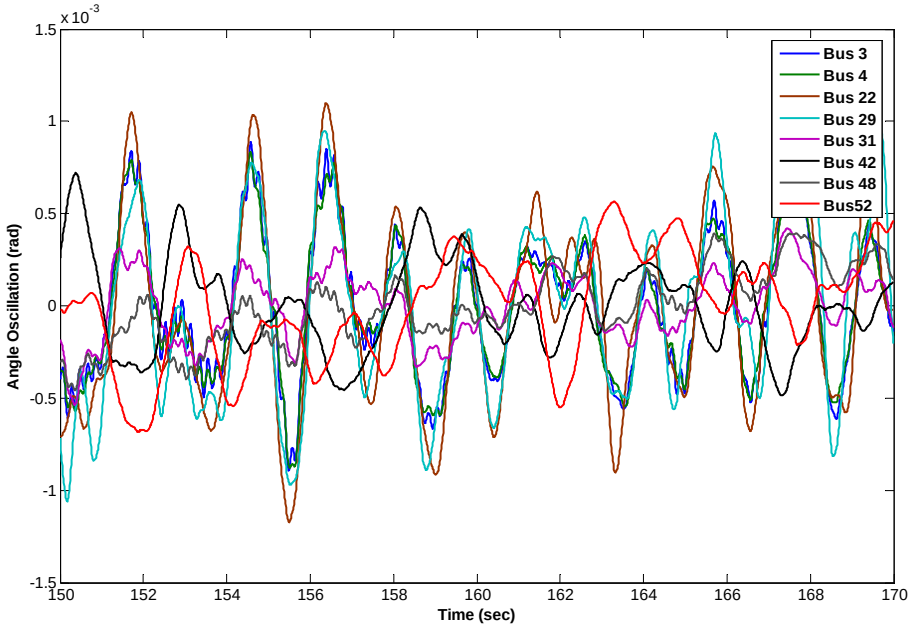

Fig. 4.7 Angle oscillation of selected non-generator buses

Low pass filtering the angle swing signals for the inter-area frequency band, the correlation coefficient is calculated so highly and positively correlated buses can be assigned to the same group. The results provide a general grouping for load buses while for the buses located in the boundaries the coherency analysis should also be applied to provide the accurate grouping and defining boundary buses and lines.

Based on the machine grouping and the results of correlation between filtered angle swings of load buses, the buses with high and positive correlation coefficient are assigned to be in the same group. The coherency results help to find the boundary buses based on the inter-area oscillation frequency between neighbouring areas. In this case, the pair of neighbour non-generator buses with highly and negative coherence in the range of inter-area frequency of the two areas are considered as boundary buses and the line connecting them as the boundary line. Similar to defining the generators in each group, finding the neighbour load buses with negative coherency might not be easy and some buses might be disputed to be in either of the areas. In such cases instead of considering the neighbour buses the penetration is increased to search for the buses with one or two buses between them to find the boundary buses. Therefore by finding these kinds of boundary buses, the load buses between them are not assigned to any group where we call them mid-area buses. This usually happens for the load buses located next to or very close to the disputed machines such as machine 10 in this case. In Fig. 4.8 the result of system grouping for generators and load buses is illustrated.

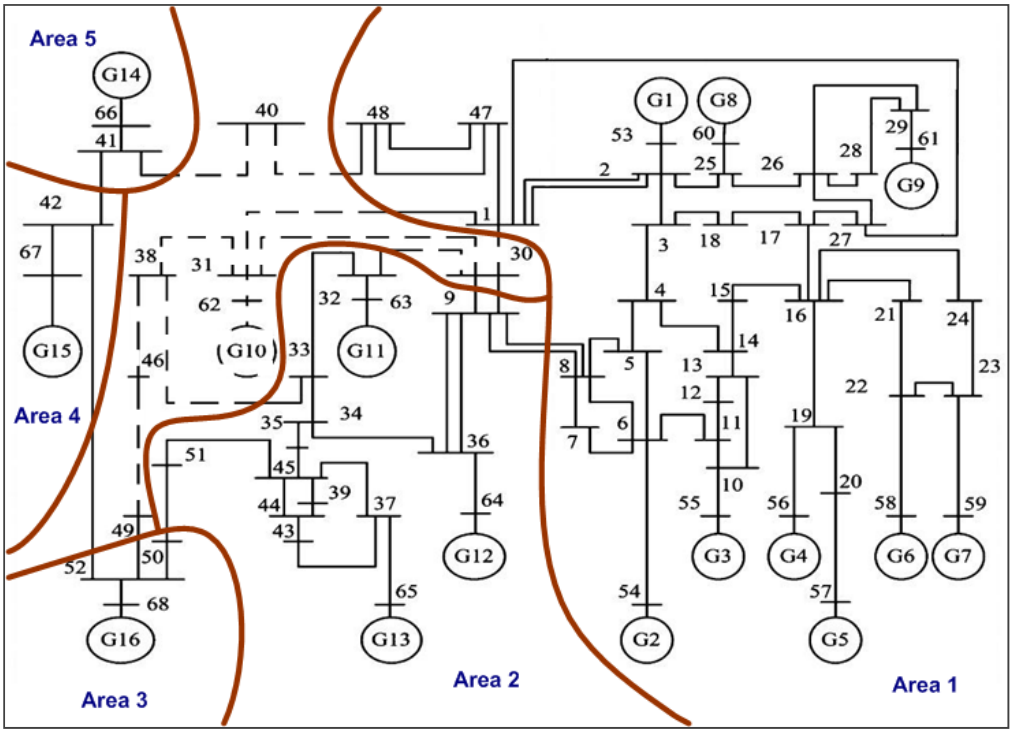

Fig. 4.8 Generator grouping and defined areas for 16 machine test system

4.4.1 Changing the operating point

The proposed area detection process, similar to other methods, finds the generator grouping and area borders for a specified load and generation level. To provide a more general approach, the system steady state load and generation is examined for several cases with values selected over a range of up to 30% change to the original operating point and in each case the area definition process described above is followed. The results show that, generators and buses which had very high correlation still remain together regardless of which steady state load and generation case is selected, but the generators and buses which are not highly correlated to any area such as generator 10 may swap from one area to another area depending on the load change. The result of generator coherency and area detection for a different

operating point of test case 2 is illustrated in Fig. 4.9 showing few changes comparing to the previous results. For real systems, some sets of load and generation levels can be defined and the area definition process can be applied for each of these levels to have a clear and more accurate vision of system behaviour which is applicable in system reduction and online control schemes of inter-area modes.

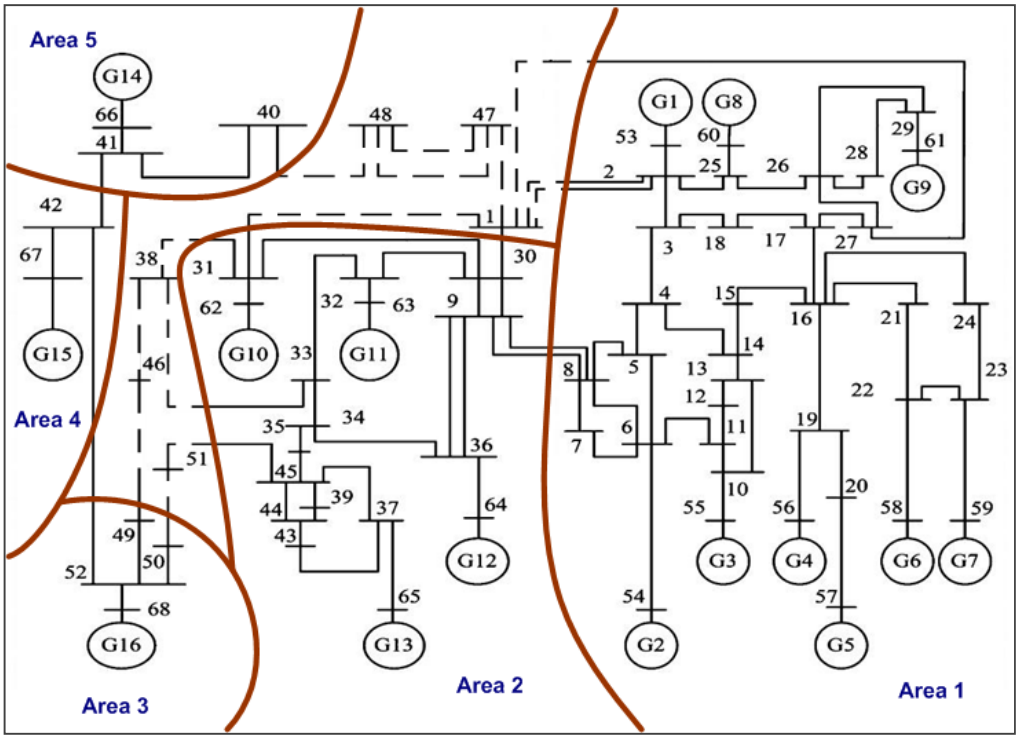

Fig. 4.9 Area detection for a different operating point in case 2

4.5 Summary

In this chapter a new approach is proposed for detecting coherent generators and defining their related non-generator buses to form areas in inter-connected power systems. The method applies random load changes as a distributed disturbance on the system and spectrum analysis on velocity changes of generators is performed to

obtain coherent generators in low frequency inter-area modes. Similar spectrum analysis is applied on the angle swing of load buses to obtain the related load buses to each group of generators and form the areas in the network. This method is applied on two test systems to validate the approach and show the feasibility and applicability of the approach in various simple and complex networks. The results shows that in complex networks it might not be possible to fully divide the system into coherent group of areas and some generators and load buses may swap between neighbor areas by changing the operating point of the system. Applying the method on several realistic operating points of a system the results shows very similar grouping of generators. By changing the operating point the general grouping does not change but the boundary generators and buses (those not assigned to any area) may be grouped with the neighbour areas. The multiple operating point approach provides more accurate representation of generator grouping and area detection in large power systems. Therefore, as a general approach the generators and buses which do not stay coherent in most of the realistic loading conditions should be modelled separately or as separate areas which is an important issue in the aspect of control of inter-area modes.

Chapter 5: Online Identification and Estimation of Equivalent Area Parameters and States

5.1 Introduction

In this chapter an approach is proposed for obtaining nonlinear area-based equivalent models of power systems to express the inter-area oscillations using synchronized phasor measurements. The process is based on the idea mentioned in Chapter 3 and 4 where multi machine power systems can be represented as multi area systems based on the coherency in the inter-area modes. Identification of the unknown parameters is an essential part of study on unknown systems. Besides due to the changes in the system operating conditions, continuous identification of important system characteristics such as loads is inevitable [50, 88]. State estimation as mentioned in Chapter 3 along with identification can provide a real time outcome for desired dynamics of large power systems.

The aim of this chapter is to provide an equivalent dynamic model to represent the inter-area dynamics of inter-connected power systems. Unlike the system reduction procedure described in Chapter 3, the parameters of the reduced model are identified by processing online PMU data. In order to represent the areas by dynamic equivalents the coherency of generators and areas must be valid in a wide range of operating conditions which is guaranteed by application of area detection approach

described in Chapter 4. The nonlinear state estimator is then designed for the reduced dynamic model to represent the angle and frequency of the areas. Several methods have been proposed for estimation of inter-area dynamic [20, 21], while in the proposed approach a Kalman filtering based method is applied for identification and estimation of equivalent area angles and frequencies.

5.2 Identification of coherent areas and reduced system parameters

In this section the procedure for reduction of coherent areas and identification of the reduced equivalent model of inter-connected power systems is presented. In order to reduce the system, coherent generators and their correspondent non-generator buses need to be defined. To make the aggregation less sensitive to any change of operation conditions, the approach described in Chapter 4 is applied to find the coherent areas in power systems. Based on this approach, random variations in all loads are applied as a disturbance to guarantee the uniform excitation of all modes and spectrum analysis is performed on the velocity and angle oscillations of generators and load buses to find the inter-area oscillation frequency band and the coherent generators and load buses. Therefore, the power system can be divided into areas which stay coherent in a wide range of operation conditions. The interactions between coherent areas can be represented by a set of simple equivalent machines and their connections as shown in Fig. 5.1.

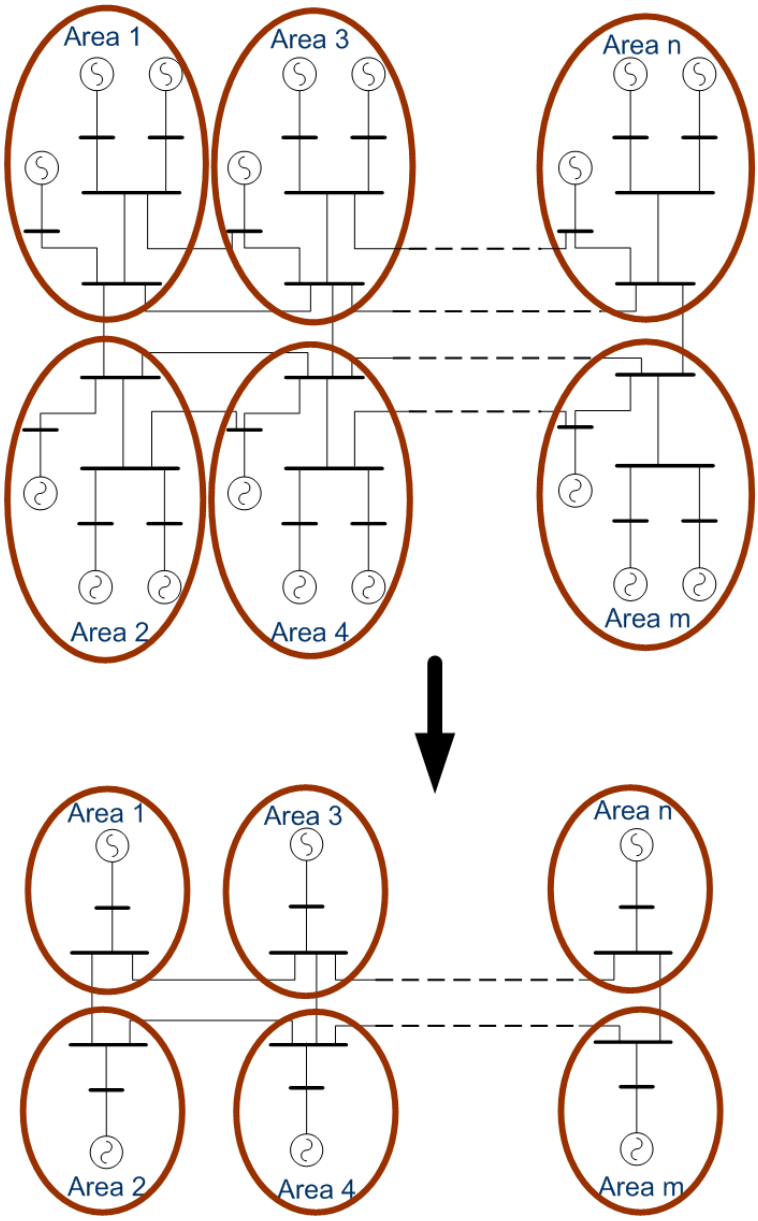

Fig. 5.1 Representation of a multi area system by equivalent generators

Equivalent generators can be represented by classical machine model and the acceleration of each equivalent machine is then described as below:

$$\ddot{\delta}_i = \frac{P_i}{J_i} - \sum_{all\ lines\ to\ i} E_i E_j \frac{\sin(\delta_{ij})}{J_i X_{ij}} - \frac{D_i}{J_i}\dot{\delta}_i \qquad (5.1)$$

Where δ_{ij} is the angle difference between equivalent areas, P_i is the difference between load and power generation in area *i*, X_{ij} is the line reactive impedance, D_i and J_i are the damping and inertia of each equivalent generator, and E_i is the generator voltage. For short time periods, the change of load demanded by customers is unpredictable. Therefore, the change of load can be modelled as white noise which implies the load can be then represented as the integral of white noise. If we take the difference between subsequent samples of these terms at a sample rate for low noise of inter-area modes, the difference of the load power contribution can be expressed as white noise w_i:

$$diff(\ddot{\delta}_i) = \frac{1}{J_i} w_i - \sum_{all\ lines\ to\ i} E_i E_j \frac{1}{J_i X_{ij}} diff\left(\sin(\delta_{ij})\right) - \frac{D_i}{J_i} diff(\dot{\delta}_i) \tag{5.2}$$

The advantage of this expression is that the unknown load term in (5.1) is reduced to additive white noise which means the identification of the acceleration can be expressed as:

$$diff(\ddot{\delta}_i) = -\left[diff\left(\sin(\delta_{i1})\right)\ \ diff\left(\sin(\delta_{i2})\right)\ \ldots\ diff\left(\sin(\delta_{in})\right)\ \ diff\left(\dot{\delta}_i\right)\right]\theta_i + \frac{w_i}{J_i} \tag{5.3}$$

$$\theta_i = [\alpha_{i1}\ \alpha_{i2}\ \ldots \alpha_{in}\ \beta_i]^T \tag{5.4}$$

Considering the area voltage to be close to *1 pu* $\alpha_{ij} = 1/J_i X_{ij}$ and $\beta_i = D_i / J_i$. Since the term $\frac{w_i}{J_i}$ is an additive white noise the estimate of θ_i can be obtained using the classical least square method. By estimation of θ_i for each area, α_{ij} and α_{ji} are obtained which implies the ratio between equivalent inertias $\frac{J_i}{J_j}$ can be identified. In

order to initiate the identification process the PMU measurements in each area are combined to obtain the area angles. The angle representing area *i* is considered to be the centre of inertia angle of area; therefore the relationship between the area angles and measurements is obtained using a number of data samples as below:

$$\delta_i = \sum_{k \in i} J_k \delta_k \Big/ \sum_{k \in i} J_k \tag{5.5}$$

$$\delta r = \Gamma \mathrm{y} \tag{5.6}$$

$$y = C_r x_r \tag{5.7}$$

Where y is the measurements, δr is the vector of area angles, Γ is the relationship between area angles and measurements in the area, x_r is the reduced system states representing area angles and frequencies, and C_r represents the relationship between reduced system states and measurements. To initiate the identification process and also to obtain the relationship between measurements and area angles, the PMU data should be filtered to reduce the effect of local modes. The inter-area frequency band is obtained for the system using the kinetic energy of the system across the spectrum while the system is disturbed by random load changes. Here the low frequency modes with higher kinetic energy can be considered as the inter-area modes.

$$E_T(f) = \sum_{k=1}^{m} 1/2 \, J_k \omega_k(f)^2 \tag{5.8}$$

In the equation above, $\omega_k(f)$ is the angular velocity of each machine and $E_T(f)$ is the total kinetic energy of the system across the spectrum. This process is completed prior to the online identification along with area detection process as mentioned above. In order to identify all the parameters of the reduced system, the

power transfer between at least two areas should be measured. To define the inter-area power transfer, the border buses and tie-line can be defined as a result of area detection approach. Therefore by installing power measurement devices on the links between boundary buses the power transfer between areas can be measured. Although power measurement can be performed on any inter-area link, installing these devices on the links with dominant inter-area mode can reduce the error. Knowing power transfer between areas and equivalent area angle differences, the inter-area admittances can be identified using power transfer equation as below:

$$X_{ij} = E_i E_j \sin(\delta_{ij}) / P_{ij} \tag{5.9}$$

Where P_{ij} is the power transfer between area *i* and area *j*, E_i and E_j are the equivalent generator voltages which are considered to be very close to *1 pu*. The inter-area admittance X_{ij} is identified using the sampled power and angle data which leads to identification of J_i and D_i based on the identified θ_i . The identification of all parameters is performed over the period of *T* which consists of at least 500 samples and the nonlinear state estimator is then designed based on the identified reduced model.

5.3 Nonlinear dynamic state estimation of the reduced system

The inter-area interactions are observed by phasor measurement units which are installed throughout the system. Visibility of local modes in the data obtained from PMUs is not desirable as it will lead into incorrect identification and estimation of the reduced area based model. To reduce the effect of local modes on the

estimation of equivalent area dynamics, a nonlinear Kalman filter is designed such that area angles and frequencies are estimated based on PMU measurements.

$$\dot{\hat{x}}_r = f(\hat{x}_r, u) + L_k(y - \hat{y}) \quad , \quad \hat{y} = C_r \hat{x}_r \tag{5.10}$$

Equation (5.10) is representing the state estimation of equivalent angles and frequencies of the reduced areas. Where $\hat{x}_r$ is the estimation of reduced system state vector, $\hat{y}$ is the measurement estimation, $f(\hat{x}_r, u)$ is the nonlinear function representing the identified reduced system model and L_k is the gain of the Kalman estimator at operating condition *k*. The Kalman gain matrix is calculated for the linearized model of the reduced system across the operating condition considering the local modes as noise in the measurements:

$$\Delta \dot{x}_r = A_k \Delta x_r + G_k w \tag{5.11}$$

$$\Delta y = C_r \Delta x_r + D_k w + v \tag{5.12}$$

Where A_k, G_k, and D_k denote the usual state and output equation matrices at the operation condition *k*, the term *w* is the process noise, and *v* summarizes the effect of local modes as the measurement noise. The actual measurement noise in PMU signals is very low which can be neglected and the only remaining noise will be the effect of non-interarea modes in the measurement data. The noise parameters are supposed to be Gaussian white noise with zero means and covariances as:

$$E\{ww^T\} = Q \tag{5.13}$$

$$E\{vv^T\} = R \tag{5.14}$$

$$E\{vw^T\} = N \tag{5.15}$$

The Kalman gain at each operation condition L_k is calculated based on linearized system state (5.11)-(5.12) and noise sequence characteristics (5.13)-(5.15). The process and measurement noises are assumed to be uncorrelated which means *N* is a zero matrix and the covariance matrices *Q* and *R* are diagonal defined as below:

$$Q = \begin{bmatrix} 0 & 0 \\ 0 & I_{n\times n} \end{bmatrix} \tag{5.16}$$

$$R : \begin{cases} R_{aa} = \sigma_a \\ R_{ab} = 0 \quad a \neq b \end{cases} \tag{5.17}$$

The submatrix related to the velocity states in *Q* matrix is set to unity as an equal disturbance on these states, since there is no prior information of whether the disturbance will perturb any particular machine or area. The PMU measurements and correspondent noises are independent from each other and have similar characteristics, but, the noise of local modes from a system disturbance may have different probability at each measurement. To simplify the representation of measurement noise, the diagonal elements of *R* can be considered as equal with a low value for $\sigma_a = \sigma$ to represent an equal effect of local modes. More accurate representation of measurement noise can be obtained by modifying *R* matrix considering different probability of local modes at each measurement point. The covariance of the modified *R* matrix can be obtained by applying the random load change as described in Chapter 4. To reduce the effect of particular modes on the measurement data, the PMUs are assumed to be installed on non-generator buses. The spectrum analysis is applied on the angle oscillation signals of the load buses and the covariance of local mode noise is obtained for each load bus

The gain of the Kalman estimator at each operating point is then calculated following the equations below:

$$\dot{P}_k = A_k P_k + P_k A_k^T - P_k C_r^T R^{-1} C_r P_k + G_k Q G_k^T = 0 \tag{5.18}$$

$$L_k = P_k C_r^T R^{-1} \tag{5.19}$$

Where P_k is the steady state error covariance of the estimation and the only positive solution of the algebraic Riccati equation (5.18). The Kalman gain L_k is obtained for each operating condition and applied to nonlinear state estimator (5.10) which is the dynamic nonlinear model estimation for reduced power system based on phasor measurement units. The Kalman estimator defines the combination of PMUs in each area to express the area angles and frequencies. Since the area angles and frequencies represent only the inter-area interactions in the power system, the output of Kalman filter must represent only the inter-area modes while ignoring the local modes.

In practice, multiple phasor measurement units are installed in each area to increase the accuracy of measurement. The loss of any PMU may result in inaccurate identification and estimation of area angles and frequencies. To overcome this problem the Kalman gain is calculated for several scenarios considering unavailability and loss of different PMUs so the Kalman estimator will continue to work properly by applying an instantaneous change in the estimator if any PMU is lost.

The Kalman estimator is designed to be updated online by the change in the operation conditions of the systems via updating the reduced system model which may result in the change of the Kalman gain matrix. As an improvement, the PMU based estimator of area angles and frequencies can be used to update the estimates in

the nonlinear parameter identification described in Section 5.2 to reduce the error in the identification process. Therefore, the approach will provide an online estimator which is updated through the live identification of system parameters as shown in Fig. 5.2.

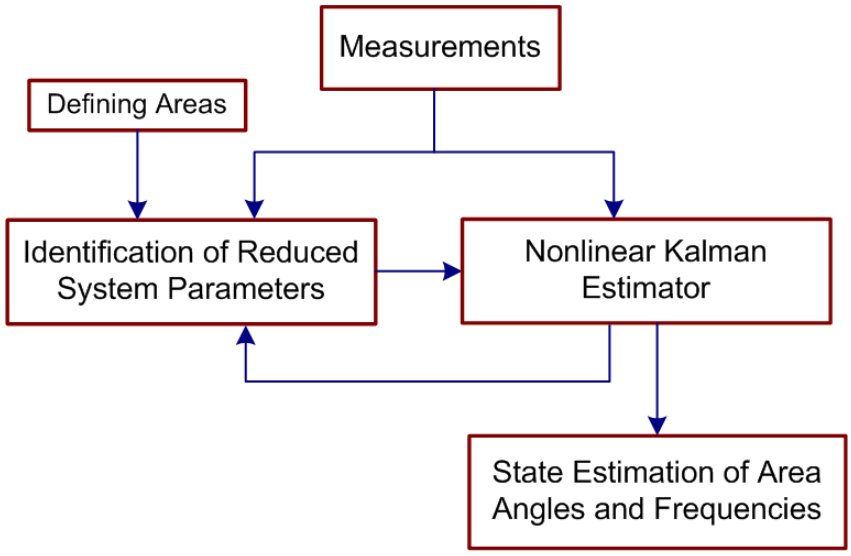

Fig. 5.2 Identification and estimation of area angles and frequencies

5.4 Simulation results

The identification and estimation approach is simulated on two test systems to show the feasibility of the proposed methods on various system types.

5.4.1 Four machine- two area system

The approach is simulated on a four machine two area system with classical generator models as Chapter 4. All transmission lines are assumed to have negligible resistance and loads are modeled as constant impedances. This system can be considered as a two area system regardless of operating conditions. To simulate the real time operation of system, a random load change of up to 3% variance at each

time step is applied to load buses and the angle oscillations of PMU buses are observed. In this system PMUs are installed on non-generator buses namely buses 5, 6, and 7 and to observe the angle oscillations without interference from particular modes that may be highly excited on generator buses. The angle oscillation at these buses resulting from a random walk perturbation is illustrated in Fig. 5.3.

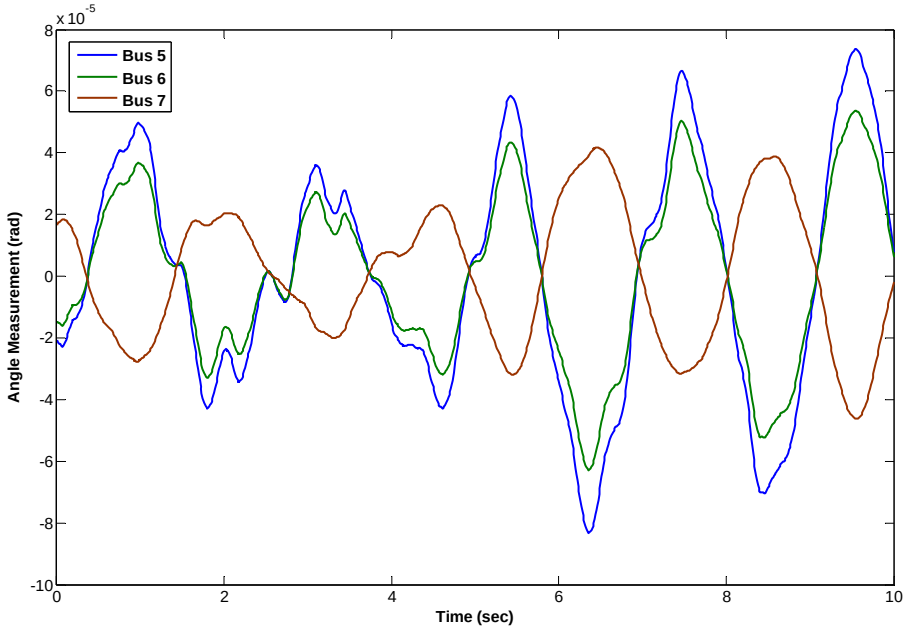

Fig. 5.3 Angle oscillation of PMU buses

In Fig. 5.3, the mean of each measurement is subtracted from recorded data for a clearer observation on angle oscillation of PMU buses. It can be observed that buses 5 and 6 are oscillating against bus 7 with the inter-area frequency, while higher frequency local modes also have significant presence in the recorded angle measurements due to the random walk load disturbance applied to the system. The power measurement unit is considered to be installed in the inter-area link between bus 6 and 7 and the identification process described in Section 5.2 is applied on the system to identify the parameters of the area based reduced system. The parameters of the original system and the identified parameters are given in Table 5.1.

Table 5.1 The parameters of the original and identified reduced system

	Original System	Reduced System
Inertia (J)	0.160 , 0.200 0.040 , 0.120	0.271 , 0.193
Damping (D)	0.060 , 0.060 0.060 , 0.060	0.108 , 0.102

The comparison between inter-area eigenvalues of the original and reduced systems as presented in Table 5.2 demonstrates less than 0.1% error in the frequency and damping ratio of eigenvalues which shows the accuracy of the identified parameters.

Table 5.2 Eigenvalue comparison of the original and identified reduced system

	Inter-area Eigenvalue	Frequency (Hz)	Damping Ratio
Original System	-0.2411 ± j2.7155	0.4322	0.0881
Reduced System	-0.2423 ± j2.7166	0.4324	0.0888

Based on the initial reduced system identification and representation of local modes as measurement noise, the Kalman filter is designed for estimation of area angles and frequencies. The Kalman gain at the current operating condition L_k is calculated as described in Section 3 applying different noise covariance for each measurement. Considering the PMU sampling frequency of 50 Hz, the identification and state estimation is updated every 20 seconds to ensure the accuracy of the approach. To show the effectiveness of the proposed identification and state estimation process, a simulation is performed on the system by applying a disturbance and the estimation of angle and frequency oscillations is illustrated in Fig. 5.4 for two cases with different operating conditions and PMU availability.

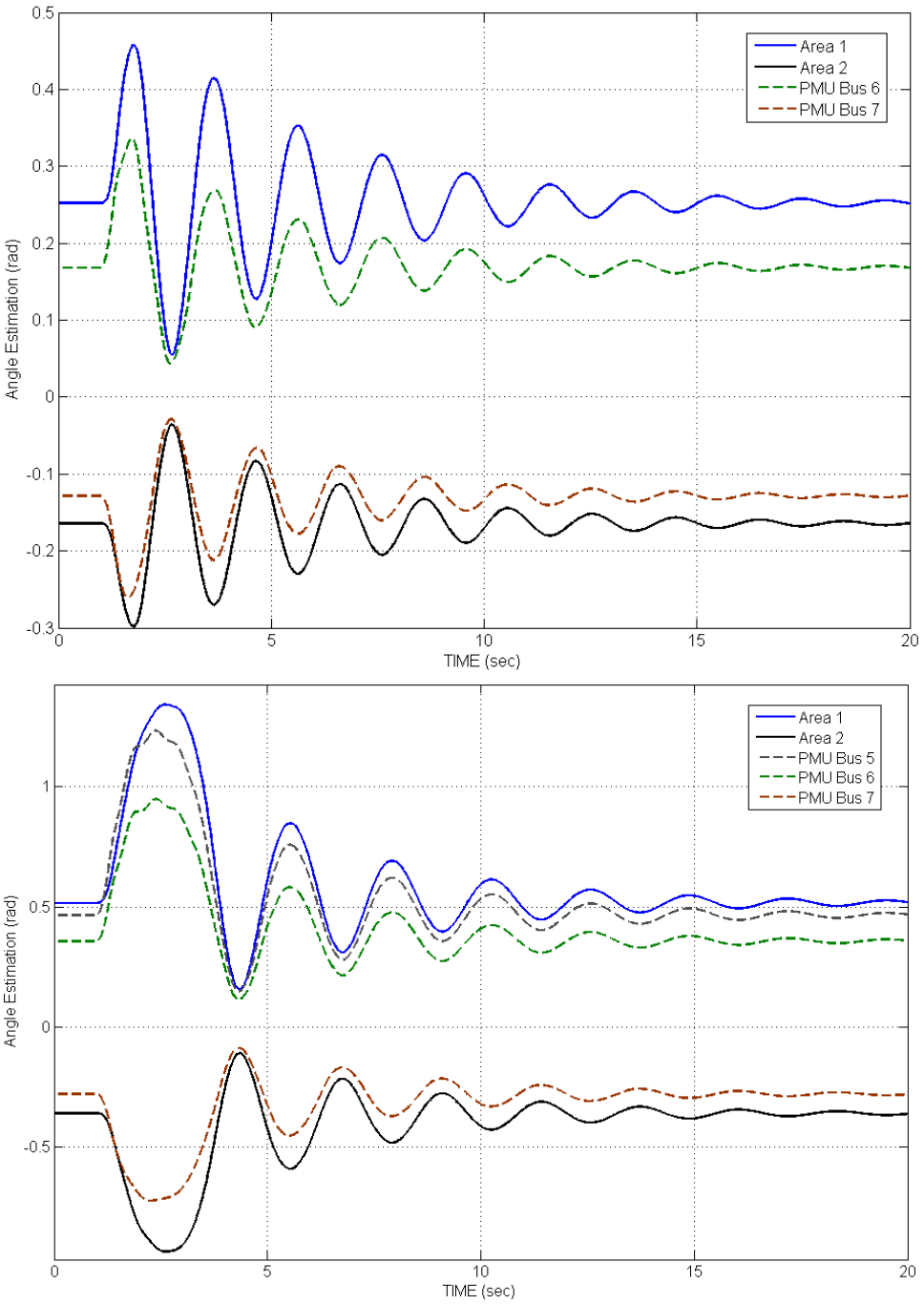

Fig. 5.4 State estimation of area angle oscillations for two operating conditions with two and three PMUs

The observation of angle oscillations in PMU buses is also included in Fig. 5.4 for comparison between the measurements and estimated area angles. Although optimal PMU placement can reduce the effect of non inter-area modes in the

measurements, the local modes are present in the angle measurement data as can be seen in Fig. 5.4. The second case in Fig. 5.4 is performed by applying a large disturbance to push the system into the nonlinear domain. Nonetheless, in both cases the nonlinear estimator output expresses only the inter-area modes of the system with no visible local modes in the estimated angle and frequency oscillations which imply the effectiveness of the Kalman estimator in the estimation of area angles and frequencies.

5.4.2 Ten machine - four area system

In this section, the proposed approach is simulated on a more complex network with ten generators. This system can be divided to four areas as shown in Fig. 5.5 where the generators at each area remain coherent for a wide range of operating conditions. The parameters of the system are given in the Appendix. By simulating the system in a similar manner to the two area case, the reduced area based model is obtained such that the reduced system is represented by four generators and the links between them based on the area borders.

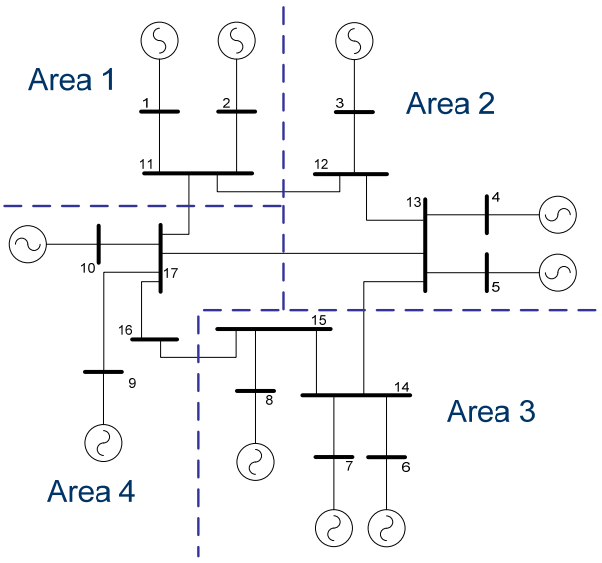

Fig. 5.5 Ten machine- four area system

In this system, there are seven possible locations for installing PMUs (installing on non-generator buses) and we simulate the system considering several scenarios with different availability of PMUs. The power transfer measurement between at least two areas is also required to obtain the parameters of the reduced system. In this case the power transfer between area 1 and 4 is measured which can be calculated by placing the two of the PMUs at buses 11 and 17 and measuring the voltage angles or measuring the voltage and current through the tie-line. The identification of reduced model is performed based on these different scenarios and a comparison between identified parameters in two cases where seven or four PMUs are installed in the network is presented in Table 5.3.

Table 5.3 The identified parameters of reduced system with different availability of PMUs

	Inertia (J)	**Damping (D)**
PMU on seven buses	0.2050 0.3965 0.3958 0.2056	0.1068 0.1614 0.1588 0.1247
PMU on four buses	0.2047 0.3934 0.3987 0.2050	0.1063 0.1618 0.1591 0.1238

It can be inferred from Table 5.3 that identification process can be performed with high accuracy in the various cases of PMU availability if the observability conditions of the Kalman filter are met. The nonlinear Kalman filter is designed for the reduced model by ignoring the local modes in the measurements in order to estimate the area angles and frequencies which represent inter-area oscillations of the system. Depending on the location of PMUs, the elements of measurement noise covariance σ_a are chosen to have low values in the range of 0.03 to 0.1 to represent the effect of local modes at each measurement point. To adjust these values, the spectrum analysis mentioned in Section 5.3 is applied on the angle oscillations of the

PMU buses resulting from a random walk perturbation and the power spectral density (PSD) for the high frequency (higher than inter-area range) noise is obtained for each measurement point. This process can also provide a scheme for finding optimal locations for phasor measurement units to monitor the inter-area oscillations of the system.

The state estimation process is applied on the system considering two cases of PMU availability. In the first case, four PMUs are considered to be installed in the system on buses 11, 13, 15, and 17 and for the second case the PMUs are available at all non-generator buses. The simulation is performed by applying a disturbance to the system considering these two scenarios. The equivalent area angle estimation is obtained by the designed Kalman filter as illustrated in Fig. 5.6 while the angle oscillation of the PMU buses are shown in Fig. 5.7 for comparison.

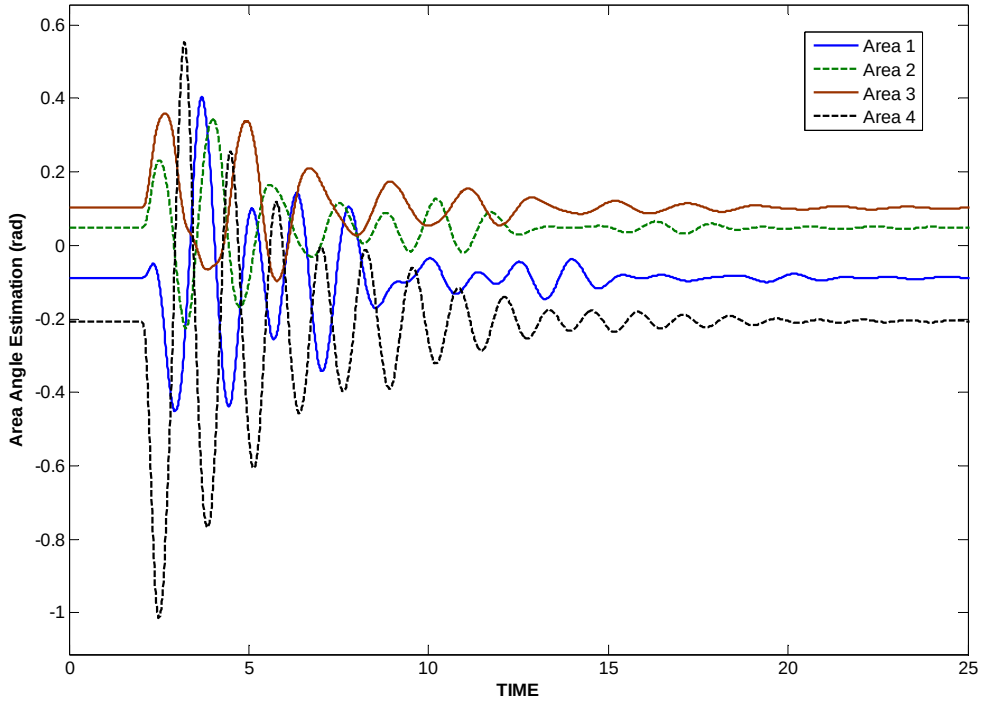

Fig. 5.6 State estimation of area angle oscillations in case 1

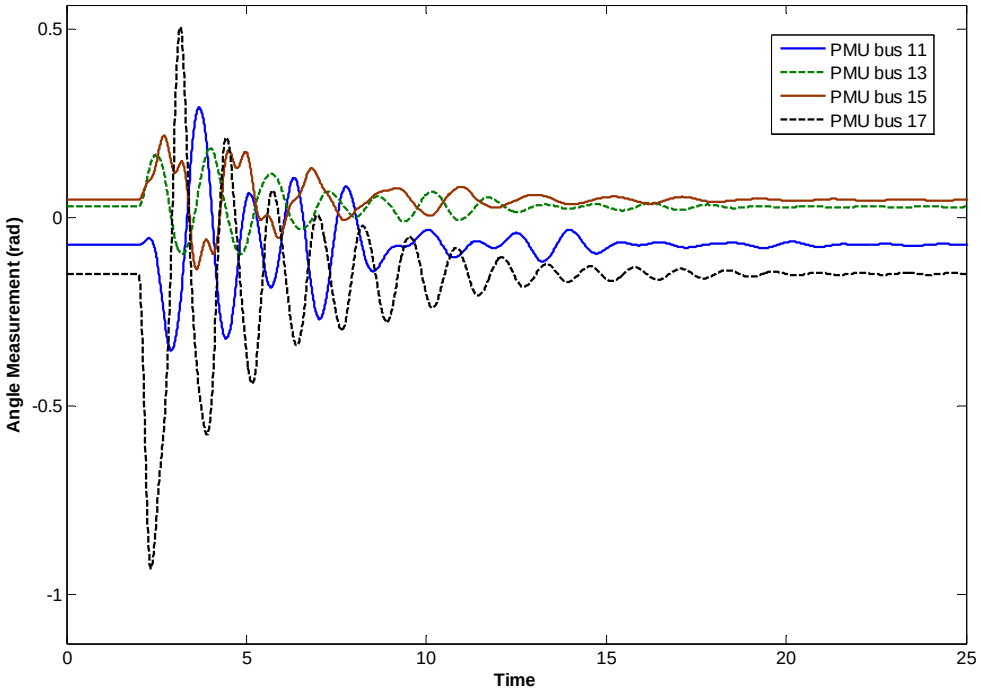

Fig. 5.7 Angle measurement from PMU buses in case 1

The result of the first case presented in Fig. 5.6 which shows the effectiveness of the approach in estimation of equivalent area angles. While the local modes are present in the measurement particularly in the measurement obtained from the PMU at bus 15 which contains higher frequency modes, the area angles are estimated with substantial reduction of local modes. In order to provide a robust approach against possible loss of measurement devices, for each case the Kalman filter is designed considering scenarios with different PMU availability. Therefore, in the second case of only four measurements, the simulation is performed with another disturbance considering loss of a PMU during the simulation which is illustrated in Fig. 5.8.

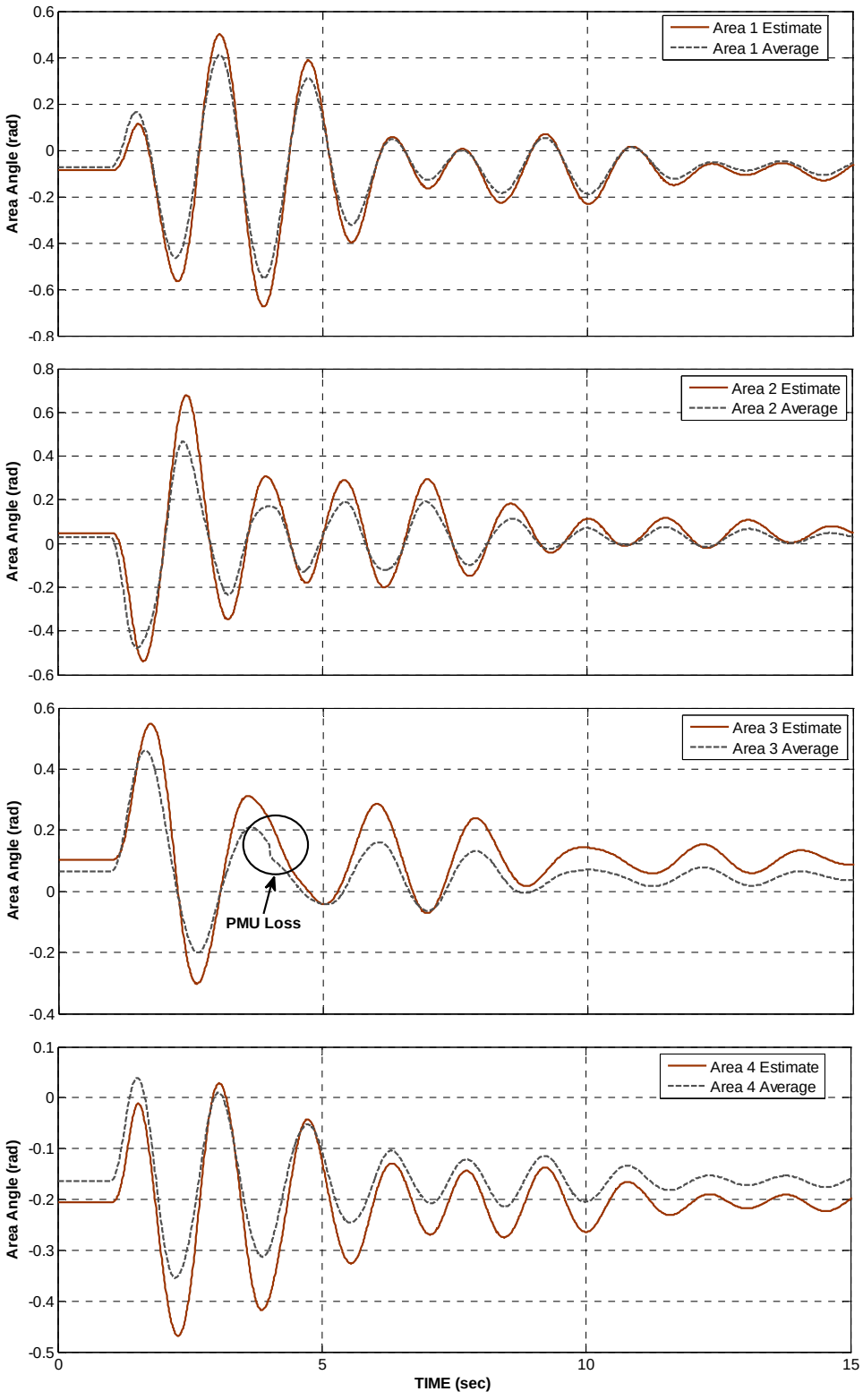

Fig. 5.8 State estimation of area angle oscillations and average of PMU measurement at each area

One way to represent area angles is the averaging of multiple PMUs in each area which is also illustrated in Fig. 5.8 for comparison between the estimated and average area angles. To show the effectiveness of the method in the worst case scenarios, the simulation is performed considering the loss of PMUs. In this case, the PMU located at bus 14 in area 3 is lost at $t=4$ *s* and the Kalman filter estimates the area angles by applying instantaneous change in the pre-calculated Kalman gain. Despite the presence of local modes in measurement data and loss of a PMU in area 3, no sudden change is observed in the estimated angles particularly in the area 3 angle estimation compared to the average area angle as seen in Fig 5.8 which proves the superiority of this approach to the averaging of PMU measurements.

5.5 Summary

In this chapter, an approach is developed for identification and estimation of equivalent area based reduced models and correspondent angles and frequencies using synchronized phasor measurement units. The generators and related non-generator buses which stay coherent in a wide range of operating conditions are defined as coherent areas and a reduced model is designed to represent the system by a set of equivalent machines and connecting links between them. The parameters of the reduced model are obtained by processing the angle measurement data obtained from PMUs installed throughout the system. The nonlinear Kalman filter is designed for the identified reduced model to estimate equivalent area angles and frequencies which represent inter-area oscillations of the system. The approach is simulated on two test systems and the results show the effectiveness of the identification and

estimation of reduced model using phasor measurement by substantial reduction of local modes in the estimated angles and robustness to the possible loss of measurement devices.

Chapter 6: Wide-area Control of Aggregated Power Systems

6.1 Introduction

Power systems are vulnerable to the disturbances which usually occur in the system due to faults. Because of the importance of power systems for the society and economy, a huge effort is undertaken to keep the system stable in the event of disturbance. The protection devices reduce the effect of faults by removing the faulted part of the system, while the controllers on the generators try to stabilize the system in the event of any disturbances.

To overcome the danger of severe disturbances, the stability of power systems can be improved by employing wide-area controllers which try to stabilize the system by applying the control actions on FACTS devices or system loads and generators. In this chapter a control approach is proposed to address the first swing and damping stability of power systems using wide-area measurements. The system aggregation and estimation of the reduced system parameters as described in previous chapters are then used to design a controller for the reduced model of a large system. This controller is then applied to the original system to stabilize the inter-area modes and thus the whole system.

6.2 Energy function based control

The stability of nonlinear systems defined as $\dot{x} = F(x)$ can be assessed using the Lyapunov Theorem [24]. Based on this theory, the system is stable if a positive definite function $V(x)$ can be found where its derivative $\dot{V}$ is negative semi-definite

along the trajectory of *x*. For power systems, a candidate Lyapunov function is based on the total energy of the system where for a *m* machine system with classic machine models the energy function is:

$$V(\delta,\omega)=\frac{1}{2}\sum_{i=1}^{m}J_i\omega_i^2-\sum_{i=1}^{m}\int_{\delta_i^s}^{\delta_i}f_i(\delta)d\delta_i \tag{6.1}$$

$$J_i\frac{d^2\delta_i}{dt^2}=f_i(\delta) \quad , \quad \omega=\dot{\delta} \tag{6.2}$$

Where δ and ω are in the centre of angle (COA) reference and f_i depends on the model of the system. The first part of the energy function V is the kinetic energy of the system and the second part is the potential energy, thus the total energy of the system can be expressed as the sum of kinetic and potential energy in the system:

$$V(\delta,\omega)=V_{KE}+V_{PE} \tag{6.3}$$

The energy function is not positive definite due to the effect of potential energy. If the potential energy is bounded within angle limits the energy function will become positive definite in this region which is called the region of attraction. Therefore, the derivative of V becomes negative semi-definite in this region. The control laws based on energy function try to yield a negative $\dot{V}$ to keep the system stable. Due to the complexity of using the total energy as the control criteria, the kinetic energy part of the energy function can be used to design the controller to stabilize the system where the derivative of system kinetic energy is:

$$\dot{V}_{KE}=\sum_{i=1}^{m}J_i\dot{\delta}_i\ddot{\delta}_i \tag{6.4}$$

In the kinetic energy based controllers the control law is usually designed based on maximum reduction of kinetic energy. The reduction of kinetic energy can enlarge the stable region of the system by applying the control law to the controlling devices.

6.3 Effect of measurement on the control design and performance

The controller may use the local or remote measurement to apply the control law on controllers such as FACTS devices. It is considered that better controlling performance can be achieved using remote measurements. To check this phenomenon, a SVC controller on a two machine system with loads on bus 3 and 5 as shown in Fig. 6.1 is examined with local and remote measurement options.

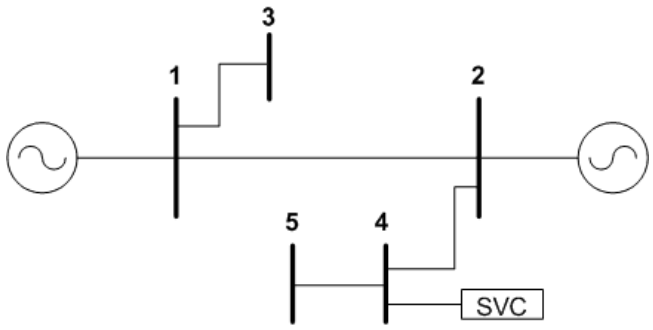

Fig. 6.1 Two generator system with SVC

The SVC controller is designed to address the first swing stability of this system. To avoid angle separation between two generators, the controller aims to maximize the power flow capacity across the link until the danger of separation is passed. The first control strategy is based on the local measurement of voltage angle at bus 4 and the second control is based on the remote angle measurement at the generator buses. Therefore, the control law for two control strategies are obtained as below:

$$u_l = \begin{cases} 1 & \ddot{\delta}_m > \varepsilon \\ -1 & \ddot{\delta}_m < -\varepsilon \\ 0 & otherwise \end{cases} \tag{6.5}$$

$$u_r = \begin{cases} 1 & \delta_{12} > \eta \\ -1 & \delta_{12} < -\eta \\ k\dot{\delta}_{12} & otherwise \end{cases} \tag{6.6}$$

$$-1 \le k\dot{\delta}_{12} \le 1 \quad , \quad |\delta_{12}| < \eta \tag{6.7}$$

Where u_l is the control law based on local measurement, δ_m is the angle measured on the SVC bus, ε is a pre-defined threshold to prevent chattering around $\ddot{\delta}_m = 0$, u_r is the control law based on remote measurement, η is a set distance from the Unstable Equilibrium Point (UEP), and *k* is a gain.

It can be inferred that local control is based on angular acceleration at the SVC bus which can be obtained by double differentiation of the local voltage angle measurement. The switching of SVC with remote measurement is determined by proximity to the system UEP which is defined by η. When the angle between generators is less than η, a linear control based on the rate of angle change $\dot{\delta}_{12}$ is applied to damp the oscillations. To see the effect of two switching laws, the system is simulated with a fault between bus 2 and 4. The critical clearing time (CCT) is obtained for uncontrolled and controlled cases which are shown in Table 6.1.

Table 6.1 Comparison between different control performances

Control type	**Critical Clearing Time (sec)**	**Improvement (%)**
No control	0.38	0%
Control based on local measurements	0.385	1.32%
Control based on remote measurements	0.47	23.68%

The results show that the controller based on local measurements can slightly improve the CCT in this system while by applying a remote measurement based SVC controller significant improvement in CCT can be achieved. This system can represent a two area system and it can be seen that using remote measurements can lead into better controlling performance in the event of fault. Therefore, remote (wide-area) measurements based controllers can improve the stability of multi-area systems by controlling the inter-area oscillations.

6.4 Damping and first swing stability

The controllers in Section 6.2 demonstrated a good performance for first swing stability while the results of the remote measurement based controller showed significant improvement of the critical clearing time. For a two machine system like the system in Fig. 6.1, a refined control law can be obtained based on reduction of the kinetic energy. This type of controller can also provide a good damping for the oscillations after severe disturbances.

Although the use of total kinetic energy based control design leads to good nonlinear damping controllers, it may not provide good first swing stability in multi-machine systems. It implies that large initial angle swings require a different control action. The work in [74] showed that short time horizon model predictive control (MPC) could be developed for suppression of the initial transients. In this approach the groups of machines in danger of separation are identified and the controller is designed for stabilizing the critical machine groups. This controller provides a good performance for first swing stability by using a control law based on the critical machine groups.

The proposed control process brings together previous works on multimode damping and on first swing stabilization. For first swing stability, several approaches have been trialled but the most promising is to control any relevant devices for the maximum reduction of the kinetic energy of the aggregate generators immediately adjacent to any weak connection link. The damping control system design is such that any control device aims to maximize the reduction rate of total kinetic energy of the system. Control actions need to target both control of the first swing instability immediately after a disturbance and damping of ongoing unstable oscillations in the network, which will result in a solution that allows for change during the disturbance from one control strategy to a different strategy. Therefore the controller will be designed as below:

$$u = \begin{cases} G_u\left(KE_{cr}\right) & t < t_{fs} \\ G_u\left(KE_T\right) & t \geq t_{fs} \end{cases} \tag{6.8}$$

Where u is the controlling actions, KE_{cr} is the kinetic energy of critical machines, KE_T is the total kinetic energy of the system, G_u is the function that shows u is calculated based on the critical and total kinetic energy, and t_{fs} is the time that criticality of first swing is passed. The controllers are designed and simulated for several systems to show the performance and details of the proposed approach.

6.4.1 Longitudinal three machine system

In the first case, the controller is designed for a longitudinal three machine system representing a reduced three area system as shown in Fig. 6.2. Due to the configuration of this system the line between buses 2 and 3 can be assumed to be the weak link, because in severe contingencies the possibility of angle separation between bus 2 and 3 is very high.

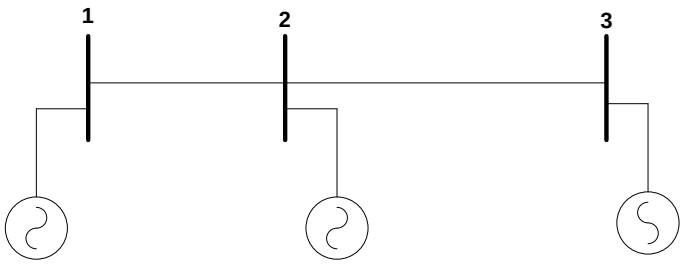

Fig. 6.2 Three machine system

A controllable series capacitor (CSC) with the susceptance ΔY_{12} is considered to be installed between buses 1 and 2 and the controlling law is designed for this device for first swing and damping stability as described before. Considering classic machine models and negligible line losses the kinetic energy based switching law is obtained:

$$Y_{12} = \bar{Y}_{12} + u\Delta Y_{12} \tag{6.9}$$

$$\dot{KE}_T = \dot{KE}_1 + (\dot{KE}_2 + \dot{KE}_3) = \dot{KE}_1 + \dot{KE}_{cr} \tag{6.10}$$

$$J_i\ddot{\delta}_i = Pm_i - Pe_i - D_i\dot{\delta}_i \tag{6.11}$$

$$\dot{KE}_T = \sum_{i=1}^{3} J_i\ddot{\delta}_i\dot{\delta}_i \tag{6.12}$$

$$\dot{KE}_1 = [Pm_1 - E_1E_2 \sin\delta_{12}(\bar{Y}_{12} + u\Delta Y_{12}) - D_1\dot{\delta}_1]\dot{\delta}_1 \tag{6.13}$$

$$\dot{KE}_2 = [Pm_2 - E_2E_1 \sin\delta_{21}(\bar{Y}_{12} + u\Delta Y_{12}) - E_2E_3 \sin\delta_{23}\,(Y_{23}) - D_2\dot{\delta}_2]\dot{\delta}_2 \tag{6.14}$$

$$\dot{KE}_3 = [Pm_{31} - E_3E_2 \sin\delta_{32}(Y_{32}) - D_3\dot{\delta}_3]\dot{\delta}_3 \tag{6.15}$$

Where $\dot{KE}_i$ is the derivative of kinetic energy at each machine and KE_{cr} is the derivative of critical kinetic energy which represents the energy of machine 2 and 3.

The switching law is obtained to maximize the reduction of kinetic energy after the disturbance.

$$\frac{\partial \dot{K}E_T}{\partial u} = \frac{\partial \dot{K}E_1}{\partial u} + \frac{\partial \dot{K}E_{cr}}{\partial u} = [-E_1 E_2 \sin \delta_{12}(\Delta Y_{12})\dot{\delta}_1] + [-E_2 E_1 \sin \delta_{21}(\Delta Y_{12})\dot{\delta}_2] \quad (6.16)$$

$$t < t_{fs} \ : \begin{cases} u = 1 & \sin \delta_{21}\dot{\delta}_2 > 0 \\ u = -1 & \sin \delta_{21}\dot{\delta}_2 < 0 \end{cases} \quad (6.17)$$

$$t \geq t_{fs} \ : \begin{cases} u = 1 & \sin \delta_{12}\dot{\delta}_{12} > 0 \\ u = -1 & \sin \delta_{12}\dot{\delta}_{12} < 0 \end{cases} \quad (6.18)$$

The control law is implemented in two stages depending on t_{fs} which determines the change in the switching strategy. In order the change the switching law, t_{fs} can be obtained by proximity to the system Unstable Equilibrium Point related to the weak link. Therefore, the angle and velocity between critical machines can determine the change in the switching law which can be therefore simplified as below:

$$t = \begin{cases} 1 & \sin \delta_{21}\dot{\delta}_2 > 0 \quad , \quad |\delta_{23}| > \eta \\ -1 & \sin \delta_{21}\dot{\delta}_2 > 0 \quad , \quad |\delta_{23}| > \eta \\ \\ 1 & \sin \delta_{12}\dot{\delta}_{12} > 0 \quad , \quad |\delta_{23}| \leq \eta \\ -1 & \sin \delta_{12}\dot{\delta}_{12} < 0 \quad , \quad |\delta_{23}| \leq \eta \end{cases} \quad (6.19)$$

Where η is a set point to change the control law which shows the criticality of the first swing is passed. Once the angle between critical machines $|\delta_{23}|$ reaches back to the set point η, the switching law is changed to the damping control based on the total kinetic energy of the system. The performance of the controller is tested by applying this control law on the CSC with the capacity of ± *0.25 pu* to provide both first swing and damping stability and the angle and angle deviation of the controlled system is illustrated in Fig. 6.3.

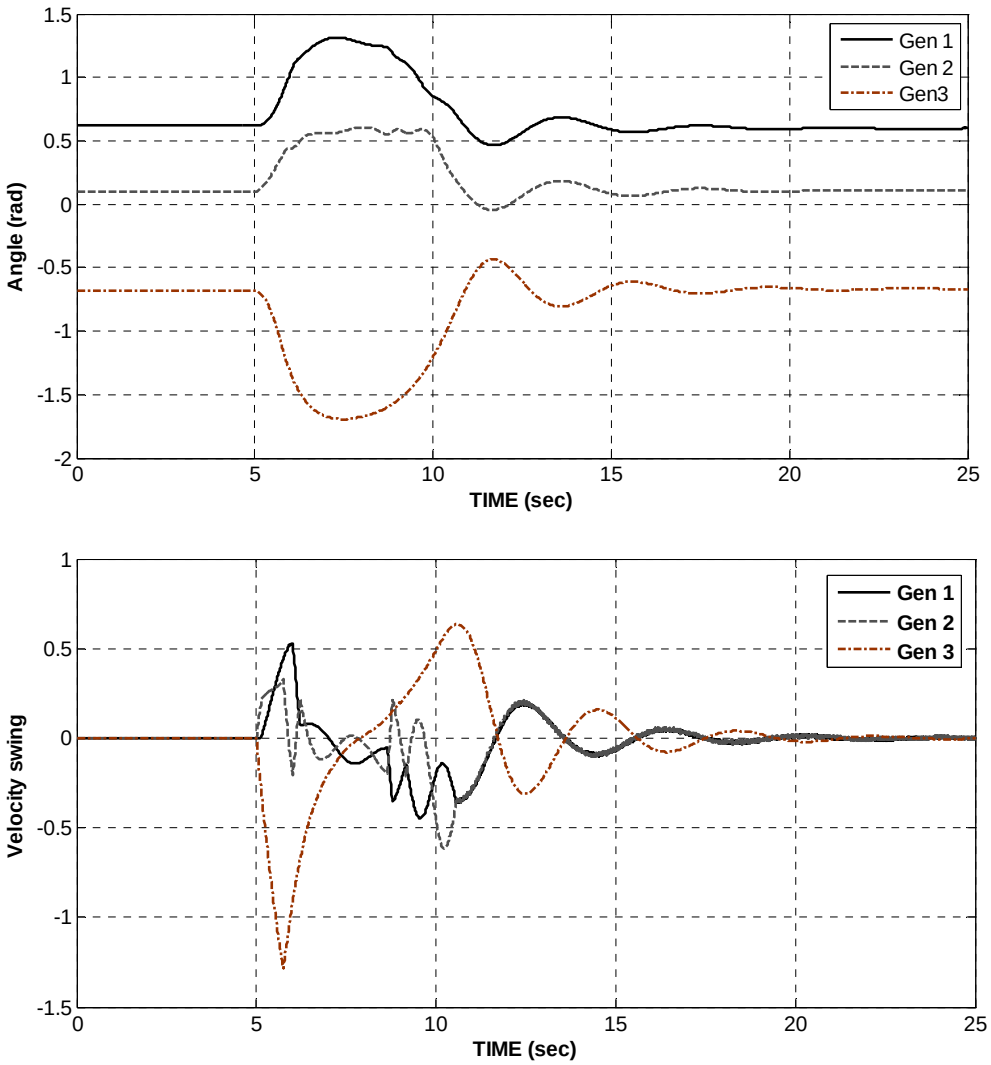

Fig. 6.3 Angle and velocity swings of the controlled system – case 1

The critical clearing time for a fault on line between bus 2 and 3 is compared for the controlled and uncontrolled system which shows a 2.7% improvement in the CCT for the controlled system. The improvement is not significant due to the location of the controlled capacitor in the system which is not located on the weak link. The CSC is only controlling the impedance between bus 1 and 2 and therefore does not have a significant effect on other modes of the system related to other machines considerably the oscillation mode between machine 2 and 3. Due to the importance of the oscillations of the critical machines, the performance of the

controller is restricted on both first swing and damping stability of this system. However, using the total kinetic energy approach for the first swing resulted in poor performance which shows the superiority of controller based on the kinetic energy of the critical machines for the first swing stability.

It is expected that a better performance can be achieved by installing the controller on the weak link which can directly affect the generators in immediate danger of separation. Therefore, the same CSC is considered to be installed between bus 2 and 3 and the control law is obtained similar to the previous case. Following the equations (6.9)-(6.18), the switching law for this case can be obtained as below:

$$Y_{23} = \bar{Y}_{23} + u\Delta Y_{23} \tag{6.20}$$

$$K\dot{E}_1 = [Pm_1 - E_1E_2 \sin\delta_{12}(Y_{12}) - D_1\dot{\delta}_1]\dot{\delta}_1 \tag{6.21}$$

$$K\dot{E}_2 = [Pm_2 - E_2E_1 \sin\delta_{21}(Y_{12}) - E_2E_3 \sin\delta_{23}(\bar{Y}_{23} + u\Delta Y_{23}) - D_2\dot{\delta}_2]\dot{\delta}_2 \tag{6.22}$$

$$K\dot{E}_3 = [Pm_{31} - E_3E_2 \sin\delta_{32}(\bar{Y}_{23} + u\Delta Y_{23}) - D_3\dot{\delta}_3]\dot{\delta}_3 \tag{6.23}$$

$$u = \begin{cases} 1 & \sin\delta_{23}\dot{\delta}_{23} > 0 \quad , \quad |\delta_{23}| > \eta \\ -1 & \sin\delta_{23}\dot{\delta}_{23} > 0 \quad , \quad |\delta_{23}| > \eta \\ \\ 1 & \sin\delta_{23}\dot{\delta}_{23} > 0 \quad , \quad |\delta_{23}| \le \eta \quad , \quad \epsilon < |\dot{\delta}_{23}| \\ -1 & \sin\delta_{23}\dot{\delta}_{23} < 0 \quad , \quad |\delta_{23}| \le \eta \quad , \quad \epsilon < |\dot{\delta}_{23}| \end{cases} \tag{6.24}$$

The control law for first swing and damping stability in this case are very similar as the controller only affects the kinetic energy of the critical machines. For damping, a threshold ϵ is used in the switching law to prevent chattering around $\dot{\delta}_{23} = 0$. To assess the performance of the controlled system with a controller on the critical link, a similar scenario is applied to the system and the angles and velocities of the machines are illustrated in Fig. 6.4.

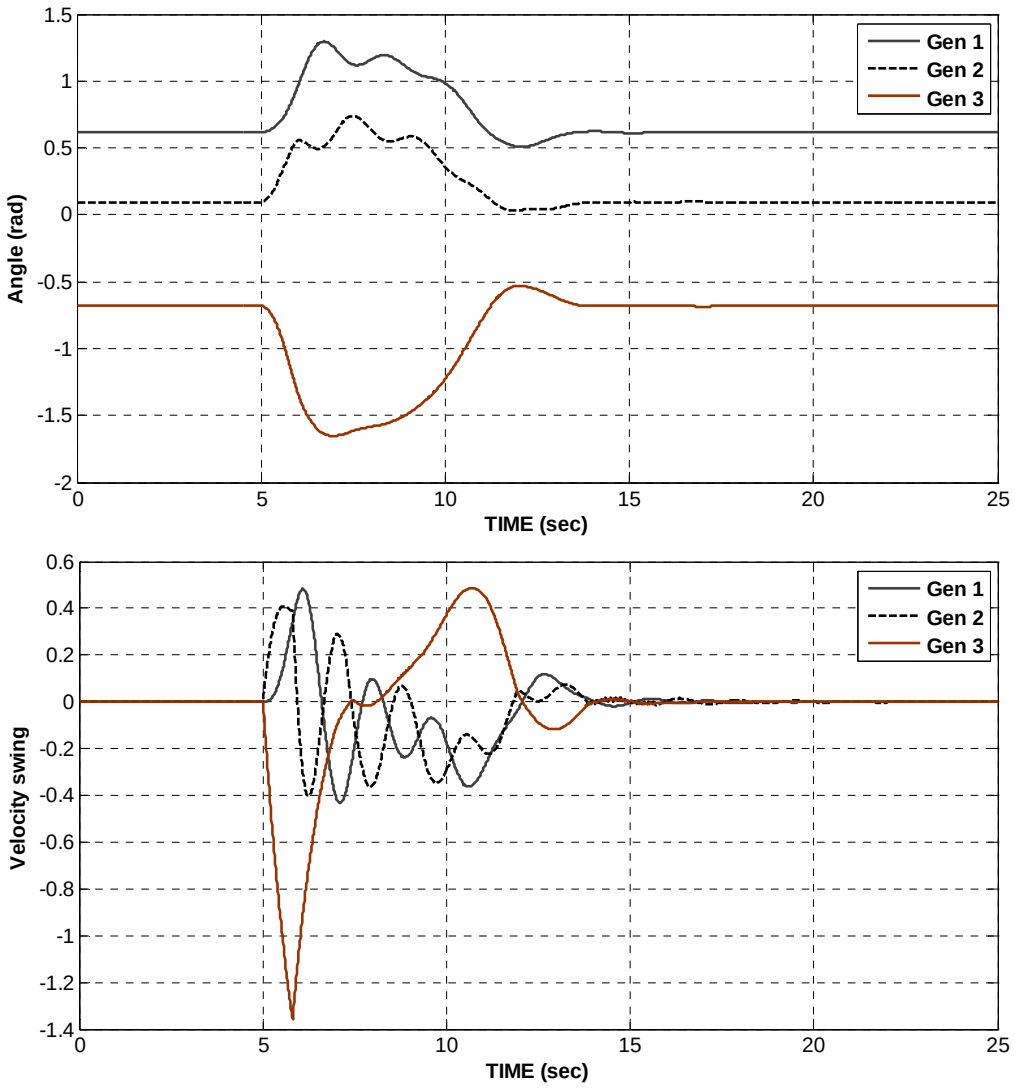

Fig. 6.4 Angle and velocity swings of the controlled system – case 2

The machine angles and velocities shown in Fig. 6.4 are obtained for the largest disturbance not resulting in system instability. For comparison, the angles and velocities of the uncontrolled system with the maximum fault duration is shown in Fig. 6.5. The critical clearing time with the controller on critical link is improved by 10.8% which shows a significant improvement compared to previous case. The damping is also improved, as the controller can damp the dominant mode of the system by reducing the total kinetic energy of the system.

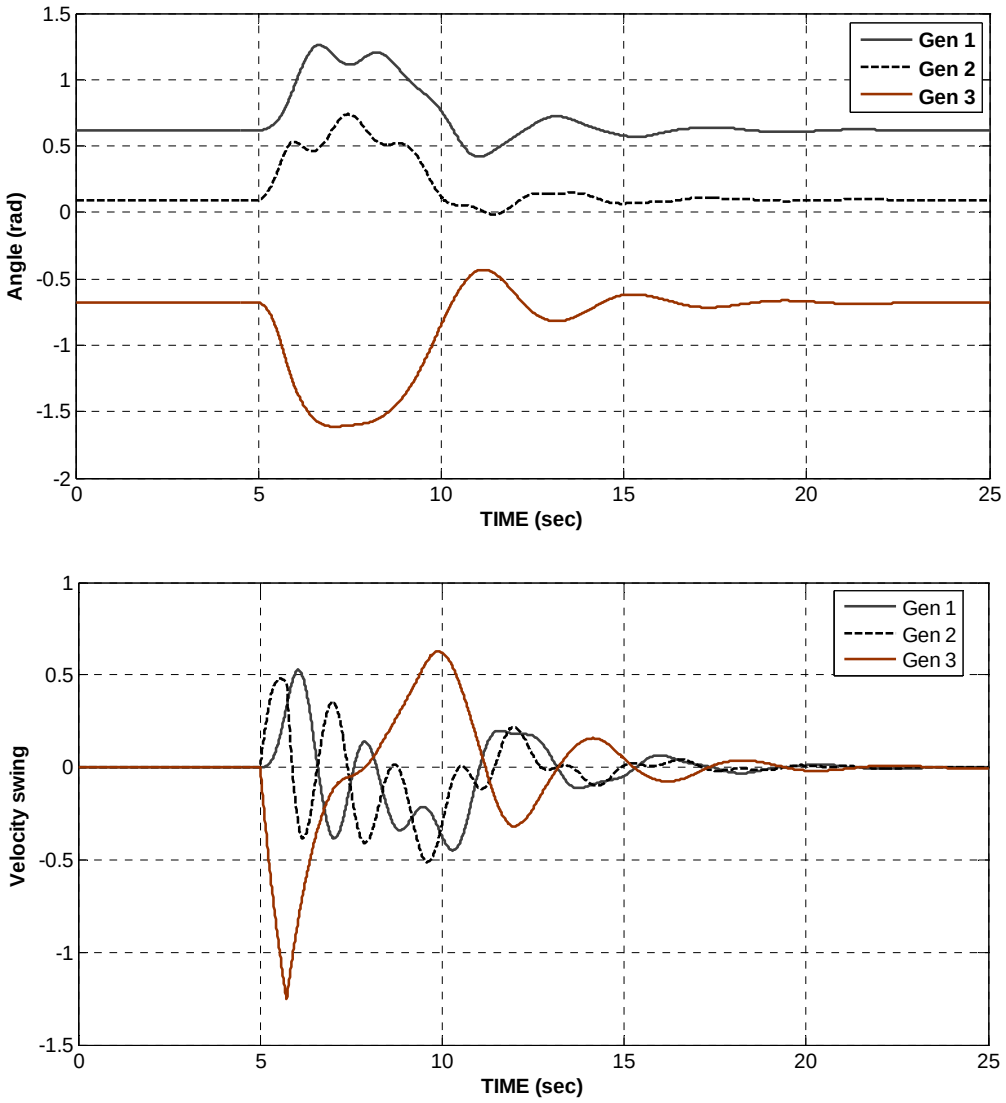

Fig. 6.5 Angle and velocity swings of the uncontrolled system

It is inferred that location of the controllable device can significantly affect the performance of the controller both in first swing and damping stability. Better performance can be observed if the device controls the kinetic energy of the critical machines. In Fig. 6.6 the control sequence corresponding to the angles and velocities of Fig. 6.4 is illustrated to show the control performance and change in the switching law from first swing to damping stability.

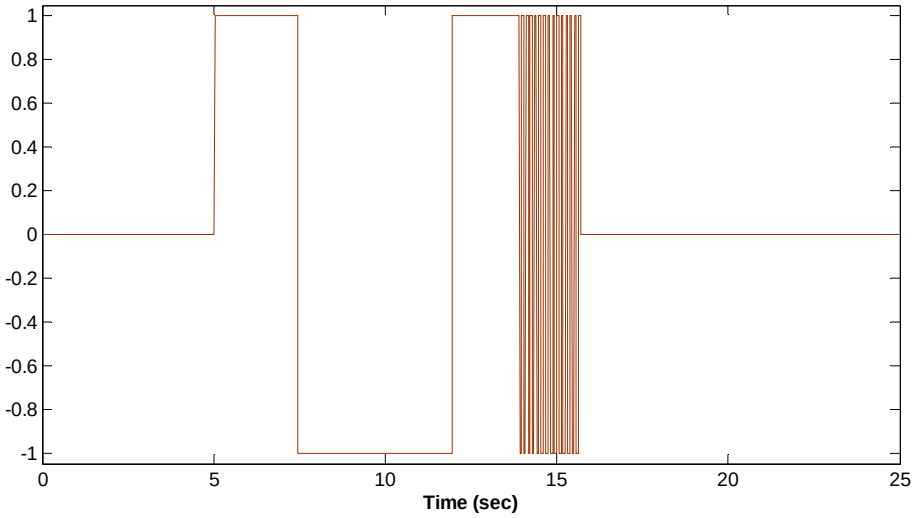

Fig. 6.6 Control sequence of the second control case

6.4.2 Three machine system with two controllers

In this case, the three machine system in previous case is extended to form a meshed network. Similar to the longitudinal system, the machines 2 and 3 are the critical machines and the line between them is the weak link. The performance of the controllers on this system is tested in several scenarios. In the first scenario, a CSC with the susceptance ΔY_{12} is considered to be available between buses 1 and 2. Due to the structure of the meshed system, the controller is not capable of providing good first swing and damping stability when a severe fault happens in the system. To provide a better stabilizing performance, two controllable series devices are considered to be available in the system. The first CSC is installed between bus 1 and 2 while the second CSC with the susceptance ΔY_{23} is installed between buses 2 and 3. The kinetic energy based switching law is then obtained:

$$Y_{12} = \bar{Y}_{12} + u_1 \Delta Y_{12} \tag{6.25}$$

$$Y_{23} = \bar{Y}_{23} + u_2 \Delta Y_{23} \tag{6.26}$$

$$u^T = [u_1 \; u_2] \tag{6.27}$$

$$K\dot{E}_1 = [Pm_1 - E_1E_2 \sin\delta_{12}(\bar{Y}_{12} + u_1\Delta Y_{12}) - E_1E_3 \sin\delta_{13}\,(Y_{13}) - D_1\dot{\delta}_1]\dot{\delta}_1 \tag{6.28}$$

$$K\dot{E}_2 = [Pm_2 - E_2E_1 \sin\delta_{21}(\bar{Y}_{12} + u_1\Delta Y_{12}) - E_2E_3 \sin\delta_{23}\,(\bar{Y}_{23} + u_2\Delta Y_{23}) - D_2\dot{\delta}_2]\dot{\delta}_2 \tag{6.29}$$

$$K\dot{E}_3 = [Pm_{31} - E_3E_1 \sin\delta_{31}(Y_{31}) - E_3E_2 \sin\delta_{32}(\bar{Y}_{23} + u_2\Delta Y_{23}) - D_3\dot{\delta}_3]\dot{\delta}_3 \tag{6.30}$$

$$\frac{\partial \dot{K}E_T}{\partial u} = \frac{\partial \dot{K}E_1}{\partial u} + \frac{\partial \dot{K}E_{cr}}{\partial u} \tag{6.31}$$

The switching control law can be obtained from (6.31) which defines the switching pattern for both first swing and damping stability. The exact solution of the control law results in co-ordinated switching of the two CSCs. However, a good performance of independent switching for two controllers is observed in [73] which shows the possibility of simplifying the control law by applying the controllers independently. Therefore, the simplified switching law for this case is obtained as below:

$$t < t_{fs} \;:\; \begin{cases} u_1 = 1 & \sin\delta_{21}\dot{\delta}_2 > 0 \\ u_1 = -1 & \sin\delta_{21}\dot{\delta}_2 < 0 \\ u_2 = 1 & \sin\delta_{22}\dot{\delta}_{23} > 0 \\ u_2 = -1 & \sin\delta_{23}\dot{\delta}_{23} < 0 \end{cases} \tag{6.32}$$

$$t \geq t_{fs} \;:\; \begin{cases} u_1 = 1 & \sin\delta_{12}\dot{\delta}_{12} > 0 \\ u_1 = -1 & \sin\delta_{12}\dot{\delta}_{12} < 0 \\ u_2 = 1 & \sin\delta_{22}\dot{\delta}_{23} > 0 \\ u_2 = -1 & \sin\delta_{23}\dot{\delta}_{23} < 0 \end{cases} \tag{6.33}$$

The control law is switched from first swing to damping stability at $t = t_{fs}$ which can be obtained similar to the longitudinal system based on the velocity difference between critical generators. To check the performance of the control system, a fault with the maximum duration not resulting in system instability is applied on the line between generator 2 and 3 and the angles and velocities of the controlled and uncontrolled system are illustrated in Fig. 6.7 and Fig. 6.8.

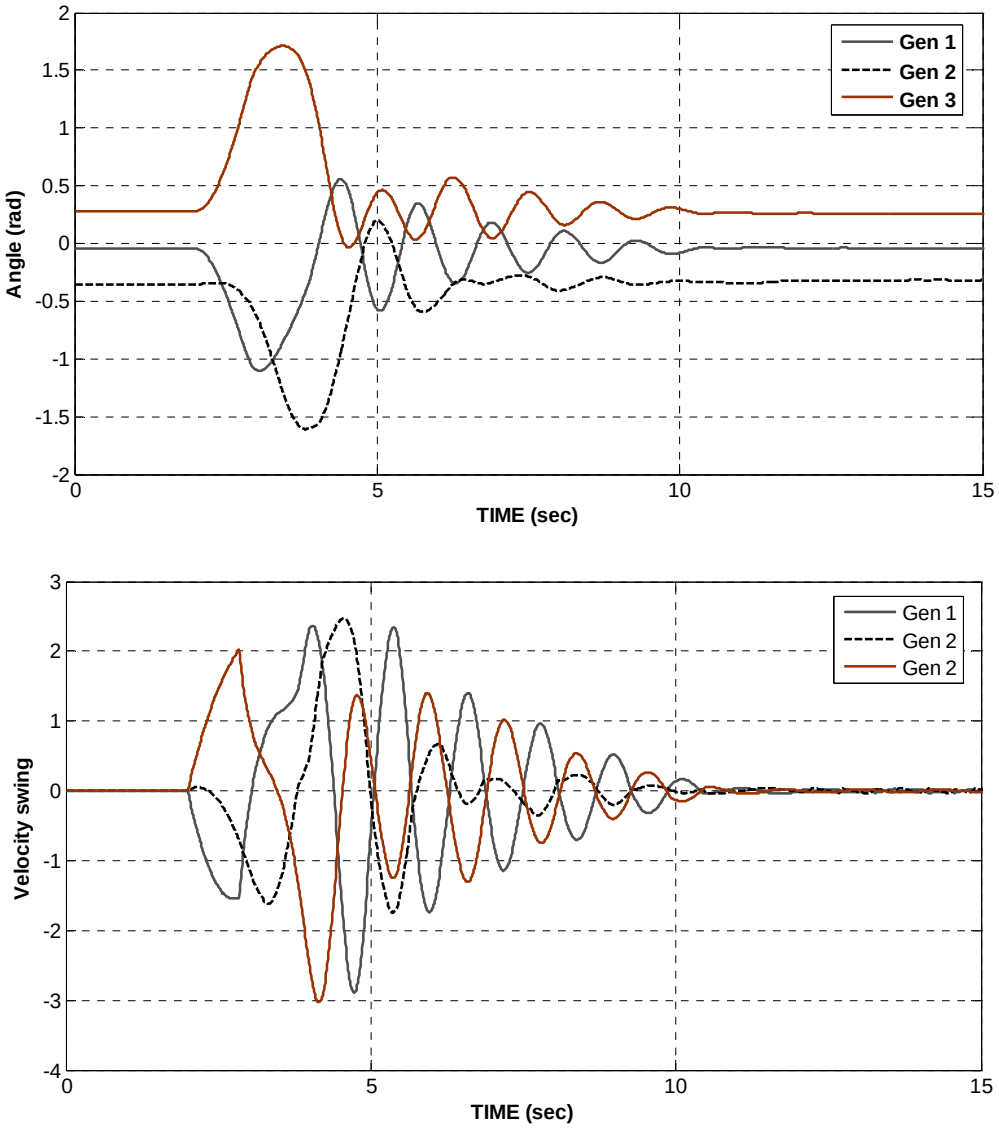

Fig. 6.7 Angle and velocity swings of the controlled meshed system

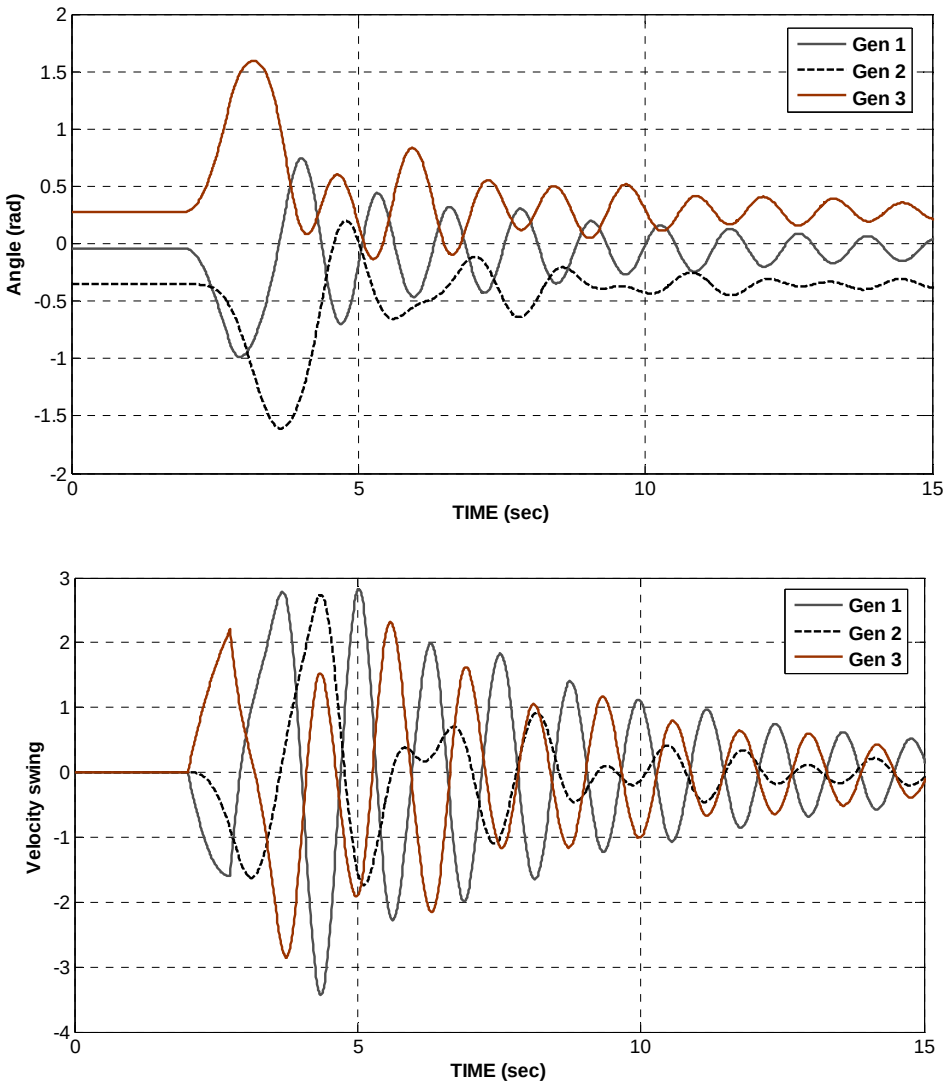

Fig. 6.8 Angle and velocity swings of the uncontrolled meshed system

The controller was able to improve the CCT by 13.2% which is a significant improvement for the first swing stability of the system. Comparing the generator swings for the controlled and uncontrolled systems as in Fig. 6.7 and 6.8 shows a significant improvement in the damping stability. Despite the fault location which was far from the controllers and the critical link, the controllers significantly improved the stability of the system which shows the effectiveness of the control

approach for both first swing and damping stability of the system. The control sequence of the controllers is shown in Fig. 6.9.

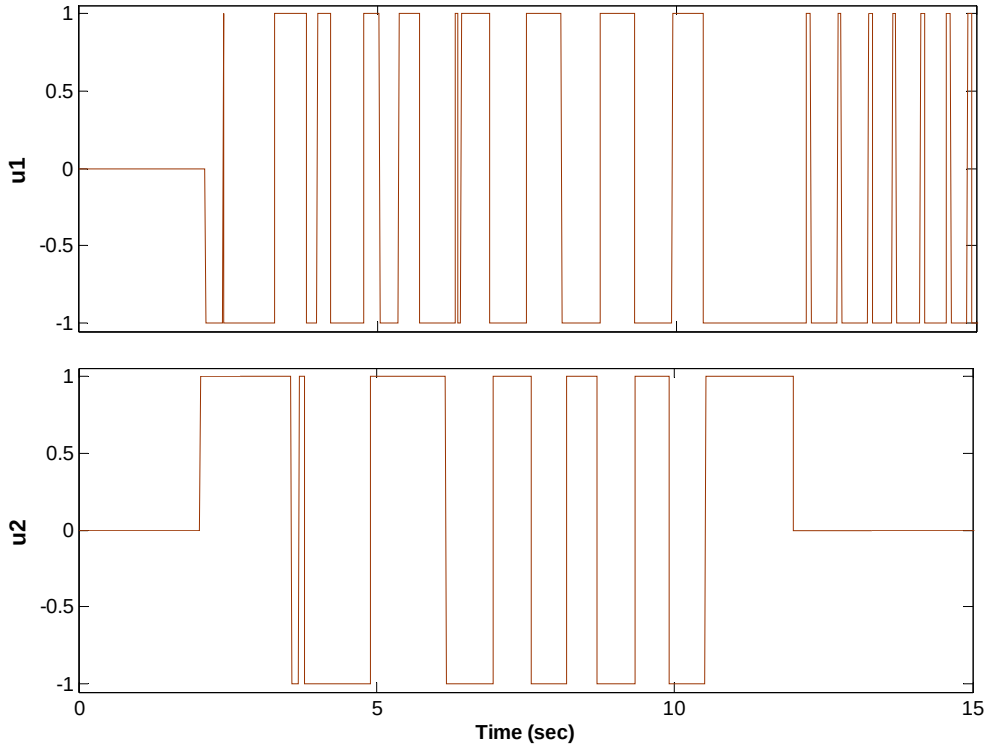

Fig. 6.9 Control sequence of the controllers in the meshed system

6.5 Wide-area control of inter-area modes

It is discussed in Section 6.3 that controllers based on remote measurements can achieve better performance in stability of power systems. The control algorithms developed in previous section also rely on remote measurement as the switching laws depend on angle and velocity differences between machines. Therefore, wide-area angle measurement is necessary to implement the proposed control approach for first swing and damping stability of power systems.

The test systems used in the previous sections can be considered as the reduced models of large systems where the aggregated generators are connected via links. The reduced model can be obtained based on the reduction approaches described in previous chapters. This implies that the proposed control methods can be applied for stabilizing the inter-area modes of power systems. Due to the importance of inter-area modes which can significantly contribute to the system instability, controlling these modes can improve the stability of power systems.

One difficulty of designing a controller for a multi-machine system is the vast number of variables which affect the control law. This increases the complexity of controller and requires extensive measurement devices across the network to implement the wide-area control system. Therefore, designing the controller based on the reduced model can be a practical approach which stabilize the inter-area modes and prevents the system instability.

The control approach described in previous sections showed a good performance for both first swing and damping stability and it can be extended to be applied on the reduced model of large systems. The coherency detection, model reduction, reduced parameters identification and estimation of angle and frequencies of the equivalent areas described in previous chapters forms the foundation for the control decisions to act on power devices such as FACTS devices or customer loads to stabilize a wide area network following a large disturbance. The control system is designed for the reduced model based on the estimation of aggregated system angles and velocities and is then applied to the real network controllers to enhance first swing and damping stability. The control approach is simulated on the test cases to show the feasibility of the proposed method.

6.5.1 Simulation on two area – four machine system

In this case, the control system is tested on the four machine system used in previous chapters. It is shown in Chapter 4, this system is a two area system in a wide range of operating conditions. A controllable series device with the capacity of *±0.1 pu* is considered to be installed between bus 6 and 7. The controller is designed for the reduced model based on state estimation of equivalent area angles frequencies described in Chapter 5 and is then applied to the original four machine system.

The only remaining issue is to model the controllable device into the reduced model and estimator. The effect of the CSCs on the inter-area impedances and the reduced admittance matrix can be obtained based on the identification of the reduced model parameters described in Chapter 5. Therefore, the inter area impedances are obtained using the PMU measurements for $Y_{67} = \bar{Y}_{67} \pm \Delta Y_{67}$ which results in identification of ΔYr_{12} for the reduced system. This process provides a mapping between the CSC of original system ΔY_{67} and reduced system ΔYr_{12} to design and implement the proposed control approach as below:

$$Yr_{12} = \bar{Y}r_{12} + u\Delta Yr_{12} \tag{6.34}$$

$$K\dot{E}r_1 = [Pmr_1 - Er_1Er_2 \sin \delta r_{12}(\bar{Y}r_{12} + \Delta Yr_{12}) - D_1\dot{\delta}r_1]\dot{\delta}r_1 \tag{6.35}$$

$$K\dot{E}r_2 = [Pmr_2 - Er_2Er_1 \sin \delta r_{21}(\bar{Y}r_{12} + \Delta Yr_{12}) - D_2\dot{\delta}r_2]\dot{\delta}r_2 \tag{6.36}$$

$$u = \begin{cases} 1 & \sin \delta r_{12}\dot{\delta}r_{12} > 0 \quad , \quad |\delta r_{12}| > \eta_r \\ -1 & \sin \delta r_{12}\dot{\delta}r_{12} < 0 \quad , \quad |\delta r_{12}| > \eta_r \\ \\ 1 & \sin \delta r_{12}\dot{\delta}r_{12} > 0 \quad , \quad |\delta r_{12}| \le \eta_r \quad , \quad \epsilon < |\dot{\delta}r_{12}| \\ -1 & \sin \delta r_{12}\dot{\delta}r_{12} < 0 \quad , \quad |\delta r_{12}| \le \eta_r \quad , \quad \epsilon < |\dot{\delta}r_{12}| \end{cases} \tag{6.37}$$

Where Yr_{12} is the equivalent admittance between area 1 and 2, Pmr_1 and Pmr_2 are the equivalent area mechanical power, and Er_1 and Er_2 are the equivalent area voltage which are assumed to be *1 pu*. The equivalent area angles and velocities δr and $\dot{\delta r}$ are obtained from PMU measurements and Kalman filter described in Chapter 5. The equivalent kinetic energy of the areas KEr define the switching law as (6.37) which has the similar properties of the control law in (6.24) where the threshold η_r defines the criteria to change the control law from first swing to damping control. In this case the total kinetic energy of the system is equal to the kinetic energy of the critical equivalent machines which results in a similar control algorithm for both first swing and damping stability.

The system is considered to have the properties described in Chapter 5 and the estimation of angles and frequencies of the equivalent areas based on the identified reduced model are used to design and implement the controller. The performance of the proposed controlling approach is tested by applying a three phase fault on bus 5 and comparing the results of the controlled and un-controlled systems. The angles and velocities of the system with the controller are illustrated in Fig. 6.10 while the uncontrolled system results are shown in Fig. 6.11. Both cases are simulated with maximum fault duration not resulting in system separation to test the most severe disturbance on the systems.

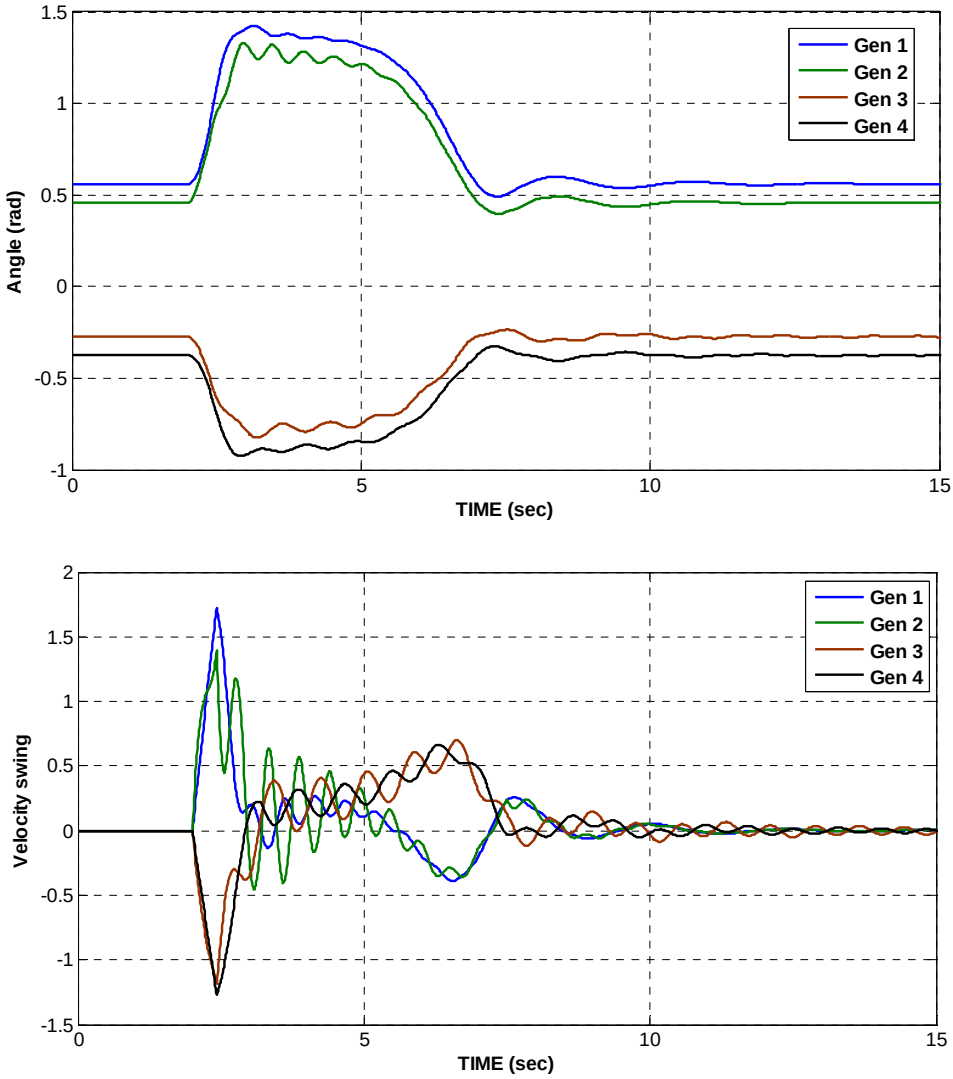

Fig. 6.10 Angle and velocity swings of the wide-area controlled system

The critical clearing time of the uncontrolled system is 0.39 sec while the CCT of the controlled system is improved by 12.82% to reach 0.44 sec. This shows a significant improvement in first swing stability of the controlled system. Comparing the results of the two scenarios as in Fig. 6.10 and 6.11, shows the effectiveness of the proposed control approach in both first swing and damping stability. The controller successfully stabilized the inter-area modes of the system which resulted in a more stable system in the case of severe disturbances. The remaining un-damped

oscillations in the controlled system are related to the local modes which are not affected by the inter-area controller. In reality, these modes can be damped by local controllers and the wide-area control system successfully discarded these modes in the control decision.

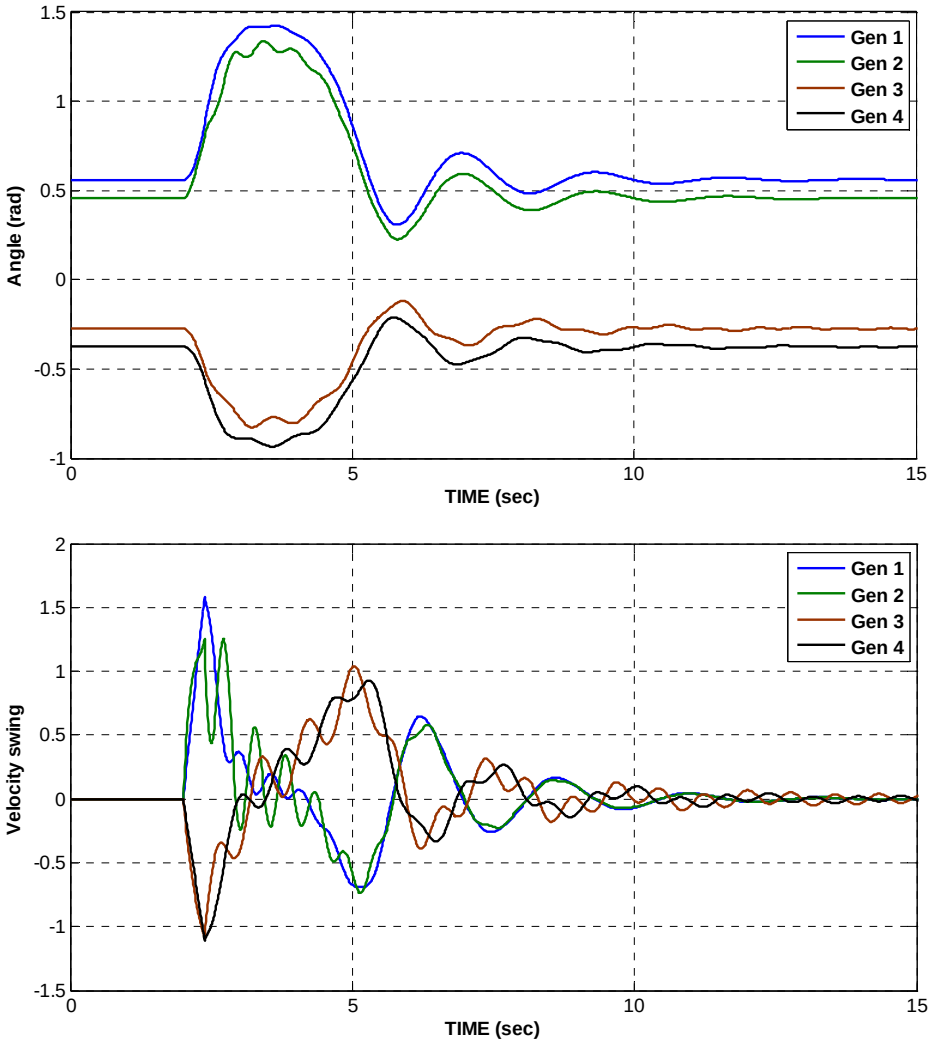

Fig. 6.11 Angle and velocity swings of the un-controlled system

6.5.2 Simulation on four area – ten machine system

In the second case, the control method is simulated on a more complex four area system shown in Fig. 5.5. Due the equivalent area parameters and impedances, the area 1 and 4 are the critical areas for a range of operating conditions. Two

controllable series capacitors are considered to be installed on the lines 11-17 and 15-16. Similar to the previous case, the controller is designed based on the estimated equivalent area parameters and is then applied to the controllable devices on the original ten machine system. The CSCs are mapped from the original system to the reduced model and the control system is designed as below:

$$Yr_{34} = \overline{Yr}_{34} + u_1 \Delta Yr_{34} \tag{6.38}$$

$$Yr_{14} = \overline{Yr}_{14} + u_2 \Delta Yr_{14} \tag{6.39}$$

$$u^T = [u_1 \; u_2] \tag{6.40}$$

$$t < t_{fs} \;:\; \begin{cases} u_1 = 1 & \sin \delta r_{43} \dot{\delta} r_4 > 0 \\ u_1 = -1 & \sin \delta r_{43} \dot{\delta} r_4 < 0 \\ u_2 = 1 & \sin \delta r_{14} \dot{\delta} r_{14} > 0 \\ u_2 = -1 & \sin \delta r_{14} \dot{\delta} r_{14} < 0 \end{cases} \tag{6.41}$$

$$t \geq t_{fs} \;:\; \begin{cases} u_1 = 1 & \sin \delta r_{43} \dot{\delta} r_{43} > 0 \\ u_1 = -1 & \sin \delta r_{43} \dot{\delta} r_{43} < 0 \\ u_2 = 1 & \sin \delta r_{14} \dot{\delta} r_{14} > 0 \\ u_2 = -1 & \sin \delta r_{14} \dot{\delta} r_{14} < 0 \end{cases} \tag{6.42}$$

Where Yr_{14} and Yr_{34} are the equivalent admittances between areas considering the effect of CSCs as ΔYr_{14} and ΔYr_{34}. The CSCs can affect the equivalent admittances between all areas; however, the change in other elements is neglected in the control design due to the dominance of the effect of the correspondent equivalent admittances. The controller is tested by applying a three phase fault on bus 16 and the angles and velocities of the controlled and uncontrolled systems are obtained as illustrated in Fig. 6.12 and 6.13 for the fault duration equal to the critical clearing time of the two cases.

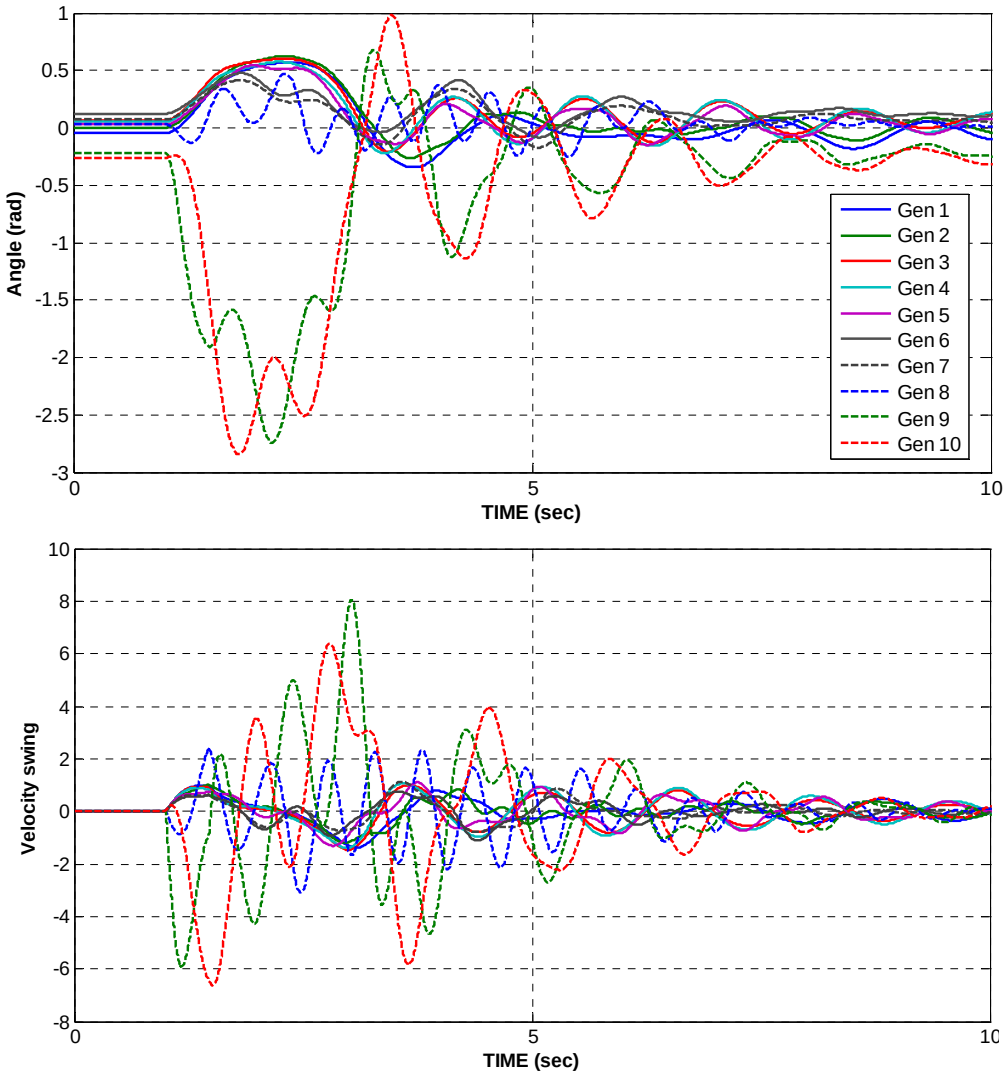

Fig. 6.12 Angle and velocity swings of the wide-area controlled four area system

The controllers improved the critical clearing time by 21.01% from 0.395 sec for the un-controlled system to 0.478 sec in the controlled system which is a significant improvement in the first swing stability of this system. Despite the longer fault duration of the controlled system, the damping is also improved which shows the effectiveness of the control approach in both first swing and damping stability improvements. Similar to the four machine case, the local modes are not damped in

the controlled system and the control algorithm effectively discarded these modes in the control design.

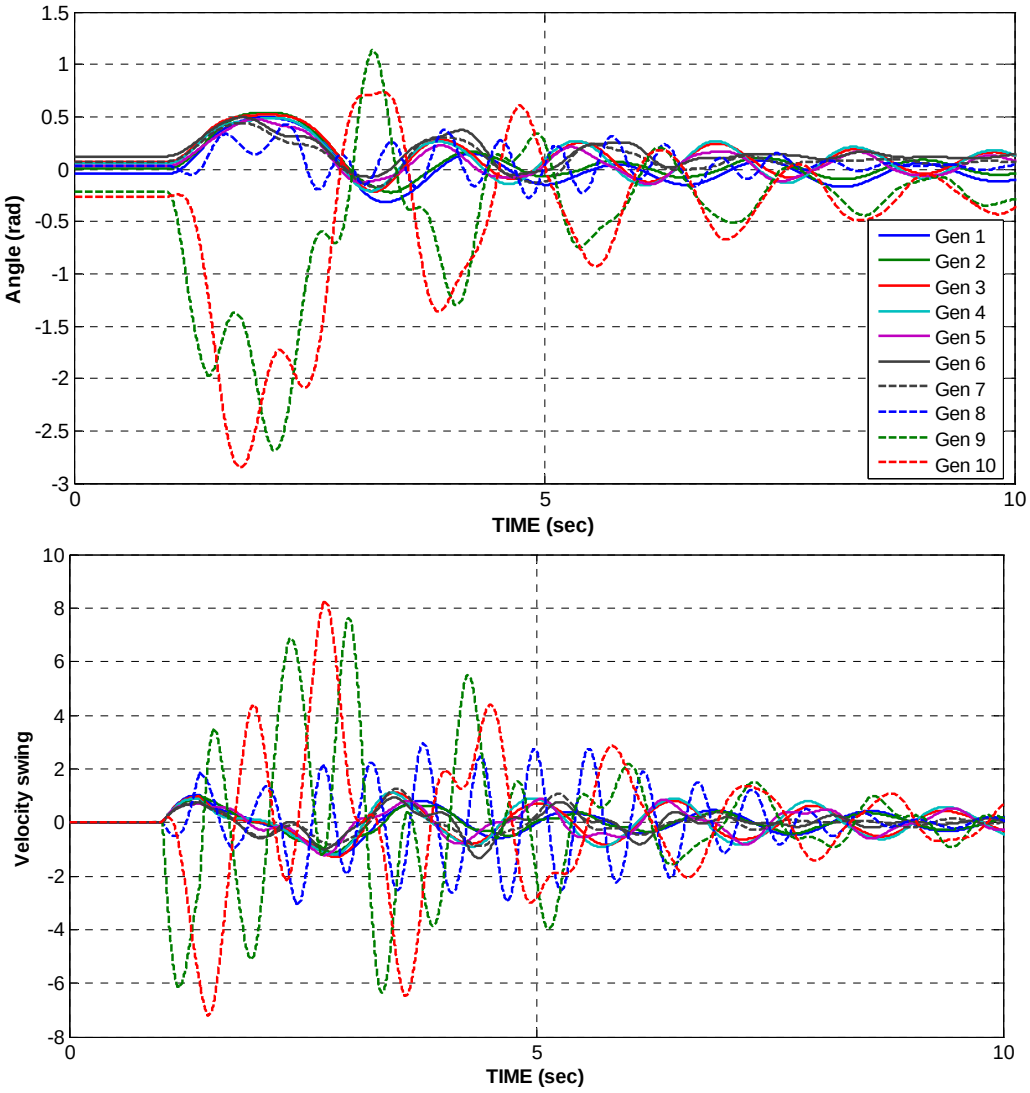

Fig. 6.13 Angle and velocity swings of the un-controlled four area system

In the simulations, the generators are modelled as classical machines and the estimation and control results showed good performances in dealing with the inter-area oscillations of the power systems. To check the feasibility of the proposed control approach, the system is simulated in a different operating condition and higher order models for the generators with the parameters given in Appendix. A

three phase fault is applied on the line between bus 11 and 12 and the angles and velocities of the controlled and un-controlled systems for the largest fault not resulting in system separation are illustrated in Fig. 6.14 and 6.15.

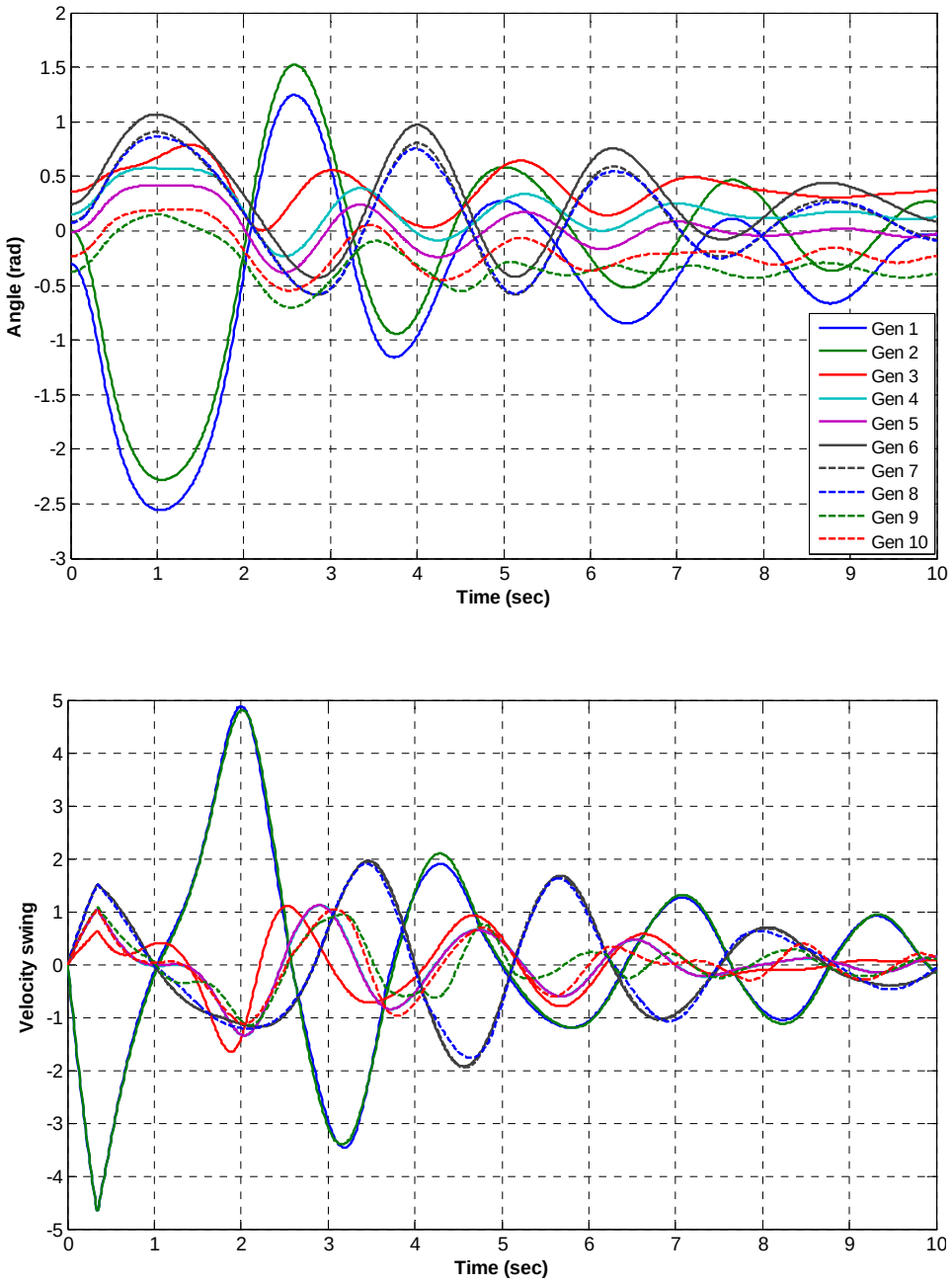

Fig. 6.14 Angle and velocity swings of the wide-area controlled four area system with higher order models

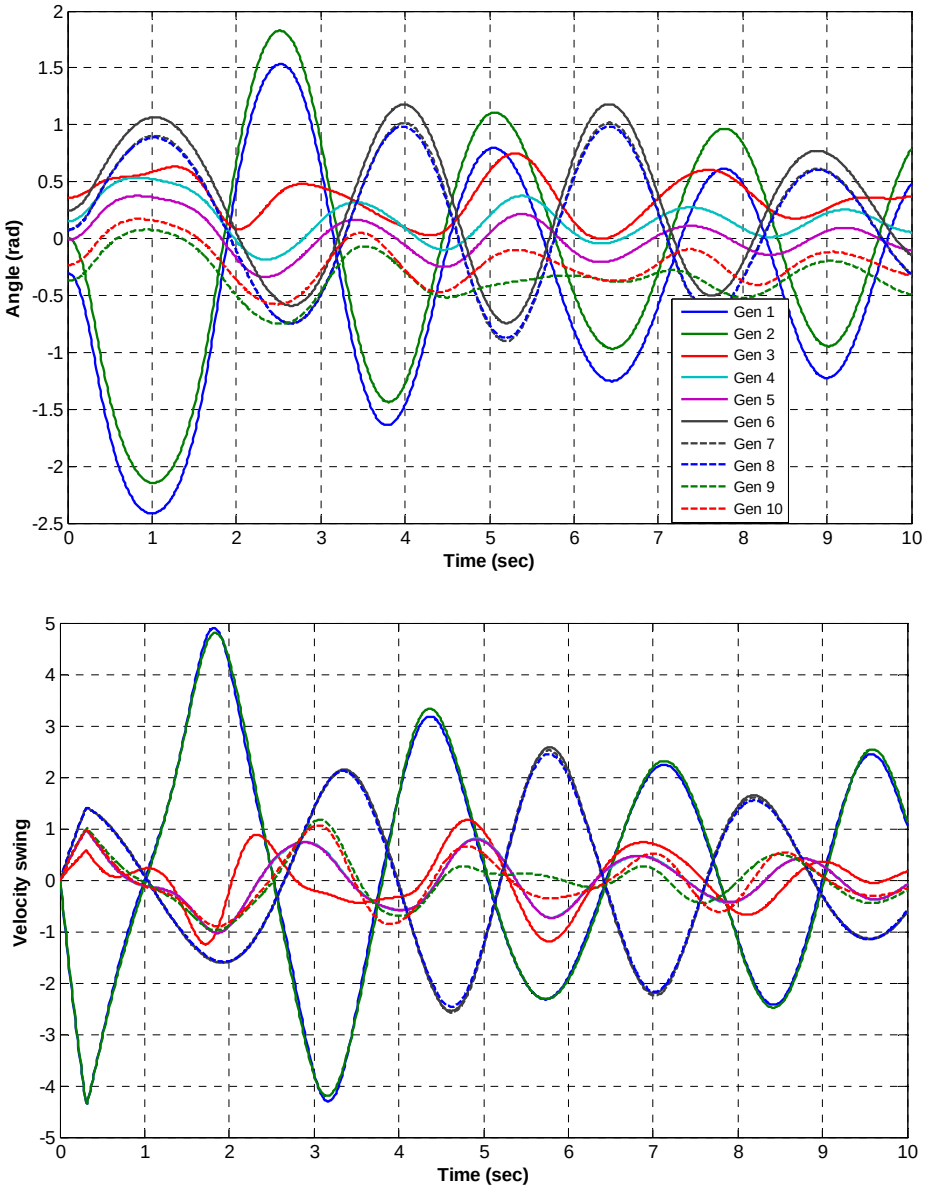

Fig. 6.15 Angle and velocity swings of the un-controlled four area system with higher order models

The critical clearing time of the controlled system is improved by 16.13% from 0.31 sec to 0.36 sec and the enhancement of damping can be observed by comparing the angles and velocities of the controlled and un-controlled systems. The control algorithms successfully improved the first swing and damping stability of the

system while higher order models were used for the generators. It can be observed that local modes are highly damped in the angles and velocities of the controlled and uncontrolled systems compared to the case with classical machine models because of the effect of higher order models and exciters. Therefore, the control algorithm can successfully stabilize and damp the inter-area modes of the system regardless of the generator models and local modes which show the applicability of this approach with real PMU measurements.

6.6 Alternative control method

The first swing and damping control methods described in previous sections are based on bang-bang type controllers. Implementing these controllers reduces the complexity of the control law and resulted in a good performance for stabilizing the power systems. The advantage of this control type is more evident in the application of wide-area controller based on reduced model which require a simple mapping between the real and reduced systems. One alternative control approach particularly for the damping stability is to use a control law based on saturation function as described in [62] :

$$u = Sat(S) = \begin{cases} 1 & S > 1 \\ \mathrm{K_s} S & -1 < S < 1 \\ -1 & S < -1 \end{cases} \tag{6.43}$$

In the equation above $\mathrm{K_s}$ is a constant and S is the switching hyperplane (the criteria for switching) where for the two area system in Section 6.5.1 $\mathrm{S} = \sin \delta r_{12} \dot{\delta} r_{12}$. This control law results in soft switching in linear region of operation and can reduce the possible chattering of the control sequence. However, the threshold in the proposed bang-bang controller could substantially reduce the chattering in the control signals and despite the good performance of this controller,

the saturation based controller can be an alternative for damping stability of power systems.

The proposed control approach uses transition criteria to change the switching law from first swing to damping stability. In the case of disturbance, the controller first operates based on the kinetic energy of the critical machines and when the immediate threat of separation is passed the control law is switched to damping stability based on total kinetic energy of the system. The controller achieved satisfactory results for both first swing and damping stability of the test system which shows the effectiveness of the method. However, the sudden change of switching law may excite some local modes in the systems controlled based on the reduced model. To overcome this issue, the sudden change in the control law can be replaced by a gradual transition pattern as below:

$$u = G_u(KE_{cr} + \beta_s KE_{nc}) \quad , \quad 0 \leq \beta_s \leq 1 \tag{6.44}$$

$$KE_T = KE_{cr} + KE_{nc} \tag{6.45}$$

Where KE_{nc} is the kinetic energy of the non-critical machines and β_s is a variable which defines the transition of the switching law from first swing to damping stability. If $\beta_s = 0$ the controller will be purely based on kinetic energy of the critical machines and if $\beta_s = 1$ the switching law will be based on total kinetic energy of the system. The transition of β_s from 0 to 1 is defined by proximity to system UEP which means if the danger of separation in first swing is reduced the variable β_s is increased to smoothly change the control pattern to damping stability. The gradual change in the switching law reduces the risk of local mode excitation and improves the controller performance. However, the results of the controller based on (6.8) did not show any excitation of local modes due to the sudden change

of switching law in the test systems which shows the effectiveness of the control approach even without smooth transition.

6.7 Summary

In this chapter, the control approaches are presented to address the first swing and damping stability based on kinetic energy of the system. The effect of wide-area measurement on control performance is studied which showed the superiority of the controller based on remote measurements. It is shown that a controller based on the kinetic energy of the machines in danger of angle separation or critical machines can provide a good first swing stability performance. Therefore, a two stage control algorithm is presented which uses the kinetic energy of the critical machines for first swing stability and then switches the control law based on the total kinetic energy of the system to damp the oscillations. The results of the test systems showed a good performance of the proposed control method in both first swing and damping stability.

In the next step, the controller is designed for the reduced model of large systems based on the reduction and estimation methods described in previous chapters. This controller is then applied to the original system by mapping the reduced and real controllers and stabilizing the inter-area modes of the system which resulted in a wide-area controller based on aggregated power systems. The proposed controller could successfully stabilize the system following a severe disturbance which shows the effectiveness of the proposed approach.

Chapter 7: Conclusions and Recommendations

The general conclusions of the thesis and recommendations for future research are presented in this chapter.

7.1 Conclusions

Development of a feasible wide-area control approach through aggregation of power systems is the main contribution of this thesis. In order to reach the goals of this research the steps as below are followed:

- Finding coherent generators and their correspondent non-generator buses which stay coherent for a wide range of operating conditions.
- Aggregating coherent generators and identifying the nonlinear dynamic parameters of the aggregated area based models.
- Estimation of the reduced system dynamic states using a nonlinear Kalman filter based on phasor measurement units.
- Designing the nonlinear control tools to address both first swing and damping stability of power systems based on the reduced dynamic model.
- Applying the developed control tools on the original power system to implement the wide-area control system.

Due to the importance of model reduction in the proposed approach, a new method is presented to reduce the entire power system into an aggregated regional model. The coherent areas are identified for the operating point of the system and the

reduction is applied on the system to represent the coherent generators by an equivalent machine. The aggregation is first applied to the linearized model of the system and the parameters of the nonlinear reduced model are obtained based on the properties of the linear reduced model and system operating conditions. To provide an estimate of reduced system states, a Kalman filter is designed for the reduced model based on the data obtained from phasor measurement units. It is demonstrated that the approach has been successful in dynamic reduction by reflecting only the inter-area modes of the power systems. Unlike the most reduction methods, this approach not only reduces the external part of the system but the entire system is reduced to create an aggregated regional model of power systems.

The described approach requires a model of whole system and the reduction is applied to the coherent generators which are obtained for the operating conditions of the system. In order to have a more general reduction process which is valid in wide range of operating conditions, a new generator coherency and area detection approach is presented. In this method a random load change known as random walk type of disturbance is applied to the system instead of a single fault for uniform excitation of all modes. The spectrum analysis is performed on velocity and angle swings of the generator and non-generator buses to obtain the coherent generators and load buses in low frequency inter-area modes. It is shown that, complex power networks might not be fully dividable into coherent areas where boundary generators and buses may swap between the neighbouring areas by changing the operating point of the system. However, by applying the proposed method on several operating points a general grouping scheme of the generators and load buses can be obtained which stay coherent for a wide range of system operating conditions.

Identification of the coherent areas for multiple operating conditions leads into a more general dynamic reduction approach to represent the system by a set of equivalent machines and links between them. The proposed reduction approach does not rely on the model of the entire system and the parameters of the reduced model are identified by processing the data obtained from synchronized phasor measurement units in the system. To estimate the equivalent area angles and frequencies a nonlinear Kalman filter is designed for the identified reduced model. The Kalman estimator demonstrated a good performance in estimation of the inter-area modes of the system in the event of disturbances by substantial reduction of local modes in the estimated angles and frequencies. Besides, the approach is shown to be robust against the possible loss of measurement units by applying instantaneous changes to the Kalman filter. The proposed approach provides a live identification process where the reduced model parameters can be updated online using the PMU measurements. It is shown that wide-area measurements can play a key role in providing a good estimate of inter-area oscillations of the system.

The dynamic reduction and state estimation methods developed in the thesis are the foundations for the ultimate goal of this research. It is shown that better performance can be achieved using the remote measurement based controllers. The developed control approach uses the kinetic energy of the critical machines for first swing stability and then control law is switched to the damping stability control based on the total kinetic energy of the system. The controller has shown good performances for both first swing and damping stability of power systems. The wide-area control system is achieved by integrating the aggregated and estimated regional model based on measurement with the proposed control approach. It is demonstrated that wide-area controller could successfully stabilize the power systems following

severe disturbances which shows the feasibility and effectiveness of the proposed control approach.

7.2 Recommendations

The following works are recommended for future research:

7.2.1 Consideration of signal delays

In wide-area measurement and control systems, PMU data needs to be transmitted to the monitoring and control centre which results in signal transmission delays. In this research the effect of this time delay in system dynamic reduction and wide-area control is not investigated which can be a topic for future research. This future research can consider signal delays in application of the Lyapunof energy function based controllers for real power systems.

7.2.2 Emergency control in the event of severe faults

In this research, the wide-area control is designed to stabilize the system in the event of disturbance by using the FACTS devices. In the event of severe disturbances where the control actions are unable to keep the system stable, emergency control methods such as load shedding and controlled islanding can be applied to reduce the risk of system-wide instability and blackout which can be investigated in future research work.

7.2.3 Considering electromechanical wave propagation phenomenon

In this research, the generators are considered to simultaneously accelerate in the event of disturbance. The other dynamic phenomenon to describe the rotor accelerations is the electromechanical wave propagation which is characterized by

travelling waves in terms of a wave equation. Developing a wide-area control algorithm to provide first swing stability enhancement against system separation caused by the wave propagation phenomenon can be a topic for future research.

7.2.4 Investigating the criteria for the aggregation based wide-area control

The model reduction and aggregation methods developed in this research are shown to be effective on different systems. However, the aggregation may not be applicable to all systems due to the coherency and other restrictions. Investigation the criteria for obtaining the aggregated model of the large power systems can be a topic for future research to find the class of systems that can be reduced.

References

[1] P. Kundur, *Power System Stability and Control*: McGraw-Hill Education, 1994.

[2] P. Kundur, J. Paserba, V. Ajjarapu, G. Andersson, A. Bose, C. Canizares, *et al.*, "Definition and classification of power system stability IEEE/CIGRE joint task force on stability terms and definitions," *IEEE Transactions on Power Systems,* vol. 19, pp. 1387-1401, 2004.

[3] M. Pavella, D. Ernst, and D. Ruiz-Vega, *Transient Stability of Power Systems: A Unified Approach to Assessment and Control*: Springer London, Limited, 2000.

[4] A. A. A. Fouad and V. Vittal, *Power system transient stability analysis using the transient energy function method*: Prentice Hall, 1992.

[5] A. Pai, *Energy Function Analysis for Power System Stability*: Springer, 1989.

[6] A. Pai, *Power System Stability: Analysis by the Direct Method of Lyapunov*: North-Holland, 1981.

[7] Z. Yun, Y. Ming-Hui, and C. Hsiao-Dong, "Theoretical foundation of the controlling UEP method for direct transient-stability analysis of network-preserving power system models," *IEEE Transactions on Circuits and Systems I: Fundamental Theory and Applications,* vol. 50, pp. 1324-1336, 2003.

[8] N. Amjady and S. F. Majedi, "Transient Stability Prediction by a Hybrid Intelligent System," *IEEE Transactions on Power Systems,* vol. 22, pp. 1275-1283, 2007.

[9] N. Amjady and S. A. Banihashemi, "Transient stability prediction of power systems by a new synchronism status index and hybrid classifier," *IET Generation, Transmission & Distribution,* vol. 4, pp. 509-518, 2010.

[10] A. G. Phadke, J. S. Thorp, and M. G. Adamiak, "A New Measurement Technique for Tracking Voltage Phasors, Local System Frequency, and Rate

of Change of Frequency," *IEEE Transactions on Power Apparatus and Systems*, vol. PAS-102, pp. 1025-1038, 1983.

[11] A. R. Messina, V. Vittal, D. Ruiz-Vega, and G. Enriquez-Harper, "Interpretation and Visualization of Wide-Area PMU Measurements Using Hilbert Analysis," *IEEE Transactions on Power Systems*, vol. 21, pp. 1763-1771, 2006.

[12] N. Hui, G. T. Heydt, and L. Mili, "Power system stability agents using robust wide area control," *IEEE Transactions on Power Systems*, vol. 17, pp. 1123-1131, 2002.

[13] W. Hongxia, K. S. Tsakalis, and G. T. Heydt, "Evaluation of time delay effects to wide-area power system stabilizer design," *IEEE Transactions on Power Systems*, vol. 19, pp. 1935-1941, 2004.

[14] S. Ray and G. K. Venayagamoorthy, "Real-time implementation of a measurement-based adaptive wide-area control system considering communication delays," *IET Generation, Transmission & Distribution*, vol. 2, pp. 62-70, 2008.

[15] D. Dotta, A. S. e Silva, and I. C. Decker, "Wide-Area Measurements-Based Two-Level Control Design Considering Signal Transmission Delay," *IEEE Transactions on Power Systems* vol. 24, pp. 208-216, 2009.

[16] A. R. Messina and V. Vittal, "Extraction of Dynamic Patterns From Wide-Area Measurements Using Empirical Orthogonal Functions," *IEEE Transactions on Power Systems*, vol. 22, pp. 682-692, 2007.

[17] I. Kamwa, S. R. Samantaray, and G. Joos, "Development of Rule-Based Classifiers for Rapid Stability Assessment of Wide-Area Post-Disturbance Records," *IEEE Transactions on Power Systems*, vol. 24, pp. 258-270, 2009.

[18] M. M. Eissa, M. E. Masoud, and M. M. M. Elanwar, "A Novel Back Up Wide Area Protection Technique for Power Transmission Grids Using Phasor Measurement Unit," *IEEE Transactions on Power Delivery*, vol. 25, pp. 270-278, 2010.

[19] J. Hauer, D. Trudnowski, G. Rogers, B. Mittelstadt, W. Litzenberger, and J. Johnson, "Keeping an eye on power system dynamics," *IEEE Computer Applications in Power,* vol. 10, pp. 50-54, 1997.

[20] J. H. Chow, A. Chakrabortty, L. Vanfretti, and M. Arcak, "Estimation of Radial Power System Transfer Path Dynamic Parameters Using Synchronized Phasor Data," *IEEE Transactions on Power Systems* vol. 23, pp. 564-571, 2008.

[21] A. Chakrabortty, J. H. Chow, and A. Salazar, "Interarea Model Estimation for Radial Power System Transfer Paths With Intermediate Voltage Control Using Synchronized Phasor Measurements," *IEEE Transactions on Power Systems,* vol. 24, pp. 1318-1326, 2009.

[22] M. Klein, G. J. Rogers, and P. Kundur, "A fundamental study of inter-area oscillations in power systems," *IEEE Transactions on Power Systems,* vol. 6, pp. 914-921, 1991.

[23] G. Rogers, *Power System Oscillation*. Norwell: Kuwler Academic, 2000.

[24] P. W. Sauer and A. Pai, *Power system dynamics and stability*: Prentice Hall, 1998.

[25] E. J. S. Pires de Souza and A. M. Leite da Silva, "An efficient methodology for coherency-based dynamic equivalents [power system analysis]," *IEE Proceedings C Generation, Transmission and Distribution,* vol. 139, pp. 371-382, 1992.

[26] T. Hiyama, "Identification of coherent generators using frequency response," *IEE Proceedings C Generation, Transmission and Distribution* vol. 128, pp. 262-268, 1981.

[27] M. H. Haque, "Identification of coherent generators for power system dynamic equivalents using unstable equilibrium point," *IEE Proceedings C Generation, Transmission and Distribution,* vol. 138, pp. 546-552, 1991.

[28] X. Wang, V. Vittal, and G. T. Heydt, "Tracing Generator Coherency Indices Using the Continuation Method: A Novel Approach," *IEEE Transactions on Power Systems,* vol. 20, pp. 1510-1518, 2005.

[29] N. Senroy, "Generator Coherency Using the Hilbert-Huang Transform," *IEEE Transactions on Power Systems,* vol. 23, pp. 1701-1708, 2008.

[30] H. A. Alsafih and R. Dunn, "Determination of coherent clusters in a multi-machine power system based on wide-area signal measurements," in *2010 IEEE Power and Energy Society General Meeting*, 2010, pp. 1-8.

[31] K. L. Lo, Z. Z. Qi, and D. Xiao, "Identification of coherent generators by spectrum analysis," *IEE Proceedings- Generation, Transmission and Distribution,* vol. 142, pp. 367-371, 1995.

[32] M. Jonsson, M. Begovic, and J. Daalder, "A new method suitable for real-time generator coherency determination," *IEEE Transactions on Power Systems,* vol. 19, pp. 1473-1482, 2004.

[33] S. B. Yusof, G. J. Rogers, and R. T. H. Alden, "Slow coherency based network partitioning including load buses," *IEEE Transactions on Power Systems,* vol. 8, pp. 1375-1382, 1993.

[34] J. H. Chow, *Time-Scale Modeling of Dynamic Networks with Applications to Power Systems*. New York: Springer-Verlag, 1982.

[35] L. Wang, M. Klein, S. Yirga, and P. Kundur, "Dynamic reduction of large power systems for stability studies," *IEEE Transactions on Power Systems,* vol. 12, pp. 889-895, 1997.

[36] R. A. Date and J. H. Chow, "Aggregation properties of linearized two-time-scale power networks," *IEEE Transactions on Circuits and Systems,* vol. 38, pp. 720-730, 1991.

[37] J. H. Chow, R. Galarza, P. Accari, and W. W. Price, "Inertial and slow coherency aggregation algorithms for power system dynamic model reduction," *IEEE Transactions on Power Systems,* vol. 10, pp. 680-685, 1995.

[38] G. N. Ramaswamy, G. C. Verghese, L. Rouco, C. Vialas, and C. L. DeMarco, "Synchrony, aggregation, and multi-area eigenanalysis," *IEEE Transactions on Power Systems,* vol. 10, pp. 1986-1993, 1995.

[39] B. Marinescu, B. Mallem, and L. Rouco, "Large-Scale Power System Dynamic Equivalents Based on Standard and Border Synchrony," *IEEE Transactions on Power Systems,* vol. 25, pp. 1873-1882, 2010.

[40] H. Kim, G. Jang, and K. Song, "Dynamic reduction of the large-scale power systems using relation factor," *IEEE Transactions on Power Systems,* vol. 19, pp. 1696-1699, 2004.

[41] M. L. Ourari, L. A. Dessaint, and D. Van-Que, "Dynamic equivalent modeling of large power systems using structure preservation technique," *IEEE Transactions on Power Systems,* vol. 21, pp. 1284-1295, 2006.

[42] A. M. Miah, "Study of a coherency-based simple dynamic equivalent for transient stability assessment," *IET Generation, Transmission & Distribution,* vol. 5, pp. 405-416, 2011.

[43] J. M. Ramirez, B. V. Hernández, and R. E. Correa, "Dynamic equivalence by an optimal strategy," *Electric Power Systems Research,* vol. 84, pp. 58-64, 2012.

[44] H. Shakouri G and H. R. Radmanesh, "Identification of a continuous time nonlinear state space model for the external power system dynamic equivalent by neural networks," *International Journal of Electrical Power & Energy Systems,* vol. 31, pp. 334-344, 2009.

[45] P. Ju, L. Q. Ni, and F. Wu, "Dynamic equivalents of power systems with online measurements. Part 1: Theory," *IEE Proceedings - Generation, Transmission and Distribution,* vol. 151, pp. 175-178, 2004.

[46] P. Ju, F. Li, N. G. Yang, X. M. Wu, and N. Q. He, "Dynamic equivalents of power systems with online measurements Part 2: Applications," *IEE Proceedings - Generation, Transmission and Distribution,* vol. 151, pp. 179-182, 2004.

[47] L. Ljung, *System identification: theory for the user*: Prentice-Hall, 1987.

[48] T. Dovan, T. S. Dillon, C. S. Berger, and K. E. Forward, "A Microcomputer Based On-Line Identification Approach to Power System Dynamic Load Modelling," *IEEE Transactions on Power Systems,* vol. 2, pp. 529-536, 1987.

[49] D. Karlsson and D. J. Hill, "Modelling and identification of nonlinear dynamic loads in power systems," *IEEE Transactions on Power Systems,* vol. 9, pp. 157-166, 1994.

[50] J. W. O'Sullivan and M. J. O'Malley, "Identification and validation of dynamic global load model parameters for use in power system frequency simulations," *IEEE Transactions on Power Systems,* vol. 11, pp. 851-857, 1996.

[51] M. Bostanci, J. Koplowitz, and C. W. Taylor, "Identification of power system load dynamics using artificial neural networks," *IEEE Transactions on Power Systems,* vol. 12, pp. 1468-1473, 1997.

[52] H. Okamoto, A. Kurita, J. J. Sanchez-Gasca, K. Clark, N. W. Miller, and J. H. Chow, "Identification of low-order linear power system models from EMTP simulations using the Steiglitz-McBride algorithm," *IEEE Transactions on Power Systems,* vol. 13, pp. 422-427, 1998.

[53] G. Ledwich, D. Geddey, and P. O'Shea, "Phasor measurement Units for system diagnosis and load identification in Australia," in *2008 IEEE Power and Energy Society General Meeting - Conversion and Delivery of Electrical Energy in the 21st Century* 2008, pp. 1-6.

[54] A. Abur and A. G. Expósito, *Power System State Estimation: Theory and Implementation*: Marcel Dekker, 2004.

[55] C. K. Chui and G. Chen, *Kalman Filtering: With Real-Time Applications*: Springer, 2009.

[56] R. E. Kalman, "A new approach to linear filtering and prediction problems," *Journal of Basic Engineering,* vol. 82, pp. 35-45, 1960.

[57] A. M. Stankovic, H. Lev-Ari, and M. M. Perisic, "Analysis and implementation of model-based linear estimation of dynamic phasors," *IEEE Transactions on Power Systems,* vol. 19, pp. 1903-1910, 2004.

[58] R. A. Wiltshire, G. Ledwich, and P. O'Shea, "A Kalman Filtering Approach to Rapidly Detecting Modal Changes in Power Systems," *IEEE Transactions on Power Systems,* vol. 22, pp. 1698-1706, 2007.

[59] P. Korba, "Real-time monitoring of electromechanical oscillations in power systems: first findings," *IET Generation, Transmission & Distribution,* vol. 1, pp. 80-88, 2007.

[60] N. R. Chaudhuri, A. Domahidi, R. Majumder, B. Chaudhuri, P. Korba, S. Ray, *et al.*, "Wide-area power oscillation damping control in nordic equivalent system," *IET Generation, Transmission & Distribution*, vol. 4, pp. 1139-1150, 2010.

[61] E. Ghahremani and I. Kamwa, "Dynamic State Estimation in Power System by Applying the Extended Kalman Filter With Unknown Inputs to Phasor Measurements," *IEEE Transactions on Power Systems*, vol. 26, pp. 2556-2566, 2011.

[62] T.-W. Chan, "Proximity-to-separation based energy function control strategy for power system stability," PhD Thesis, Queensland University of Technology, Brisbane, 2003.

[63] D. N. Kosterev and W. J. Kolodziej, "Bang-bang series capacitor transient stability control," *IEEE Transactions on Power Systems*, vol. 10, pp. 915-924, 1995.

[64] C. Jaewon and J. H. Chow, "Time-optimal control of power systems requiring multiple switchings of series capacitors," *IEEE Transactions on Power Systems*, vol. 13, pp. 367-373, 1998.

[65] M. H. Haque, "Evaluation of First Swing Stability of a Large Power System With Various FACTS Devices," *IEEE Transactions on Power Systems*, vol. 23, pp. 1144-1151, 2008.

[66] M. H. Haque, "Improvement of first swing stability limit by utilizing full benefit of shunt FACTS devices," *IEEE Transactions on Power Systems*, vol. 19, pp. 1894-1902, 2004.

[67] M. H. Haque, "Damping improvement by FACTS devices: A comparison between STATCOM and SSSC," *Electric Power Systems Research*, vol. 76, pp. 865-872, 2006.

[68] C. Jaewon and J. H. Chow, "Time-optimal series capacitor control for damping interarea modes in interconnected power systems," *IEEE Transactions on Power Systems*, vol. 12, pp. 215-221, 1997.

[69] B. Chaudhuri and B. C. Pal, "Robust damping of multiple swing modes employing global stabilizing signals with a TCSC," *IEEE Transactions on Power Systems*, vol. 19, pp. 499-506, 2004.

[70] A. B. Leirbukt, J. H. Chow, J. J. Sanchez-Gasca, and E. V. Larsen, "Damping control design based on time-domain identified models," *IEEE Transactions on Power Systems*, vol. 14, pp. 172-178, 1999.

[71] E. W. Palmer, "Multi-Mode Damping of Power System Oscillations," PhD Thesis, University of Newcastle, 1998.

[72] M. Ghandhari, G. Andersson, and I. A. Hiskens, "Control Lyapunov functions for controllable series devices," *IEEE Transactions on Power Systems* vol. 16, pp. 689-694, 2001.

[73] E. Palmer and G. Ledwich, "Switching control for power systems with line losses," *IEE Proceedings- Generation, Transmission and Distribution*, vol. 146, pp. 435-440, 1999.

[74] J. J. Ford, G. Ledwich, and Z. Y. Dong, "Efficient and robust model predictive control for first swing transient stability of power systems using flexible AC transmission systems devices," *IET Generation, Transmission & Distribution*, vol. 2, pp. 731-742, 2008.

[75] A. Chakrabortty, "Wide-Area Damping Control of Power Systems Using Dynamic Clustering and TCSC-Based Redesigns," *IEEE Transactions on Smart Grid*, vol. 3, pp. 1503-1514, 2012.

[76] E. De Tuglie, M. Dicorato, M. La Scala, and P. Scarpellini, "A corrective control for angle and voltage stability enhancement on the transient time-scale," *IEEE Transactions on Power Systems* vol. 15, pp. 1345-1353, 2000.

[77] J. Jung, L. Chen-Ching, S. L. Tanimoto, and V. Vittal, "Adaptation in load shedding under vulnerable operating conditions," *IEEE Transactions on Power Systems*, vol. 17, pp. 1199-1205, 2002.

[78] J. J. Ford, H. Bevrani, and G. Ledwich, "Adaptive load shedding and regional protection," *International Journal of Electrical Power & Energy Systems*, vol. 31, pp. 611-618, 2009.

[79] H. You, V. Vittal, and W. Xiaoming, "Slow coherency-based islanding," *IEEE Transactions on Power Systems,* vol. 19, pp. 483-491, 2004.

[80] Y. Bo, V. Vittal, and G. T. Heydt, "Slow-Coherency-Based Controlled Islanding—A Demonstration of the Approach on the August 14, 2003 Blackout Scenario," *IEEE Transactions on Power Systems,* vol. 21, pp. 1840-1847, 2006.

[81] Y. Haibo, V. Vittal, and Y. Zhong, "Self-healing in power systems: an approach using islanding and rate of frequency decline-based load shedding," *IEEE Transactions on Power Systems,* vol. 18, pp. 174-181, 2003.

[82] K. Sun, D. Z. Zheng, and Q. Lu, "Searching for feasible splitting strategies of controlled system islanding," *IEE Proceedings- Generation, Transmission and Distribution,* vol. 153, pp. 89-98, 2006.

[83] C. L. Zhang and G. F. Ledwich, "A new approach to identify modes of the power system based on T-matrix," in *Sixth International Conference on Advances in Power System Control, Operation and Management (ASDCOM 2003)* 2003, pp. 496-501.

[84] E. W. Palmer and G. Ledwich, "Optimal placement of angle transducers in power systems," *IEEE Transactions on Power Systems,* vol. 11, pp. 788-793, 1996.

[85] G. Ledwich and E. Palmer, "Modal estimates from normal operation of power systems," in *IEEE Power Engineering Society Winter Meeting*, 2000, pp. 1527-1531 vol.2.

[86] D. J. Trudnowski, "Estimating Electromechanical Mode Shape From Synchrophasor Measurements," *IEEE Transactions on Power Systems,* vol. 23, pp. 1188-1195, 2008.

[87] S. M. Kay, *Modern spectral estimation: theory and application*: Prentice Hall, 1988.

[88] P. Jazayeri, W. Rosehart, and D. T. Westwick, "A Multistage Algorithm for Identification of Nonlinear Aggregate Power System Loads," *IEEE Transactions on Power Systems,* vol. 22, pp. 1072-1079, 2007.

Publications Arising from the Thesis

Journal papers

(1) **A. Vahidnia**, G. Ledwich, E. Palmer, and A. Ghosh, "Generator coherency and area detection in large power systems," *IET Generation, Transmission & Distribution*, vol. 6, pp. 874-883, 2012.

(2) **A. Vahidnia**, G. Ledwich, E. Palmer, and A. Ghosh, "Dynamic equivalent state estimation for multi-area power systems with synchronized phasor measurement units," *Electric Power Systems Research*, vol. 96, pp. 170-176, 2013.

(3) **A. Vahidnia**, G. Ledwich, E. Palmer, and A. Ghosh, "Online identification and estimation of equivalent area parameters using synchronized phasor measurements," under revision *IET Generation, Transmission & Distribution*, 2013.

(4) **A. Vahidnia**, G. Ledwich, E. Palmer, and A. Ghosh, "Wide-area control through aggregation of power systems," to be submitted to *IEEE Transactions on Power Systems*, 2013.

Conference papers

(5) **A. Vahidnia**, G. Ledwich, E. Palmer, and A. Ghosh, "Interpreting regional frequencies from synchronized phasor measurement in multi-area power systems," in *2011 IEEE Power and Energy Society General Meeting*, pp. 1-7, 2011.

(6) **A. Vahidnia**, G. Ledwich, E. Palmer, and A. Ghosh, "Identification of reduced equivalent models of power system areas using phasor measurement units," to be submitted to *2013 Australasian Universities Power Engineering Conference (AUPEC)*, 2013.

(7) **A. Vahidnia**, G. Ledwich, E. Palmer, and A. Ghosh, "Wide area controls for first swing and damping stability enhancement," to be submitted to *2013 Australasian Universities Power Engineering Conference (AUPEC)*, 2013.

(8) **A. Vahidnia**, G. Ledwich, A. Ghosh, and E. Palmer, "An improved genetic algorithm and graph theory based method for optimal sectionalizer switch placement in distribution networks with DG," *2011 Australasian Universities Power Engineering Conference (AUPEC)*, 2011.

Appendix

The parameters of the test systems used in the simulations are presented in this Appendix.

- **Four machine system**

The four machine - two area system is used in the simulations with two different sets of generator parameters as shown in Table A.1 and Table A.2: The first set is used in Chapter 3 while the second set is used in other chapters.

Table A.1 The dynamic parameters of the four machine system (first set)

	Gen 1	**Gen 2**	**Gen 3**	**Gen 4**
Inertia (J)	0.80	0.20	0.60	1.0
Damping (D)	0.25	0.25	0.25	0.25

Table A.2 The dynamic parameters of the four machine system (second set)

	Gen 1	**Gen 2**	**Gen 3**	**Gen 4**
Inertia (J)	0.160	0.040	0.120	0.200
Damping (D)	0.060	0.060	0.060	0.060

- **16 machine – 68 bus system**

The 16 machine test system is shown in Fig. A.1 and the generator parameters of this system are presented in Table A.3.

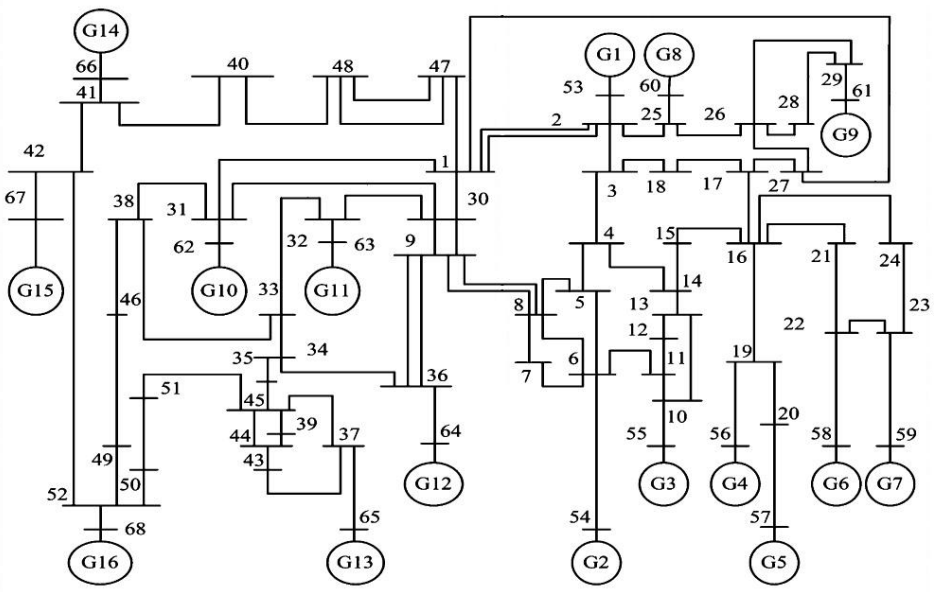

Fig. A.1 The 68 bus – 16 machine test system

Table A.3 The dynamic parameters of the 16 machine system

Generator	Bus No	Inertia (J)	Damping (D)	V_gen (pu)
1	53	0.0541	0.0271	1.045
2	54	0.2101	0.1050	0.98
3	55	0.2106	0.1053	0.983
4	56	0.1767	0.0883	0.997
5	57	0.1770	0.0885	1.011
6	58	0.2345	0.1172	1.05
7	59	0.1836	0.0918	1.063
8	60	0.1662	0.0831	1.03
9	61	0.2141	0.1071	1.025
10	62	0.1853	0.0926	1.01
11	63	0.1702	0.0851	1
12	64	0.5220	0.2610	1.0156
13	65	2.5963	2.5465	1.011
14	66	1.5915	0.7958	1
15	67	1.5915	1.5915	1
16	68	2.5969	2.5969	1

- **Ten machine – four area system**

The generators of 10 machine system used in Chapter 6, have similar characteristics to the four machine system as presented in Table A.4.

Table A.4 The dynamic parameters of the 10 machine system

Generator Number	Inertia (J)	Damping (D)
1	0.16	0.060
2	0.04	0.060
3	0.12	0.060
4	0.20	0.060
5	0.08	0.060
6	0.16	0.060
7	0.20	0.060
8	0.04	0.060
9	0.08	0.060
10	0.12	0.060

- **Three area test system**

The generator parameters of the three machine (area) system as applied for both longitudinal and meshed systems are shown in Table A.5.

Table A.5 The dynamic parameters of the three area system

	Gen 1	Gen 2	Gen 3
Inertia (J)	0.150	0.100	0.150
Damping (D)	0.10	0.10	0.10

- **Higher order ten machine system**

The parameters of the generators and exciters for the ten machine system with higher order models are shown in Table A.6 and A.7 where identical dynamic parameters are used for the generators.

Table A.6 The generator parameters of the ten machine system

H	r_a	x'_d	x'_q	x_d	x_q	T'_d	T'_q	x_l
24.3	0	0.057	0.0911	0.29	0.28	6.7	0.41	0.028

Table A.7 The exciter parameters of the ten machine system

K_a	T_a	Vr_{min}	Vr_{max}	K_e	T_e	K_f	T_f	c_1	c_2
5	0.06	-1	1	-0.052	0.5	0.08	1	0.08	0.314